Chapter 4

Results and Discussion

4.1 Introduction

In this chapter, the fabrication of the ZnO nanostructures grown on bare and gold-coated silicon substrates by a chemical vapor transport and condensation (CVTC) route using carbothermal reaction under different growth conditions are studied. The ZnO nanostructures fabricated were characterized using field emission scanning electron microscopy (FESEM), energy dispersive x-ray spectroscopy (EDX), x-ray diffraction (XRD), photoluminescence measurements (PL) and high resolution transmission electron microscopy (HRTEM). A systematic study, including the effect of growth parameters and growth mechanism of ZnO nanostructures synthesized on bare and gold-coated silicon substrates will be discussed in detailed in sections 4.2 and 4.3, respectively. In section 4.4, a comparative study on ZnO nanostructures grown without catalyst and using gold catalyst will be reported. The PL measurements of ZnO nanostructures will be presented in section 4.5. Different morphologies of ZnO nanostructures grown on the different substrates as well as growth mechanisms will be presented in section 4.6. Finally, the growth morphology, structure, and the optical properties of P-doped ZnO nanostructures fabricated on silicon substrate will be reported in section 4.7.

4.2 Parametric study of ZnO nanostructures grown without catalyst

As mentioned in session 2.9, the control of the size and the shape of ZnO nanostructures are not easily obtained and the role of growth parameters on ZnO nanostructures is still not fully understood. Arguments were raised on the effect of growth parameters on ZnO nanostructures growth mechanism. In general, the motivation was to obtain mass production and high quality with low cost of ZnO nanostructures [121]. In this study, the effect of growth parameters such as deposition temperatures, gas flow rate, deposition time and ZnO:C mass ratios on the growth of ZnO nanostructures have been investigated. The effects of different parameters on the morphology and properties of the ZnO nanostructures produced by non-catalytic carbothermal process and at atmospheric pressure will be discussed in detailed.

4.2.1 Effect of location of the silicon substrate from the source

To study the effect of location of Si substrate during the growth process on the formation of ZnO nanostructures, the syntheses of ZnO nanostructures were performed at 6, 11, 15 and 19 cm downstream away from the source materials. The deposition conditions were kept as follows; furnace temperature was 1200°C, Ar gas flow rate 40 sccm, deposition time for 30 min and the mass ratio of ZnO:C was 1:1. The source material was put at the center of the furnace and the furnace temperature was kept constant for 7.5 cm downstream the center of the furnace. Typical FESEM images of the ZnO nanostructures that have been obtained on silicon substrates at different locations from the source materials are shown in Fig. 4.1. In addition, Fig. 4.2 shows the corresponding EDX spectra for each sample.

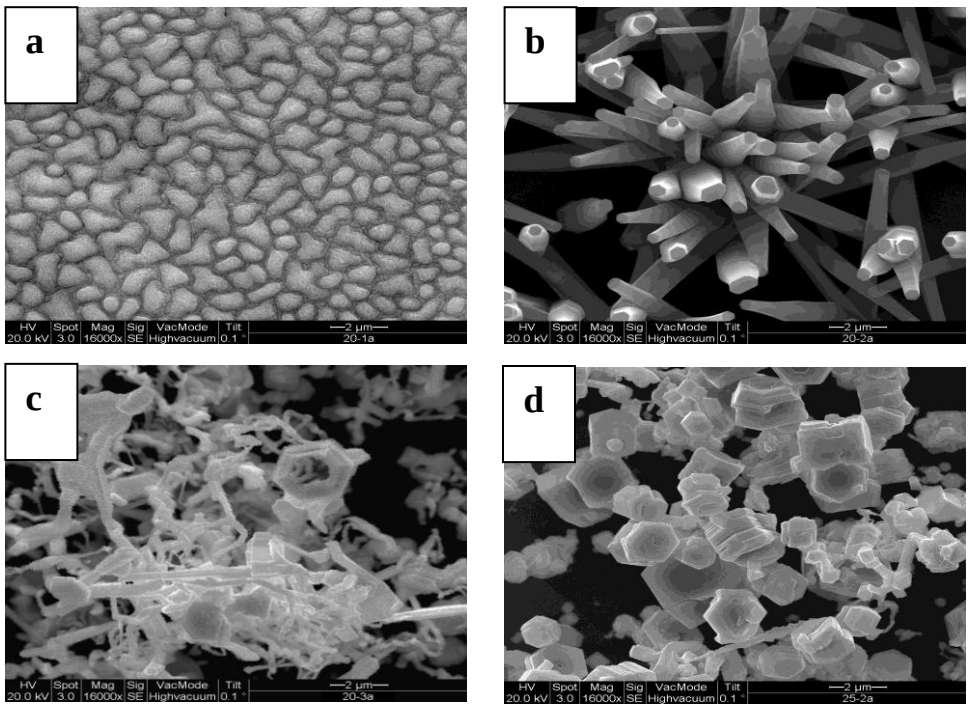

Fig. 4.1. FESEM images of ZnO nanostructures grown on silicon substrates located at (a) 6 cm, (b) 11 cm, (c) 15 cm and (d) 19 cm from the source. The furnace temperature was 1200°C. Ar gas flow rate was 40 sccm. The deposition time was 30 min. The mass ratio of ZnO:C was 1:1.

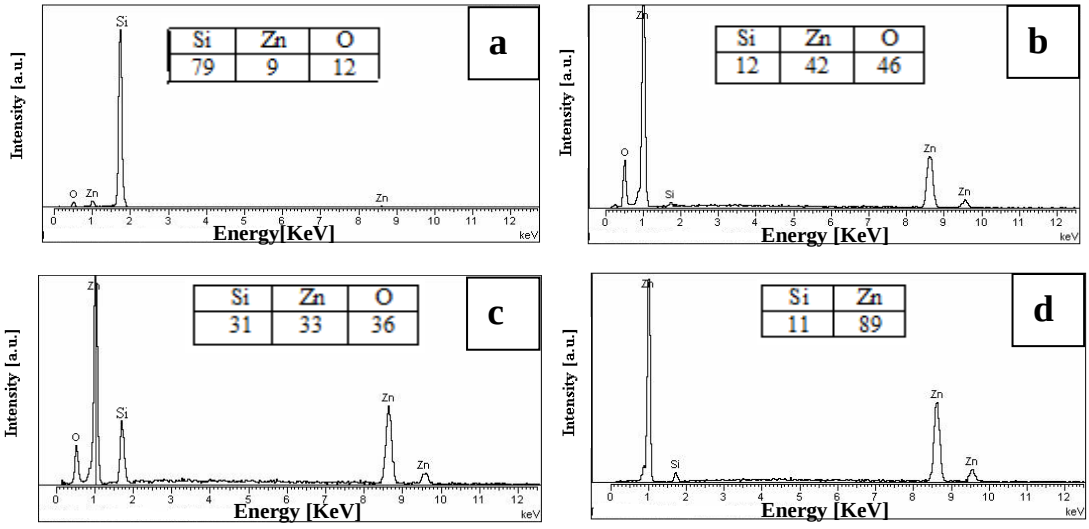

Fig. 4.2. EDX spectra of ZnO nanostructures grown on silicon substrates located at (a) 6 cm, (b) 11cm, (c) 15 cm and (d) 19 cm away from the source material. The furnace temperature was 1200°C. Ar gas flow rate was 40 sccm. The deposition time was 30 min. The mass ratio of ZnO:C was 1:1.

In Fig. 4.1 (a), a complete film of ZnO was formed with particles of a few micrometers in size and clearly, no specific nanostructures were observed for the sample located at 6 cm from the source. Composition analysis of the sample was performed by EDX. Fig. 4.2 (a) shows that the atomic proportion of Zn element was very small compared to silicon (the Si-related peak in the spectrum comes from the Si substrate). This indicates that at short distance from the source, the silicon substrate has higher local temperature than the boiling temperature of the Zn (907°C) and as a result, this leads to re-evaporate of Zn atoms from the substrate without being oxidized. At 11 cm away from the source, aligned ZnO nanowires were formed upon silicon substrate as demonstrated in Fig. 4.1 (b). The average diameter of these nanowires was about 50 nm to 200 nm and the length was 4-8μm. The EDX spectrum in Fig. 4.2 (b) showed that the percentage of Zn and O were increased compared to silicon and this shows that a high yield of ZnO nanowires was produced. The atomic ratio of Zn:O is 0.91:1, which shows that the nanostructures were O rich. Fig. 4.1 (c) shows irregular shapes of ZnO nanostructures with non-aligned nanowires that were formed in large quantity for the sample at 15 cm. The corresponding EDX result in Fig. 4.2 (c) showed significant increase in the Zn and O peaks relative to the silicon peak. Overall, EDX for the samples located at 6, 11 and 15 cm have the atomic ratio of O higher than the Zn which indicates that there is excessive oxygen in the as-grown ZnO nanostructures. The reason for the O-rich may be due to the large ratio of surface to volume of the ZnO nanostructures makes more oxygen absorbing on the surface.

For the silicon substrate which was located 19 cm away from the center, microstructures in the form of Zn disks were obtained as shown in Fig. 4.1 (d). The corresponding EDX (Fig. 4.2 (d)) shows that no oxygen was found and the microstructures disks were metallic Zn. This is a direct evidence of the carbothermal mechanism of the ZnO nanostructures formation where reduction of ZnO occurred in ZnO/C mixture at elevated temperatures to produce Zn, which evaporated and redeposit on the substrates. ZnO nanostructures were formed upon oxidation of the redeposit Zn. Details of the ZnO formation mechanism will be given in section 4.2.6.

Fig. 4.3 shows the XRD patterns of the samples grown on Si(100) substrates at different locations from the source material. The strong intensity and narrow width of ZnO diffraction peaks indicate that the resulting products were of high crystallinity, where more than one diffraction peak appeared on the XRD patterns indicating the polycrystalline nature of ZnO nanostructures.

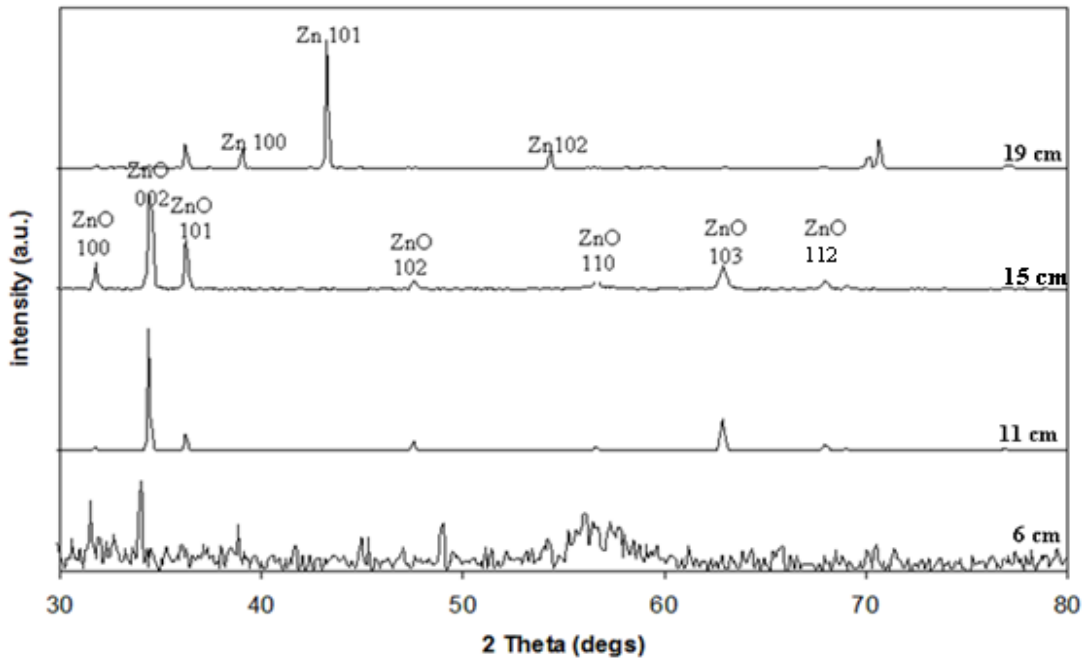

Fig. 4.3. XRD patterns of ZnO nanostructures deposited on the Si(100) substrates at different locations from the source. The furnace temperature was 1200°C. Ar gas flow rate was 40 sccm. The deposition time was 30 min. The mass ratio of ZnO: C was 1:1.

As shown in Fig. 4.3, apart from the ZnO diffraction peaks, no other peaks, such as Zn peaks, were detected in the samples located at 6, 11 and 15 cm. The XRD diffraction peaks can be assigned to (100), (002), (101), (102), (110), (103) and (112) phase of the standard polycrystalline ZnO peaks. Similar results were reported by Jung *et al* [122]. For the sample located at 19 cm from the source, strong Zn (100), (101), and (102) diffraction peaks were observed which indicates that the prepared sample at this location was mainly composed of a metallic Zn. Very weak ZnO (1 0 0), (0 0 2), and (1 0 1) peaks were observed in the sample located at 6 cm. Moreover, the broad ZnO diffraction peak at 2θ=56.59° indicates that the resulting products possess a very small size of crystal. and possibly were amorphous. It is noticeable that the (002) peak at 34.3° is dominated suggesting a preferred orientation of the ZnO nanorods obtained at 11 cm. This corresponds

with the align nanorods as observed in the FESEM image in Fig. 4.1 (b). In general, at different substrate locations, different ZnO nanostructures were formed in agreement with Li *et al* [71] and Umar *et al* [72]. Silicon substrates have different local temperatures at different locations from the source. As a result, different ZnO morphologies was obtained on substrates at high and low temperature zones. This is because the concentration and diffusion rate of vapor component are different. At high substrate temperature, vapor has a small chance to nucleate and deposit on the surface. This may be due the re-evaporated of vapor from the substrate when it gains sufficient energy to evaporate. For that reason, a thin film of ZnO was observed at substrate located at 6 cm away from the source. In lower temperature region, (substrate at 19 cm location from the source) a small amount of vapor arrived since most of the material settled at the substrate upstream. In addition, zinc structures were only deposited on substrate therefore, any zinc vapor arrived to the substrate it solidified instantly without oxidized.

4.2.2 Effect of furnace temperature

To study the effect of furnace temperature, a mixture of (1:1) ZnO:C powders loaded into the center of the a horizontal tube furnace with four different furnace temperatures 1200°C, 1100°C, 1000°C and 950°C, respectively. The Si substrates were kept at 11 cm from the source. Ar gas flow rate was 40 sccm. The deposition time was 30 min. Fig. 4.4 shows typical FESEM images of the samples grown at different source temperatures.

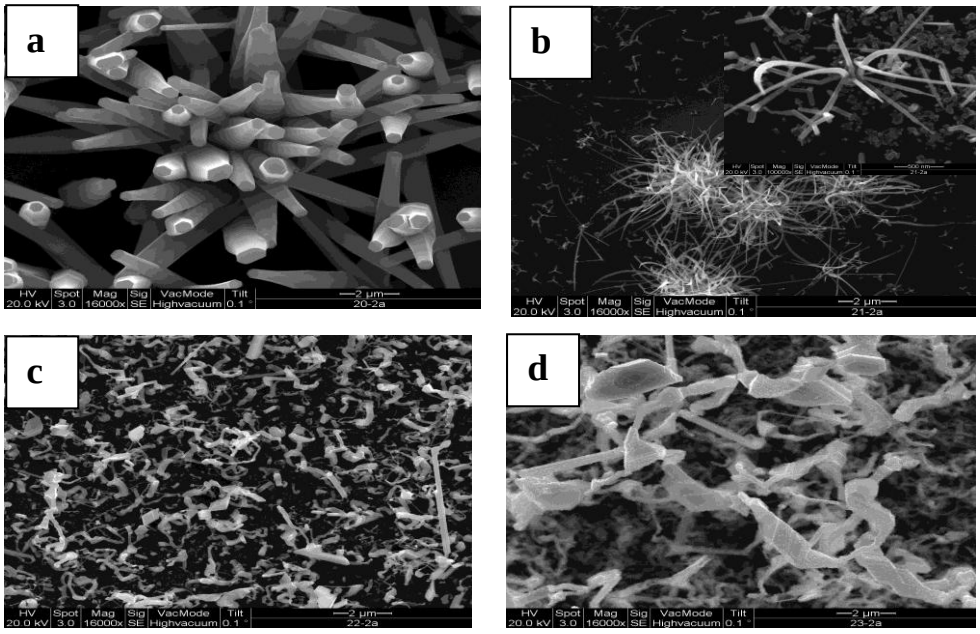

Fig. 4.4. FESEM images ZnO nanostructures formed on Si substrates at (a) 1200°C, (b) 1100°C, (c) 1000°C and (d) 950°C furnace temperatures. The Si substrates were kept at 11 cm from the source. Ar gas flow rate was 40 sccm. The deposition time was 30 min. The mass ratio of ZnO:C was 1:1.

Aligned nanowires with 50 nm to 200 nm diameters and 4-8 μm lengths were formed on the substrate when the furnace temperature was 1200°C as illustrated in Fig. 4.4 (a). At 1100°C, nanoflowers and nanotetrapods were synthesized on the substrate as shown in Fig. 4.4 (b). The length of the nanotetrapods is about 300 nm with a diameter of 50 nm whereas the nanoflowers have a 3 μm length with diameters ranging from 50 nm to 100 nm. A representative EDX spectrum of these nanostructures is shown in Fig. 4.5 (a). Peaks associated with Zn and O atoms are seen in this EDX spectrum. The Si-related peak in the spectrum comes from the Si substrate. The peak comparison also shows that there is a fair amount of nanomaterials deposited over the substrate. Fig. 4.4 (c) and Fig. 4.4 (d) possess similar morphology because they are grown with almost the same furnace temperature. In addition, these nanostructures have the same composition of

Zn and O as illustrated in Fig. 4.5 (b). It is quite clear that there is an oxygen deficiency for sample grown at 1000°C furnace temperature. This is may due to the low concentration of vapors caused by carbothermal reaction.

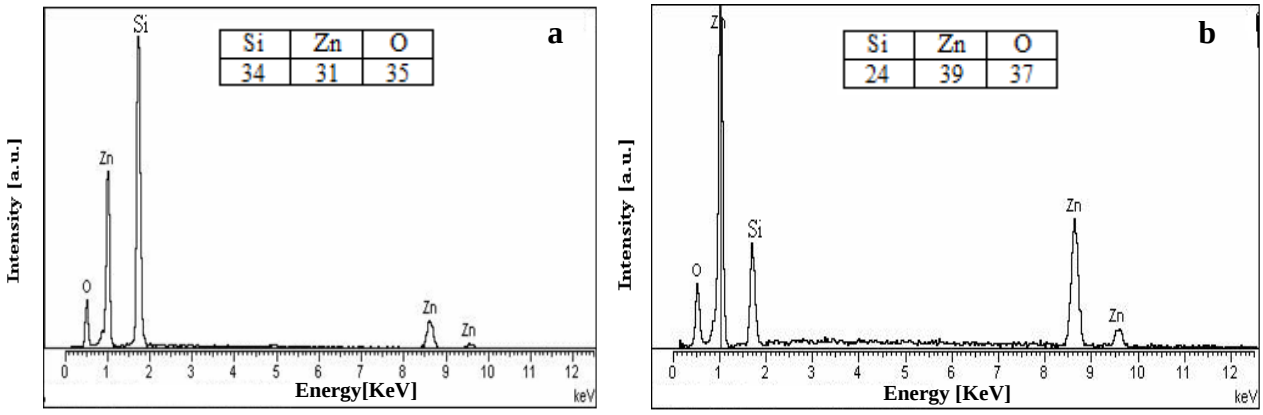

Fig. 4.5. EDX spectra of ZnO nanostructures grown on Si substrates at (a) 1100°C and (b) 1000°C furnace temperatures. The Si substrates were kept at 11 cm from the source. Ar gas flow rate was 40 sccm. The deposition time was 30 min. The mass ratio of ZnO:C was 1:1.

To determine the crystallinity and the crystal phase of the deposited products grown at different furnace temperature, x-ray diffraction (XRD) was used. The results are shown in Fig. 4.6. The diffraction peaks for all examined samples corresponded to hexagonal wurtzite structure of ZnO. The diffraction peak at 2θ=34.4° can be assigned to (002) hexagonal structure of bulk ZnO. This indicates the preferential (002) growth of ZnO on the silicon substrate. Fujimura *et al.* [123] suggested that the surface energy of the (002) orientation is the lowest in the ZnO crystal. All XRD spectra confirm that as the furnace temperature increased, high density, good crystallinity, and well alignment ZnO crystalline is obtained. XRD result revealed that the crystallinity of the ZnO nanostructures grown at 950 °C was of lower quality. As a result, the growth morphology of ZnO nanostructures is

strongly depend on the furnace temperature because the density of vapor component that generated from carbothermal reaction is different at different furnace temperatures [124]. At a higher furnace temperature, a higher vapor pressure was produced and hence, the vapor of the source material diffuses away from the source area along the gas flow direction. At low furnace temperature, the vapor pressure is lower so, the nucleation of the nanostructures was preformed at different directions.

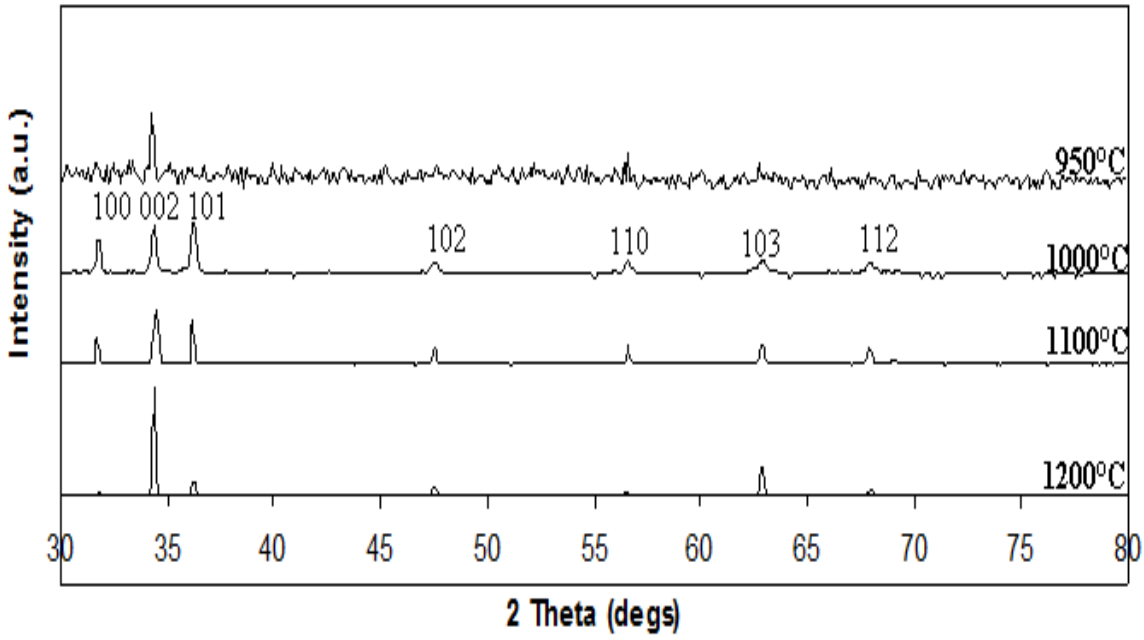

Fig. 4.6. XRD patterns of the deposited ZnO products on silicon substrates at different furnace temperatures. The Si substrates were kept at 11 cm from the source. Ar gas flow rate was 40 sccm. The deposition time was 30 min. The mass ratio of ZnO:C was 1:1.

4.2.3 Effect of Argon flow rate

The growth of ZnO nanostructures was performed under various Ar flow rates, including 10, 30, 50 and 70 sccm for substrates located at 11 cm away from the source. The source was ZnO:C (1:1) heated at 1100°C for 15 min. Typical FESEM pictures indicate the morphologies of ZnO nanostructures grown on silicon substrates at different Ar flow rates as shown in Fig. 4.7.

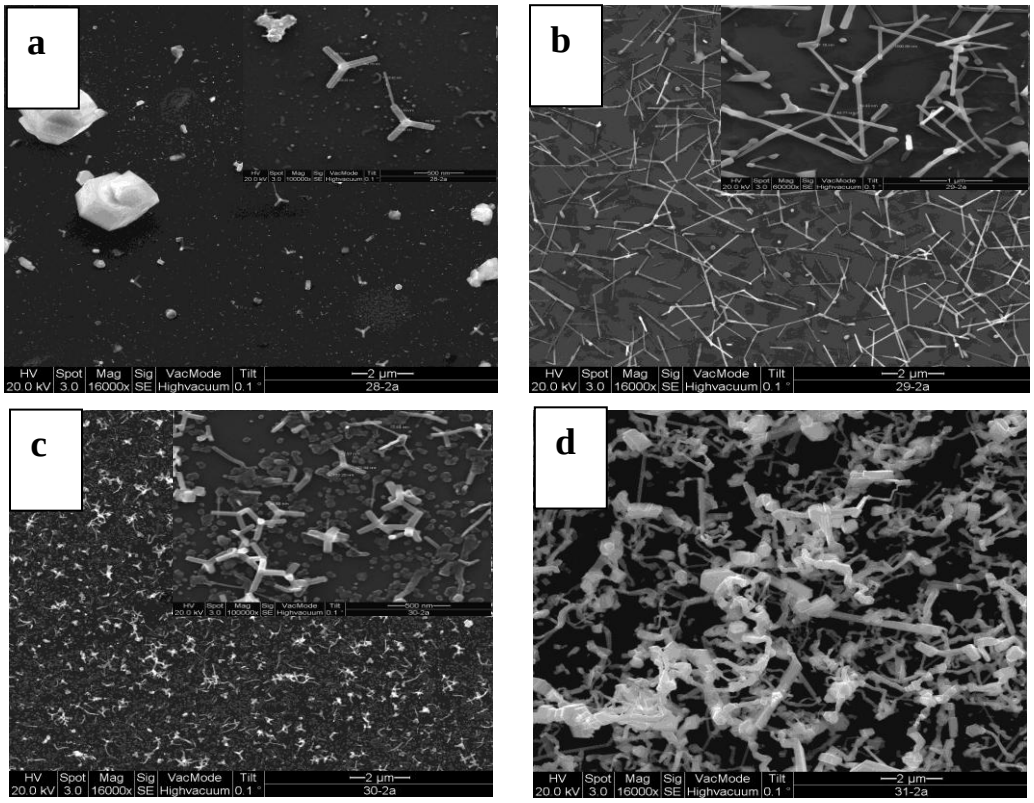

Fig. 4.7. FESEM images of ZnO nanostructures formed at (a) 10 sccm, (b) 30 sccm, (c) 50 sccm and (d) 70 sccm Ar flow rates. The silicon substrates were located at 11 cm away from the source which is ZnO:C (1:1) heated at 1100°C furnace temperature for 15 min.

The samples grown with the flow rates of 10, 30, and 50 sccm are shown in Fig. 4.7 (a), (b) and (c), all the samples have almost the same ZnO nanostructures which consisted mostly of nanotetrapods with hexagonal legs. ZnO nanostructures synthesized at a flow rate of 30 sccm have the longest average length of 1.5 μm while, those grown at 50 sccm exhibit the shortest average length of 200 nm. The smallest average diameter of 45 nm is obtained at 30 sccm and 50 sccm Ar flow rates. As the flow rate increased to 70 sccm, irregular shape and dendritic ZnO nanostructures were formed. ZnO nanotetrapods with different sizes were obtained on silicon substrates at different flow rates because supersaturation of ZnO vapors is different at different flow rates [125]. The reduction in tetrapod dimensions is directly linked to a lower supersaturation of vapor phase rather than the effect of temperature on the growth of tetrapods. Attempting to further decrease the size of ZnO tetrapods by reducing the supersaturation of the vapor phase, the flow rate of the carrying gas was further tuned to 70 sccm.

XRD spectra (Fig. 4.8) supported our argument on the effect of Ar gas flow rate on the ZnO product grown on silicon substrates. ZnO grown under 50 sccm and 30 sccm exhibit the same diffraction peaks but, the one grown under the 50 sccm flow rate has higher intensity peaks, indicating that more dense of ZnO nanostructure were grown obtained. On the other hand, samples grown under 10 sccm and 70 sccm, demonstrated lower crystalline quality. The XRD spectra were similar to those of amorphous structures. In summary, the density of ZnO nanostructures was found to increase rapidly as Ar flow rate increased because of the increased of Zn vapor and CO gas that they were carried by Ar gas to the substrate. In addition, the ZnO nanotertapods deposited at higher flow rates are denser than those deposited at lower flow rates because of the flow of carrier gas in the

system can greatly increase the rate of transport of vapor atoms from the source to the substrate.

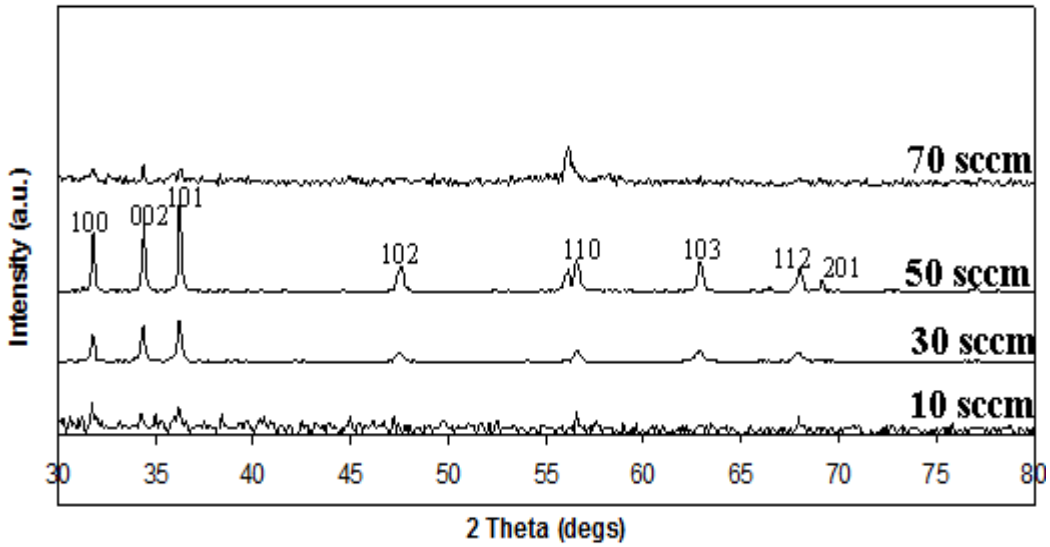

Fig.4.8. XRD patterns of the different ZnO nanostructures grown at different Ar gas flow rates. The silicon substrates were located at 11 cm away from the source, which is ZnO:C (1:1) heated at 1100°C for 15 min.

4.2.4 Effect of deposition time

The deposition time was varied to study the effect of it. The Si substrates are placed 11cm away from the source. The deposition time was varied, i.e. at 15, 30, 45 and 60 min, respectively. The ZnO:C mass ratio, Ar flow rate and furnace temperature are set 1:1, 40 sccm and 1100°C, respectively. Fig. 4.9 illustrates FESEM micrographs of ZnO products grown on silicon substrate grown at different deposition times. Fig. 4.10 (a) and (b) show the EDX spectra of 15 min and 60 min ZnO nanostructures formed on the silicon substrates.

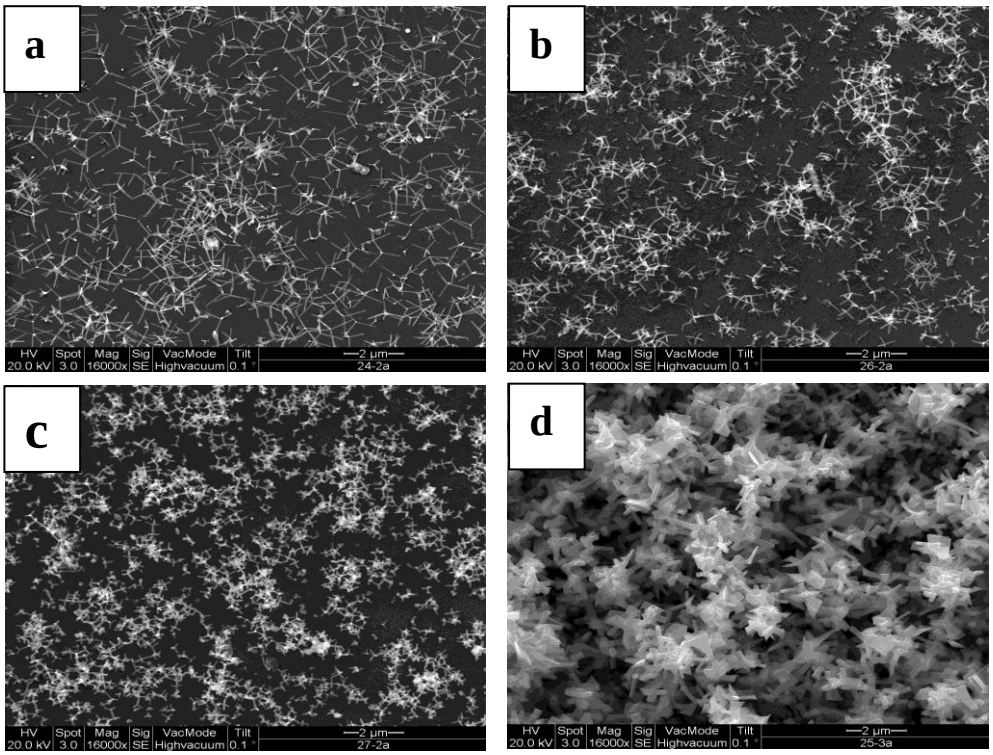

Fig. 4.9. FESEM images of ZnO nanostructures deposited for (a) 15 min, (b) 30 min, (c) 45 min, and (d) 60 min. The silicon substrates were located at 11 cm away from the source, which is ZnO:C (1:1) heated at 1100°C under 40 sccm Ar flow rate.

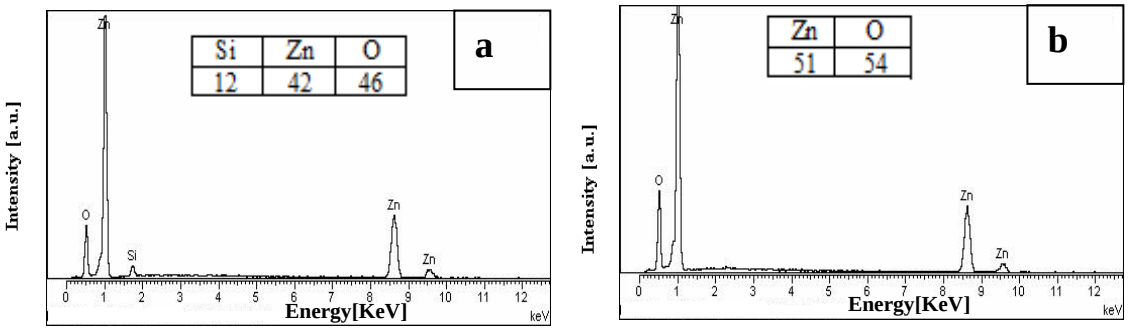

Fig. 4.10. EDX spectra of ZnO nanostructures grown with (a) 15 min and (b) 60 min growth time. The silicon substrates were located at 11 cm away from the source, which is ZnO:C (1:1) heated at 1100°C under 40 sccm Ar flow rate.

For EDX results, there is no silicon peak detected for the sample with 60 min deposition time. However, the silicon peak was observed for the sample 15 min deposition time. This result gives a good evidance to the high yield of ZnO nanostructures grown at 60 min depostion time. It is interesting to note that in all FESEM images, nanotetrapods were only formed upon the silicon substrates. As the deposition time increased, shorter nanotetrapods with large diameters were formed. Short ZnO nanotetrapods with large diameter are obtained for the samples with 60 min deposition time. The longest nanotertrapod legs were obtained for the sample with 15 min deposition time with 700 nm tall and 30 nm width. The largest nanotetrapod diameter of 200 nm with 400 nm length was formed in the sample with 60 min deposition time. It is worth to point out that when the deposition time was increased from 45 min to 60 min, ZnO nanostructures were changed from nanotertrapods to the sheet form. The deposition time plays a key role in controlling the shapes of ZnO nanostructures. The same result was reported by Tak *et al.* [103]. The variety of ZnO nanostructure forms was found to increase with increasing deposition time.

Fig. 4.11 shows typical XRD patterns of the as-synthesized ZnO nanostructures obtained at different deposition time. No diffraction peaks of metallic Zn or other impurities can be observed besides ZnO peaks. XRD spectra clearly reveal that as deposition time was increased higher densities of ZnO products were formed. In addition, (100), (002) and (101) peaks have been observed with almost the same intensities for the samples with 15 min to 45 min deposition time. In contrast, the highest intensity of (002) peak, at 60 min deposition times is observed. This shows that those nanostructures are aligned along the c-axis. In other words, this indicates that as the time increases, the (002) face becomes the preferred growth direction for ZnO nanostructures. Thus, it could be

concluded that the amount of ZnO nanostructures production is increased with the deposition time due to the increase of vapor components that was carried by the Ar gas to the silicon substrates.

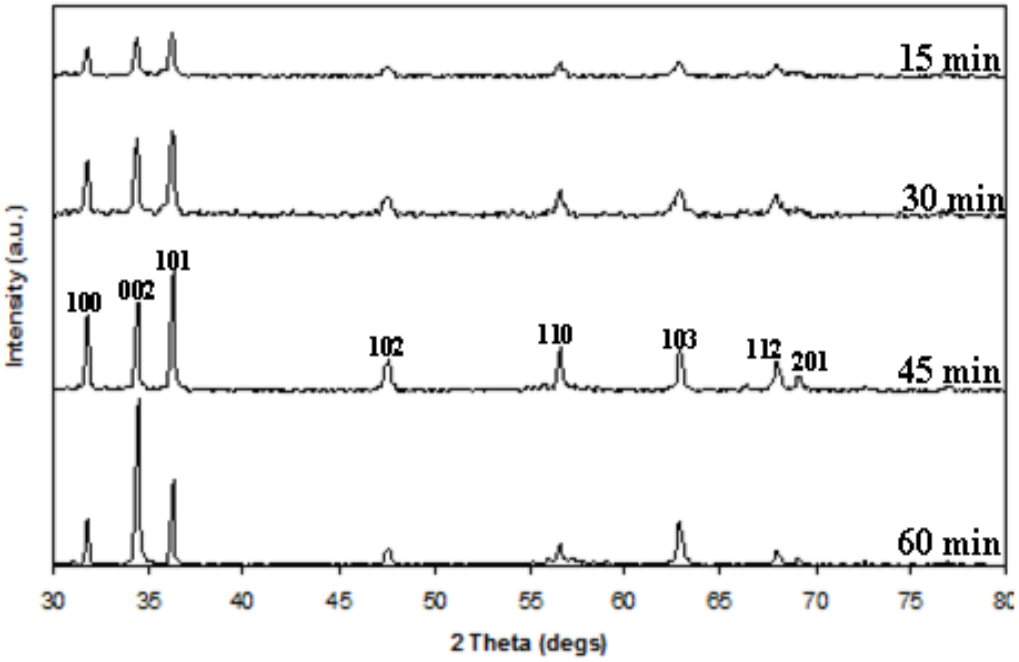

Fig. 4.11. XRD patterns of as-synthesized ZnO nanostructures obtained at different deposition times. The silicon substrates were located at 11 cm away from the source, which is ZnO:C (1:1) heated at 1100°C under 40 sccm Ar flow rate.

4.2.5 Effect of ZnO:C mass ratio

To study the effects of ZnO:C mass ratio, the mass ratio was varied from (1:1) to (2:1), (1:2) (3:1) and (1:3). The Ar flow rate was fixed at 30sccm and the furnace temperature was fixed at 1100°C. The substrate was located at 11 cm from the source. The deposition time 15 min was kept constant at 15 min during the growth process. The FESEM images of ZnO nanostructures grown in silicon substrates for each trial are shown in Fig. 4.12.

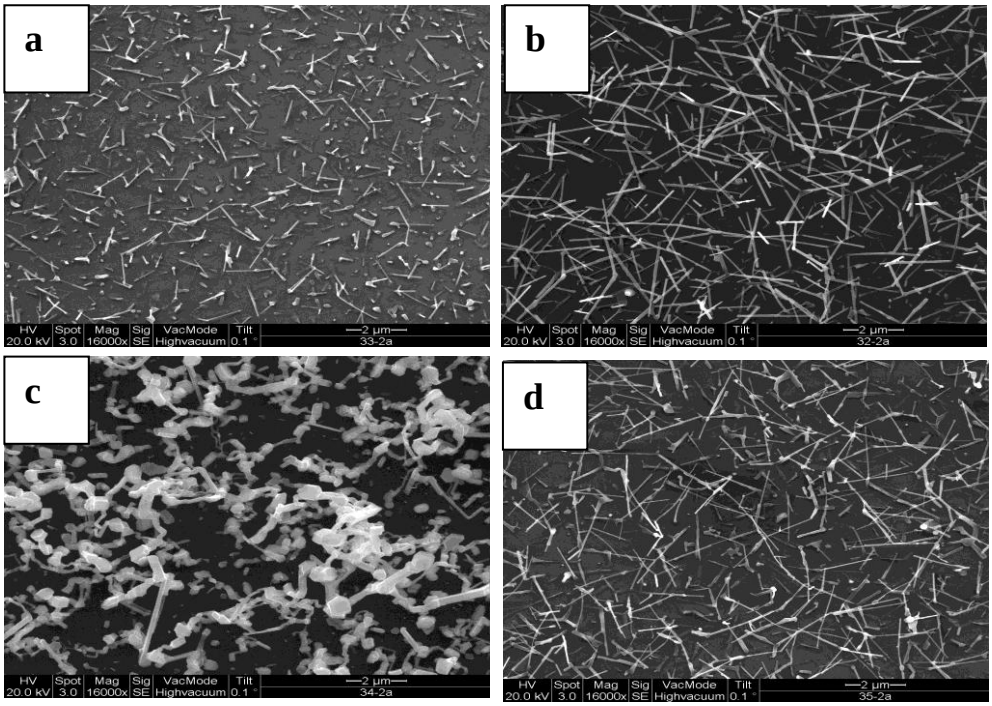

Fig. 4.12. FESEM images of ZnO nanostructures obtained from the ZnO:C source ratios of (a) (2:1), (b) (1:2), (c) (3:1) and (d) (1:3). The Si substrates were located at 11 cm away from the source under 30 sccm Ar flow rate. The source was heated at 1100°C for 15 min.

It is worthy to note that ZnO nanostructures could not be obtained by heating ZnO powder without carbon powder at our experiment conditions due to the high melting point of ZnO powder (1975 °C). Less ZnO products were obtained when a small quantity of carbon powders were mixed with ZnO powders as reactants. When excess carbon powders were added into the reactants, the length of nanostructures increased significantly. This result agrees well with that of Chen *et al*. [69]. They reported that the growth rates of ZnO nanostructures become faster as the ratio of carbon increased.

As shown in Fig. 4.12 (a), the typical diameter and length of ZnO nanotetrapods are about 50–100 nm and 0.5-1 μm, respectively. According to FESEM images, the growth density of tetrapods increases as the mass ratio of carbon increased. Fig. 4.12 (b) shows ZnO tetrapods formed at ZnO:C (1:2) with tallest legs of 1.5–2 μm and they having almost the same diameter comparing to Fig. 4.12 (a). As the mass of carbon was increased to three times than ZnO mass, the length of tetrapod legs increase to 3 μm (Fig. 4.12 (d)). This indicates that the increased of carbon mass ratio appears to lengthen the tetrapods, and not to alter their diameter. In contrast, when the ratio of ZnO: C was 3:1, the morphology quality of silicon substrate was worsen. Therefore, the growth rates become slow and shapeless ZnO nanostructures were formed.

Figure 4.13 showed EDX spectra of ZnO nanostructures synthesized at different mass ZnO:C ratios. The peaks at Zn and O signals were observed indicating Zn was oxidized with O and formed zinc oxide nanostructures. Figure 4.13 (a) and (d) showed high intensities of Zn and O signals, confirming a high yield of ZnO nanostructures. The atomic ratio of Zn to O are determined to be 0.7:1 for (2:1), 1.2:1 for (3:1), 1.7:1 for (1:2) and 1:1 for (1:3) Zn:O ratios respectively. It can be seen that the atomic content of oxygen is high for the sample prepared (2:1) ZnO:C ratio, and the content is lower for samples prepared with other ZnO:C ratios. For the samples prepared with (3.1), (1:2) and (1:3) ZnO:C mass ratios, the ratio of oxygen to zinc (O/Zn) is larger than 1 and becomes closer to 1 for the sample prepared with (3:1) ZnO:C ratio.

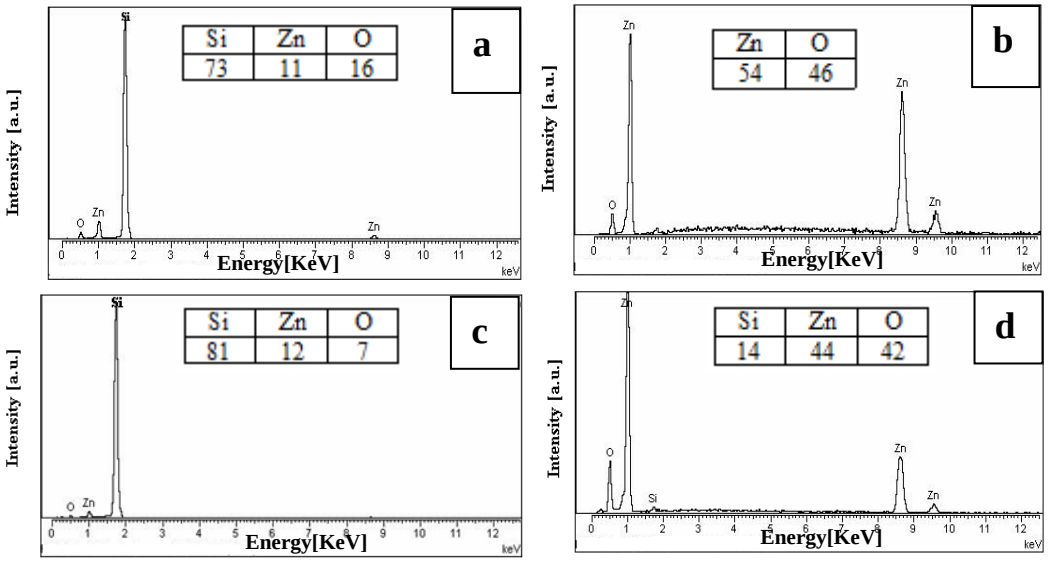

Fig. 4.13. EDX spectra of ZnO nanostructures synthesized by using (a) (2:1), (b) (1:2), (c) (3:1) and (d) (1:3) ZnO:C mass ratios. The Si substrates were located at 11 cm away from the source. Ar flow rate was 30 sccm. The source was heated at 1100°C for 15 min.

The XRD patterns of ZnO nanostructures that prepared with different mass ZnO:C ratios are illustrated in Fig. 4.14. As the mass of carbon ratio increases, the density and the crystallinity of ZnO nanostructures are improved. In addition, XRD patterns show that the ZnO (002) peaks are predominant, indicating that the preferred growth of ZnO nanostructures are in the (002) direction. The ZnO nanostructures grown at 3:1 and 2:1 ZnO:C ratios have large size of crystals. They seem to be amorphous in their structures according to XRD result. In summary, ZnO:C mass ratio is one of the key parameters for ZnO nanostructure sizes. It was found that the density ZnO nanostructures increased as the mass ratio of carbon increased. Therefore, the carbon can enhance the ZnO reduction forward resulting of a high concentration of vapor components which affect positively the ZnO growth rate.

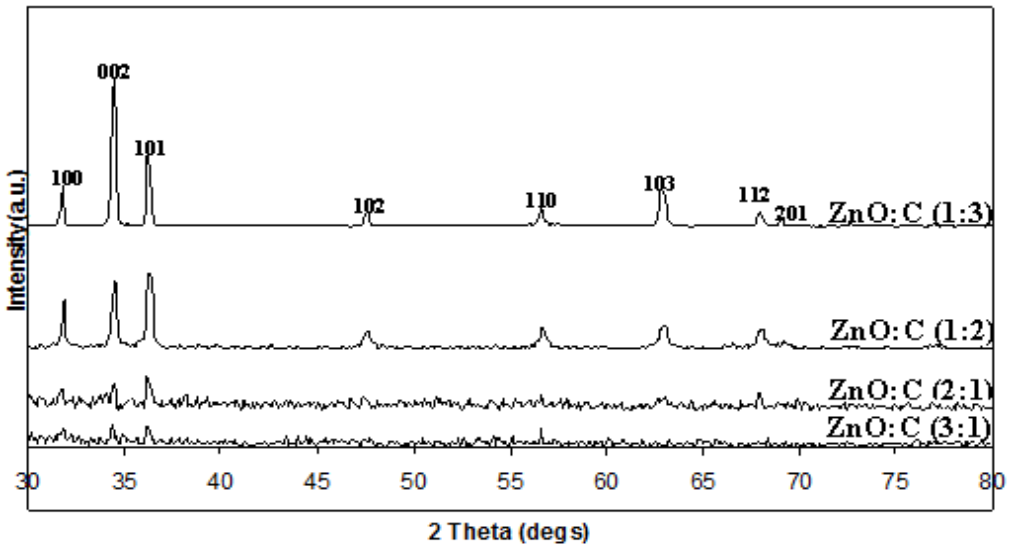

Fig. 4.14. XRD spectra of ZnO grown using different ZnO:C mass ratios. The Si substrates were located at 11 cm away from the source. Ar flow rate was 30 sccm. The source was heated at 1100°C for 15 min.

4.2.6 Summary of the growth mechanism of ZnO nanostructures

The growth of ZnO nanostructures without metal catalyst has been demonstrated by various methods. In this study, the mechanism of ZnO nanostructures formation on bare silicon substrates has been suggested to be a self–catalytic vapor–liquid–solid (VLS) process as illustrated in section 2.10.2. This mechanism works as the same as vapor–liquid–solid process except no external metal catalyst has been introduced upon the substrate, while some metal droplets that form from the chemical reaction work as self-catalyst for nanostructures propagation. Here, Zn, Zn-suboxides and ZnO work as self-catalyst for ZnO nanostructures propagation. The possible reaction process is discussed as follows. To facilitate the production of ZnO nanostructures at atmospheric pressure the growth reduction is utilized to decompose high-melting-point (1975°C) into low-melting-point. Simply, this happened when ZnO powder is mixed with graphite powders to form Zn and CO gas as illustrated in Eq. (4.1).

$$ZnO_{(solid)} + C_{(solid)} \rightarrow Zn_{(gas)} + CO_{(gas)} \quad \text{---------- 4.1}$$

As more CO gas generated from Eq. (4.1), more ZnO reacted to Zn vapor and CO_2 gas as shown in Eq. (4.2).

$$ZnO_{(solid)} + CO_{(gas)} \rightarrow Zn_{(gas)} + CO_{2\ (gas)} \quad \text{---------- 4.2}$$

However, there are three possible reactions occurred after the decomposition on ZnO:

(1) Zn and CO_2 vapors were then transported or diffused to a low temperature region (downstream of carrier gas flow), which they reacted to form ZnO droplets and CO gas which depart the tube as shown in Eq. (4.3).

$$Zn_{(gas)} + CO_{2(gas)} \rightarrow ZnO_{(\ liquid\ )} + CO_{(gas)} \quad \text{---------- 4.3}$$

(2) Zn did not oxidized completely and Zn-suboxides ZnO_X , $x < 1$ droplets were formed.

(3) A part of the unoxidized Zn vapor condensed on the substrate to form liquid droplets.

According to this study, there are some evidences which have been reported to support the carbothermal reduction and self–catalytic vapor–liquid–solid (VLS) growth mechanism. A thick black layer deposited on the inner wall of the quartz tube on downstream end had been observed and these black layers were dissolved in a diluted HCl solution. It indicates that there are plenty of Zn sources with a vapor phase and it can not be oxidized completely in the system. Moreover, Zn structures have been formed upon silicon surface as indicated in Fig 4.1 (d). These two observations gave a direct evidence to the reduction of ZnO to Zn and a part of the Zn vapor was condensed to form liquid droplets, which are the preferred sites to absorb ZnO or ZnO_X , $x < 1$ vapor species. It means that the Zn/ZnO or Zn/ZnO_X liquid droplets will be formed and ZnO nanostructures will grow from the supersaturated liquid droplets. In addition, the Zn droplets act as a reactant and a

catalyst. Using this hypothesis, the following steps were proposed for nucleation and growth of ZnO nanostructures from the carbothermal reaction according to the model sketched in Fig. 4.15. Zn vapor is produced by a reduction of ZnO powder by graphite at a high temperature (Eq. (4.1)). Then, Zn vapor is transported to the Si substrate downstream the gas flow (as shown in Fig. 4.15 (A)). As illustrated above, Zn can be oxidized to ZnO, partially oxidized to ZnO_X , $x < 1$ and non oxidized (Zn) as is transported by the carrier gas into the lower temperature zone as illustrated in Eq. (3).After that, the Zn, ZnO and ZnO_X or could be alloy of them are deposited on the surface of silicon substrate and they are formed liquid droplets (as shown in Fig. 4.15 (B)). These droplets aggregate on the surface of substrate to minimize their surface tension (as shown in Fig. 4.15 (C)). The droplets serve as the nuclei for nanostructure growth. They have the same function as gold catalyst in VLS growth. In other words, liquid droplets have a high accommodation coefficient function as a nucleation site. In addition, the droplets absorb the vapors that are generated from the carbothermal redaction. When a supersaturated solution is achieved, ZnO will crystallize and then, segregates out from the droplets at some favored sites leading to form ZnO nanostructures (as shown in Fig. 4.15 (D)). In addition, the alloy droplets become smaller and smaller, while the reaction continues, and the nanostructures are synthesized. The growth of ZnO nanostructures continues as long as appropriate quantities of CO/CO_2 and the source metal reactants are available. Finally, when the source metal is exhausted entirely, the growth terminates.

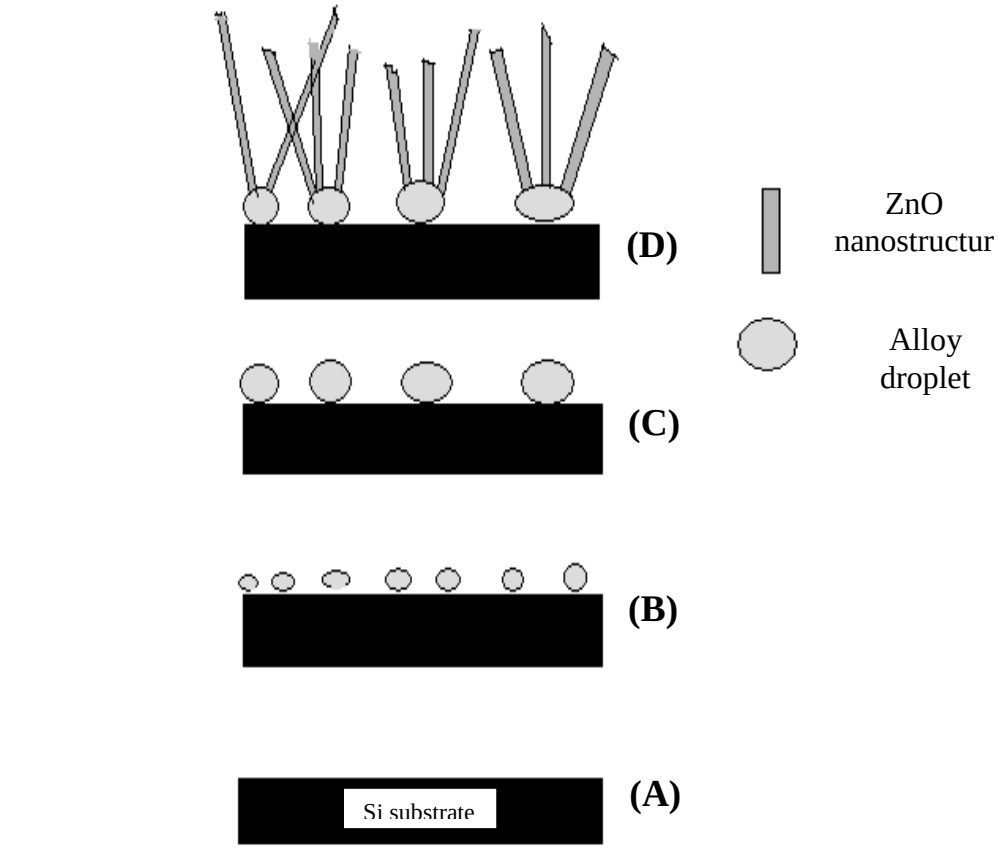

Fig. 4.15. A schematic diagram illustrated the steps for nucleation and growth of ZnO nanostructures from carbothermal reaction according to self–catalytic (VLS) process.

In this study, the growth mechanism of ZnO nanostructures from the Zn/ZnOx droplets in the light of the SEM, EDX and HRTEM results has been postulated. Based on high-resolution TEM result, no tip particles was observed at the ends of the nanostructures as shown in Fig. 4.16. In contrast, a wide base at bottom of ZnO nanostructures was observed as shown in Fig. 4.17. TEM result confirms that the alloy droplets that are worked as a self-catalytic was found at the bottom of nanostructures and this type of growth is called root growth [126].

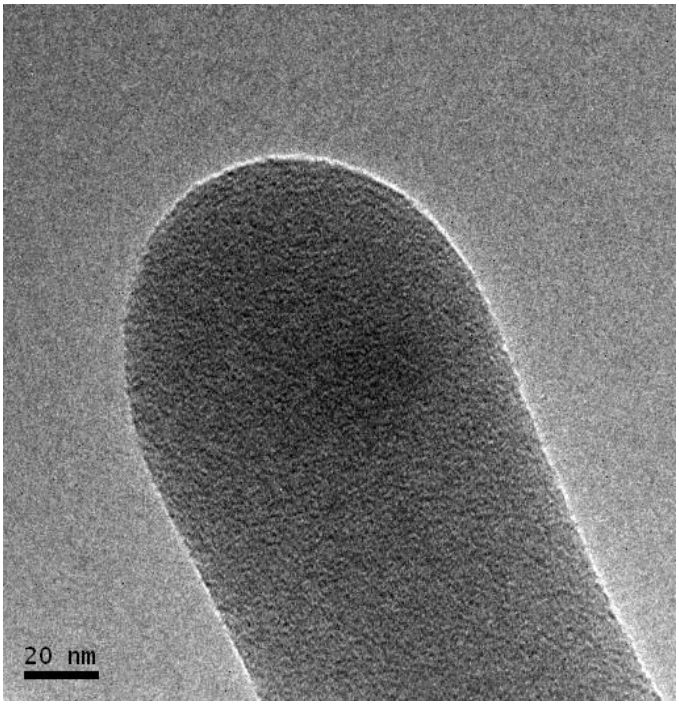

Fig. 4.16. TEM image showing that no tip particle was observed at the end of ZnO nanostructures.

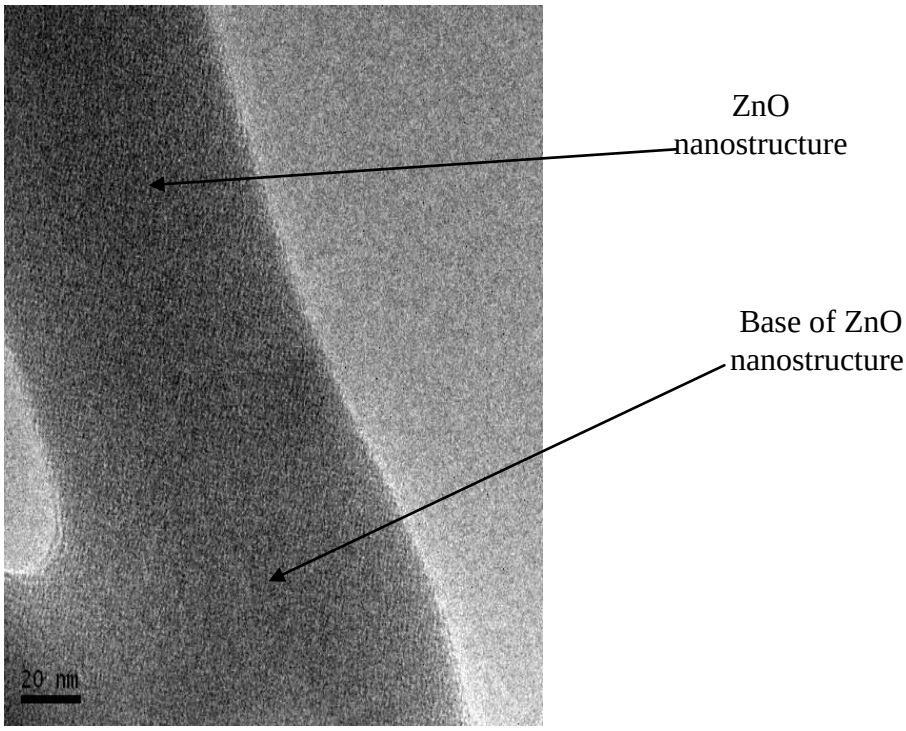

Fig. 4.17. TEM image showing that a wide base at the bottom of nanostructures was observed.

Moreover, FESEM results show more evidences for supporting the argument which that has been introduced in Fig. 4.15. Fig. 4.18 (a) and (b) show very thick clusters agglomerate on the surface of silicon substrate and EDX result indicates that these clusters are Zinc-rich. The Zinc-rich clusters were formed may be due the aggregation of alloy droplets that deposited on silicon substrate according to Fig. 4.15(C). Furthermore, Fig. 4.18 (b) shows that aligned ZnO nanowires were nucleating from the same position, while in Fig. 4.18 (d), is indicating two ZnO nanowires were also grown from the same point (demarcated by the circle). These two examples give strong evidence that these ZnO nanorods seem to be nucleated and guided through a catalyst as the same to VLS process. Since no catalyst has been used in this study, the growth mechanism of ZnO nanostructures on silicon substrate was attributed to self catalytic VLS.

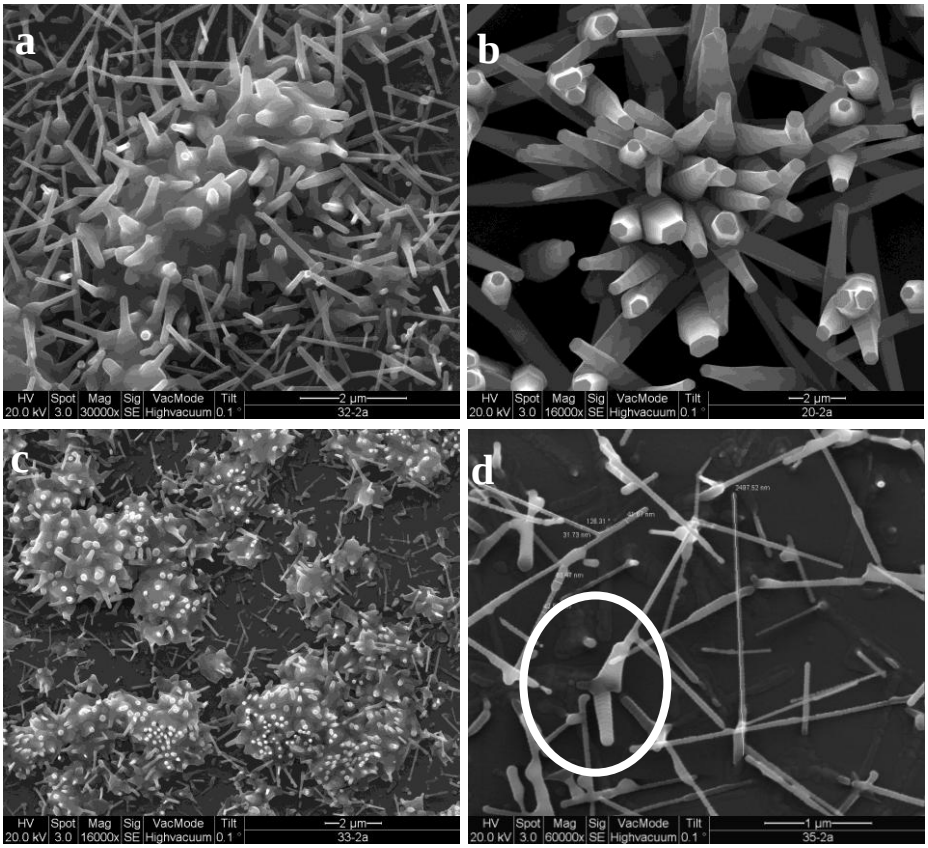

Fig. 4.18. FESEM image of ZnO nanostructures grown on silicon substrates via self catalytic VLS growth mechanism.

Interestingly, EDX result shows that the root and the stem of ZnO nanostructure are consisted of different atomic ratios of Zn. According to this result, the base of ZnO nanostructure had a Zn- rich ratio comparing to the stem as illustrated in Fig. 4.19. As result, this is also a strong evidence to support role of the Zn liquid droplet which acts as both a reactant and a catalyst during the growth process of ZnO nanostructures without using a foreign metal catalyst.

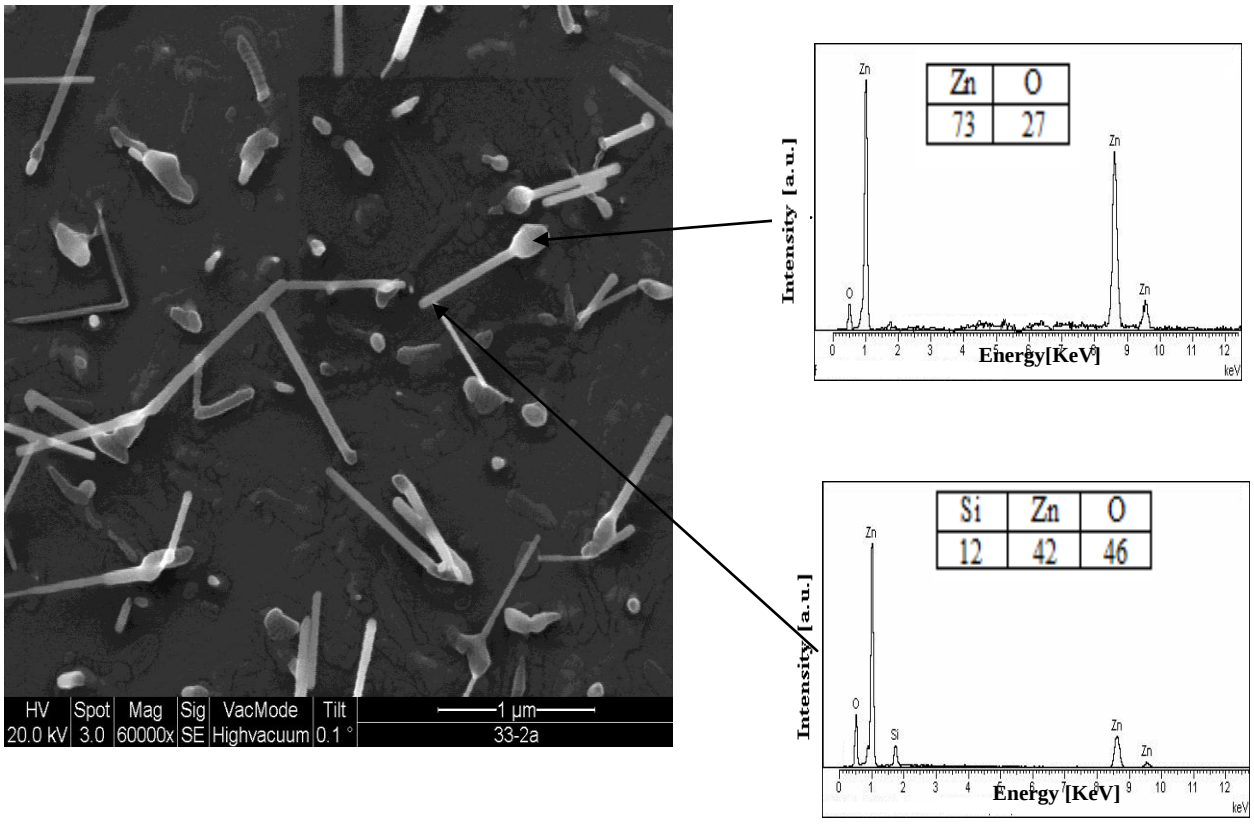

Fig. 4.19. EDX signals showing that the different components between the root and the stem of ZnO nanostructures grown on the bare silicon substrate.

4.3 Parametric study of ZnO nanostructures grown with gold as catalyst

In this section, the growth process of ZnO nanostructures using gold as acatalyst will be discussed. Gold is commonly chosen as a catalyst in ZnO nanofabrication due to its low melting point and tendency to form spherical droplets on common substrates. The growth mechanism of ZnO nanostructures assisted by gold will be explained. The effects of different parameters on the catalytic growth of ZnO nanostructures using gold as a catalyst will be presented in details.

4.3.1 Effect of gold-coated silicon substrate treatment

In order to investigate the effect of substrate treatment, two gold-coated substrates were used in ZnO nanostructure growth using the same experimental conditions (Growth temperature was 1200°C, Ar flow rate was 20 sccm, ZnO:C mass ratio was 1:1 and growth time was 60 min). One of the gold-coated substrate was pre-annealed at 700 °C for 30 min under 40 sccm Ar flow rate, whereas the other sample was introduced directly into the furnace without pre-annealing. Fig. 4.20 (a) and (b) show FESEM and EDX results for ZnO nanostructures grown with and without pre-annealed Si/Au substrates, respectively.

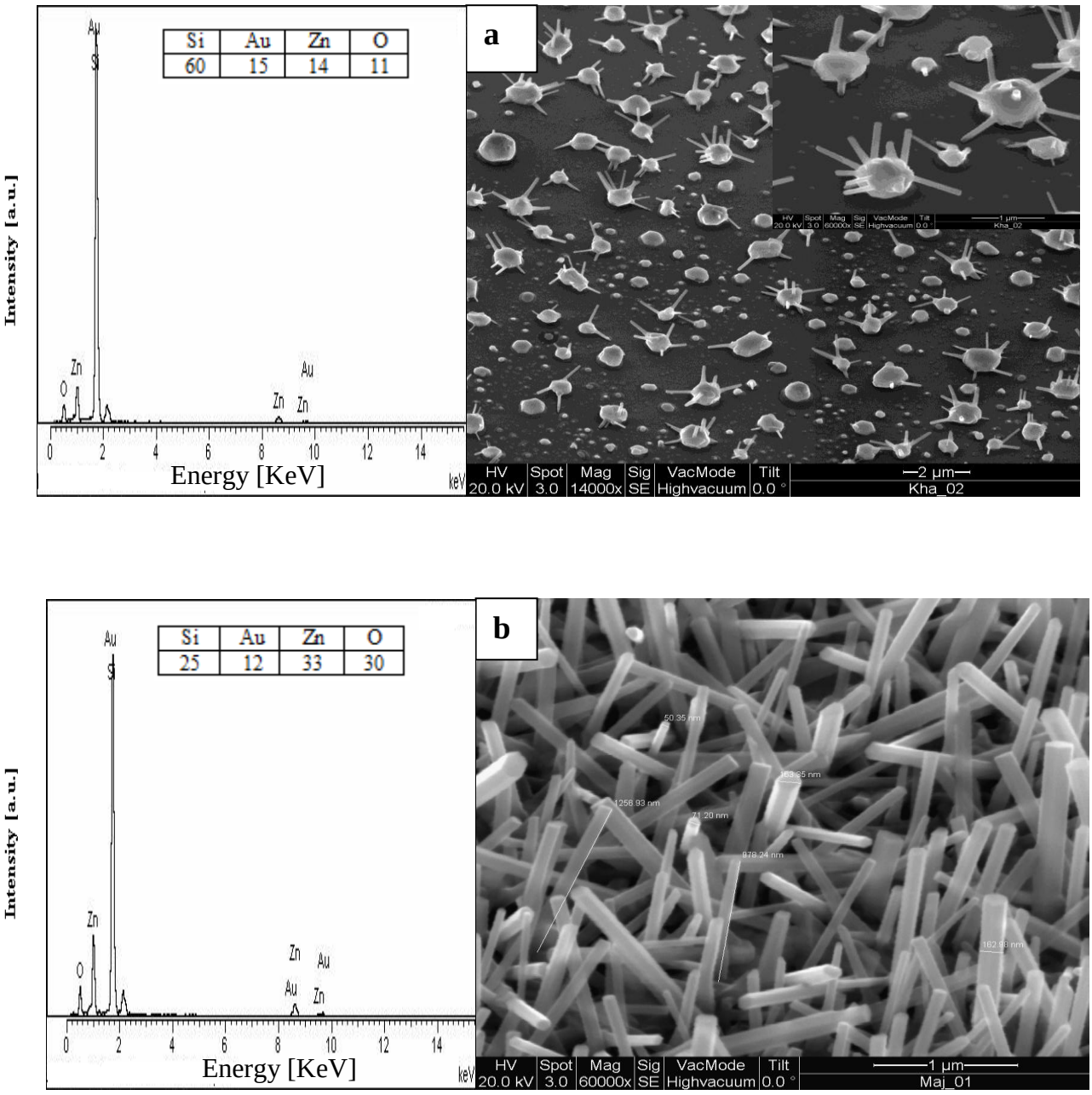

Fig. 4.20. FESEM and EDX of ZnO nanostructures grown on (a) non-annealed (b) pre-annealed Si/Au substrates (Growth temperature was 1200°C, Ar flow rate was 20 sccm, ZnO:C mass ratio was 1:1 and growth time was 60 min).

For the non-annealed substrate, FESEM image shows that the grown structures of ZnO nanomulti-wires were propagated from the spherical microstructured Au balls as illustrated in Fig. 4.20 (a). The nanowires are 1–2 μm in length and 30–100 nm in diameters. EDX spectra result confirms that the grown nanostructures are indeed those of ZnO, other peaks represent the detected Au catalyst and Si substrate materials, respectively. In addition, no defects of impurities are deducted through FESEM and EDX results. Fig. 4.20 (b), in contrast, shows FESEM image which demonstrates semi-aligned ZnO nanowires with hexagonal shapes grown upon pre-annealed Si/Au substrates. The average length and diameter of ZnO nanowires are 1–2 μm and 30–100 nm, respectively. The semi-aligned ZnO nanowires have a high growth density compared to that of nanowires grown on non pre-annealed substrate. EDX result shows that the compositions of semi-aligned nanowires are similar to those of nanomulti-wires as shown in Fig. 4.20 (a) and Fig. 4.20 (b), respectively.It can be concluded that the pre-annealing process of deposited gold film plays an important role in the increment of ZnO nanostructures growth density. Thus, the pre-annealing process reduced the agglomeration of catalyst droplets on the substrate surface. Hence, more distribution of catalyst droplets is caused by pre-annealing process, resulting in more being nanostructures formed on the surface. Fig. 4.21 illustrates FESEM image of the distribution of gold droplets on silicon substrate after annealing at 700 °C for 30 min under 40 sccm Ar gas at atmospheric pressure. The gold droplets are ranging in diameter from 20-300 nm. EDX result demonstrates that only Au and Si peaks exist and no other peaks are present as shown in Fig. 4.22.

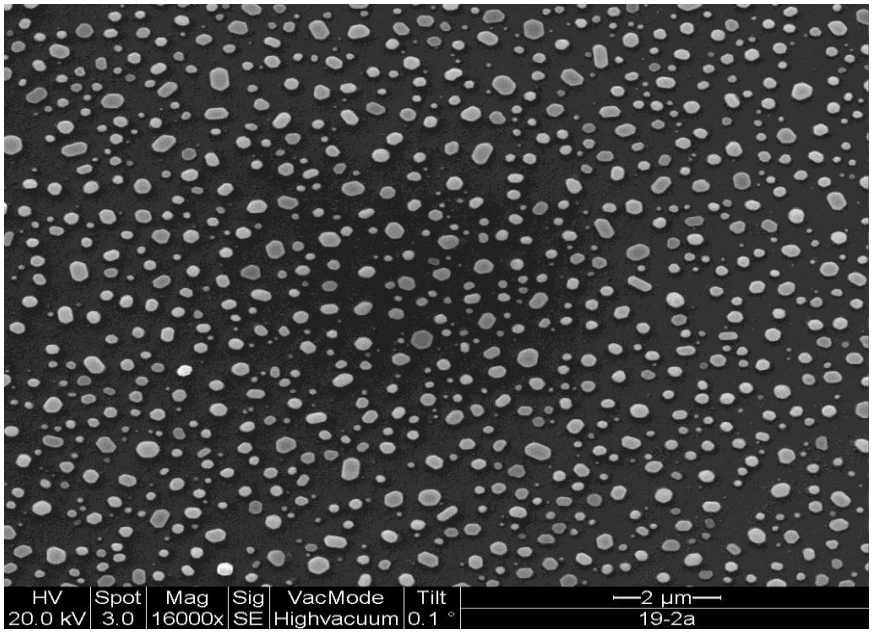

Fig. 4.21. FESEM image of the distribution of gold droplets on the silicon substrate after annealing process at 700 °C for 30 min under 40 sccm Ar gas at atmospheric pressure.

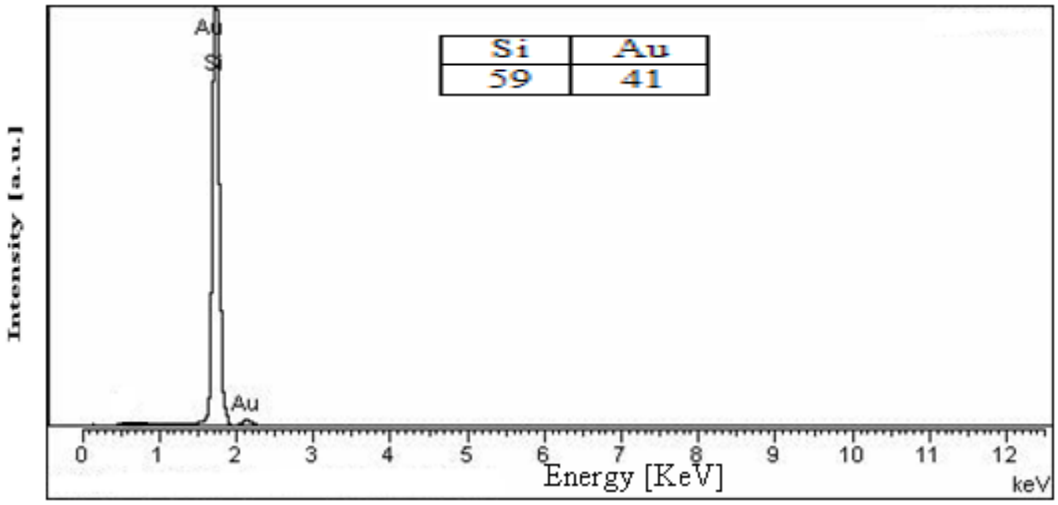

Fig. 4.22. EDX spectrum of gold droplets on silicon substrate after annealing process.

4.3.2 Effect of the location of the gold-coated silicon substrate from the source

In order to study the effect of locations of gold-coated silicon substrates during the growth process, the synthesis of ZnO nanostructures was performed at 6, 11, 15 and 19 cm downstream away from the source materials under the following conditions: 1200°C furnace temperature, 40 sccm Ar gas flow rate, 30 min deposition time and (1:1) ZnO:C mass ratio. Typical FESEM images of the ZnO products grown on the gold-coated silicon substrates are shown in Fig. 4.23.

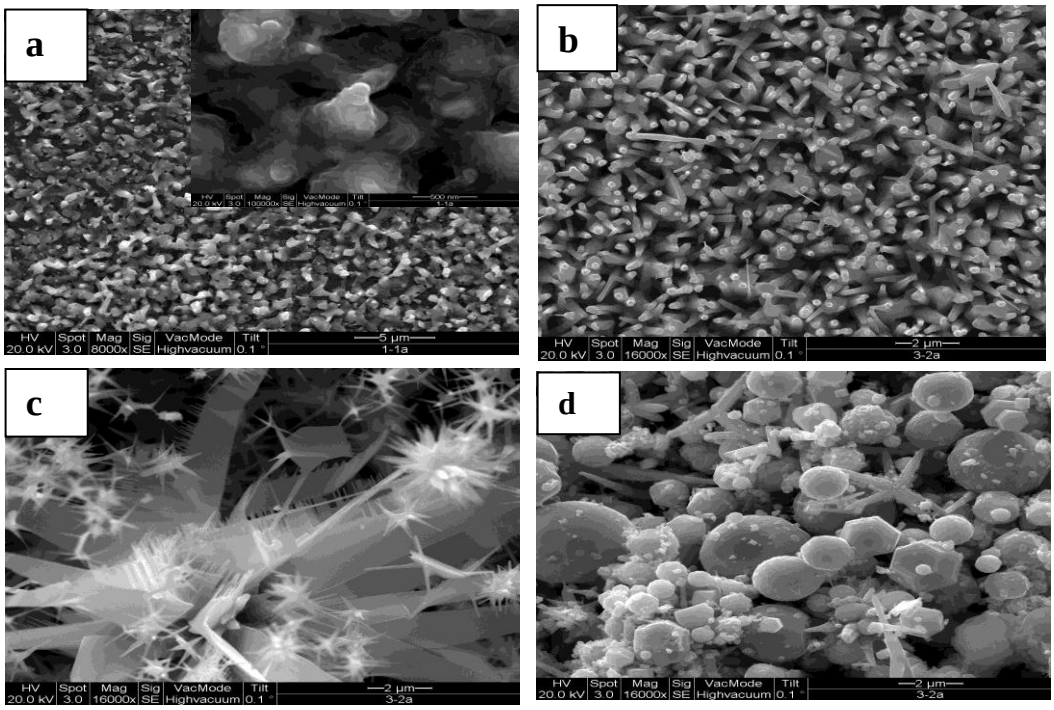

Fig. 4.23. FESEM images of ZnO nanostructures grown on gold–coated silicon substrates placed at (a) 6 cm, (b) 11 cm, (c) 15 cm and (d) 19 cm downstream of the source. The furnace temperature was 1200°C. Ar gas flow rate was 40 sccm. The deposition time was 30 min. The mass ratio of ZnO:C was (1:1).

There are different ZnO nanostructure morphologies observed in FESEM images, depending on the placed locations of the nanostructures from the reactant. As shown in Fig. 4.23 (a), when the substrate was placed at 6 cm away from the source, ZnO and Au microstructures were formed as a continuous cluster. Energy dispersed x-ray spectroscopy (EDX) (Fig. 4. 24 (a)) shows that the atomic proportion of silicon is large. This indicates that the thickness of the cluster is small. At 11 cm, aligned ZnO nanowires are observed in a large quantity. The average diameter of these nanowires is about 50 nm to 500 nm and the length is 3- 5 μm as shown in Fig. 4.23 (b). At 15 cm, the surface morphology of the nanostructures changes into plates and combs shapes with increasing substrate location as shown in Fig. 4.23 (c). The average diameter of ZnO nanoplates is 2 μm. Moreover, the usual width of the backbones of the nanocombs is about 400 nm to 1 μm, and the thickness is around 50–100 nm, while the length is up to several tens of microns. The teeth of the combs have diameters ranging from about 50 to 100 nm and length ranging from hundreds nanometers to several microns. EDX spectra in Fig. 4.24 (b) and (c) show that the atomic mass of silicon decreases as the location of the substrates is increased. This indicates that as the distance increases, more dense ZnO nanostructures are formed and this due to the diffusion rate of vapor components is increased as the substrate temperature is decreased. In the last substrate which is located 19 cm away from the source, highly dense Zn microstructures; nanocages and nanoballs, with very low ZnO nanostructures were formed as shown in Fig. 4.23 (d). This may due to the low substrate temperature, which leads to uncompleted oxidization of Zn. EDX result shows a very high atomic proportion of Zn compared to O as well as no Si peak was detected as illustrated Fig. 4.24 (d).

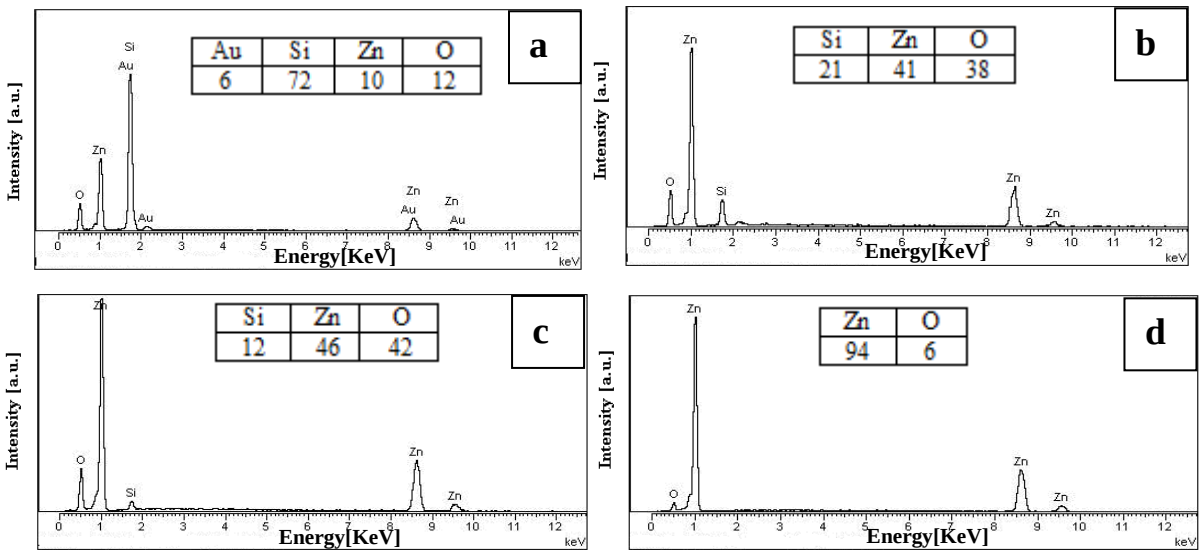

Fig. 4.24. EDX spectra of ZnO nanostructures grown on Si/Au substrates at(a) 6 cm, (b) 11 cm, (c) 15 cm, (d) 19 cm away from the source. The furnace temperature was 1200°C. Ar gas flow rate was 40 sccm. The deposition time was 30 min. The mass ratio of ZnO:C was (1:1).

In addition, the EDX results indicate that the atomic ratio of Zn:O is 0.8:1 for the sample located at 6 cm, which shows that the nanostructures are O rich. This can be attributed to the high growth temperature, which makes more oxygen absorption on the surface of ZnO nanostructures. On the other hand, EDX result (Fig. 4.24(b) and Fig. 4.24(b)) shows that the nanostructures consist of Zn and O elements at an approximate atomic ratio of 1:1, which indicates that the deposited ZnO nanostructures are stoichiometric. For ZnO nanostructures grown at 19 cm, in contrast, the ratio of oxygen to zinc (O/Zn) is 15.7:1, indicates that the grown nanostructures are mainly metallic Zn.

In order to study the atomic structures and defects of grown ZnO nanostructures on gold-coated silicon substrates, XRD analyses have been used. Fig. 4.25 shows the XRD patterns of the samples at different locations from the source.

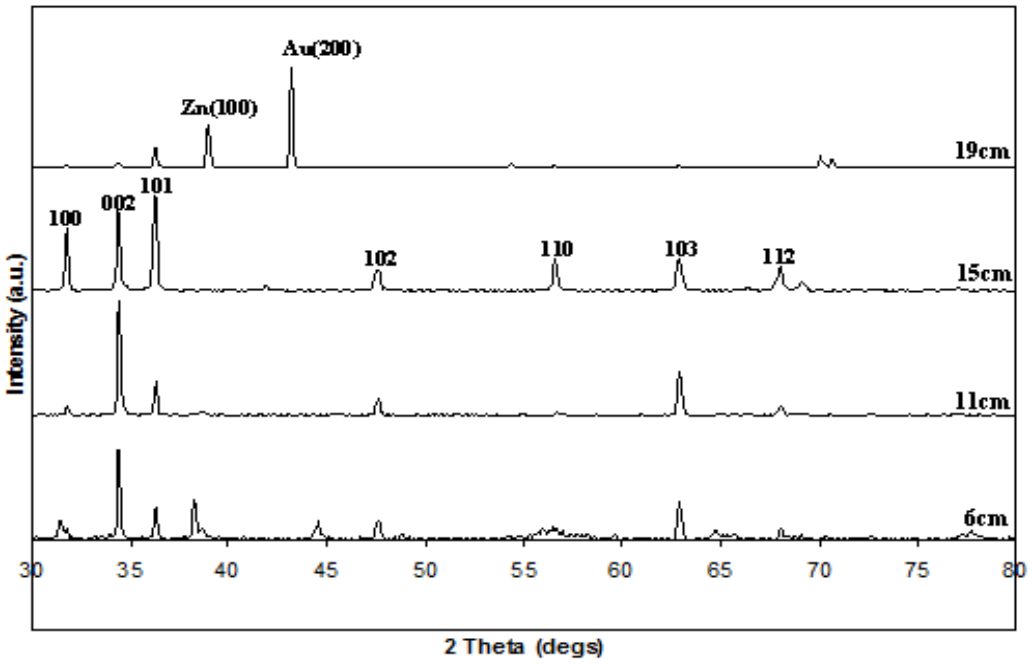

Fig. 4.25. XRD patterns of ZnO grown on the gold-coated silicon substrate at different locations from the source. The furnace temperature was 1200°C. Ar gas flow rate was 40 sccm. The deposition time was 30 min. The mass ratio of ZnO:C was (1:1).

As shown in Fig. 4.25, the XRD diffraction peaks can be assigned to (100), (002), (101), (102), (110), (103) and (112) for the standard polycrystalline ZnO structure. At substrate located at 19 cm from the source, strong Zn (100) and Au (200) diffraction peaks are observed which indicates that the prepared sample at this location is mainly composed of a great number of Zn and gold with little oxidation. It is interesting to note that the gold peak can not be detected by EDX may be due to the limitation of EDX detector. The (002) ZnO is the strongest peak observed at 6 cm and 11 cm substrate locations, which indicates that the preferred growth direction of ZnO nanostructures is perpendicular to the substrate and this result agrees well with FESEM result (Fig. 4.23(a) and Fig. 4.23(b)). For the substrate which is located at 6 cm, the wide width of ZnO diffraction peak at 2θ=56.59° indicates that the resulting products have very small sized crystals and products are amorphous. At 15 cm substrate location, the (101) peak has a slight high intensity than the other peaks, revealing that the preferred orientation of nanostructures is along (101) direction. It is noticeable that no other peaks corresponding to Zn or Au are observed on the substrate that was located at 15 cm. This reveals that ZnO grown in the Si/Au substrate is highly dense. As such, the substrate location plays an important role on the formation of ZnO nanostructures. Different morphologies for ZnO nanostructures are observed at different substrate locations. The same result was reported by Umar *et al* [72].

4.3.3 Effect of furnace temperature

A mixture of (1:1) ZnO:C powders was placed at the centre of the horizontal tube furnace set at four different source temperatures 1200°C, 1100°C, 1000°C and 950°C, respectively. The gold-coated silicon substrates were kept at 11 cm from the source. Ar gas flow rate was set at 40 sccm. The deposition time was 30 min. Fig. 4.26 shows typical FESEM images of the samples grown at different furnace temperatures while, Fig. 4.27 shows the EDX results for the same samples.

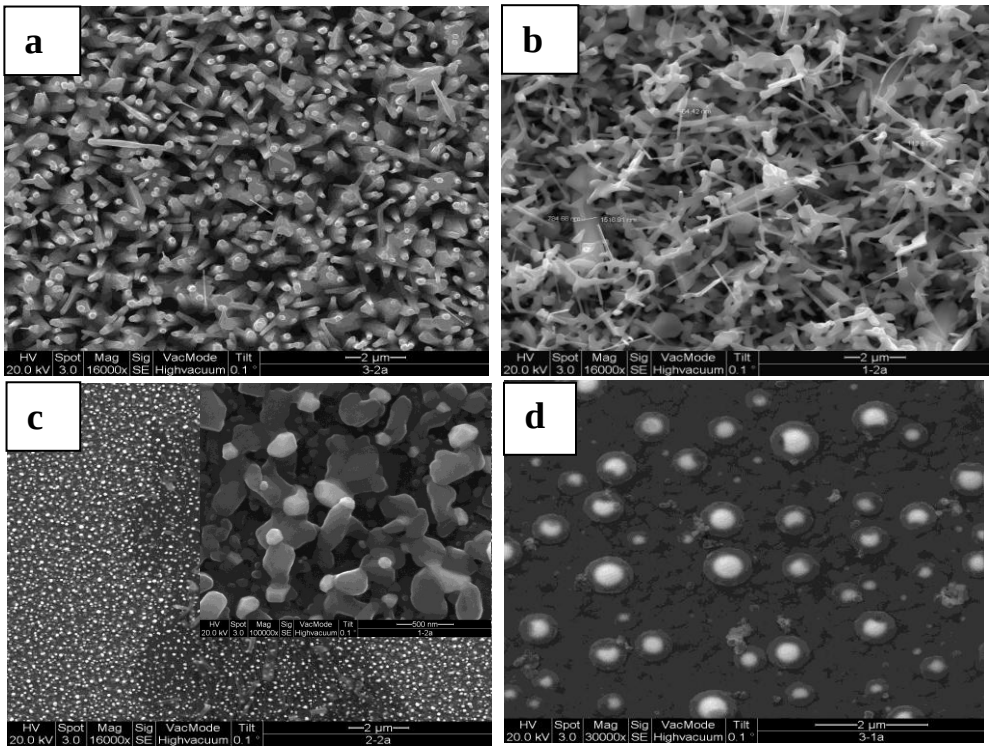

Fig. 4.26. FESEM images of ZnO nanostructures formed on gold-coated silicon substrates at (a) 1200°C, (b) 1100°C, (c) 1000°C and (d) 950°C furnace temperatures. The substrates were kept at 11 cm far from the source. Ar flow rate was 40 sccm. The deposition time was 30 min and the mass ratio of ZnO:C was 1:1.

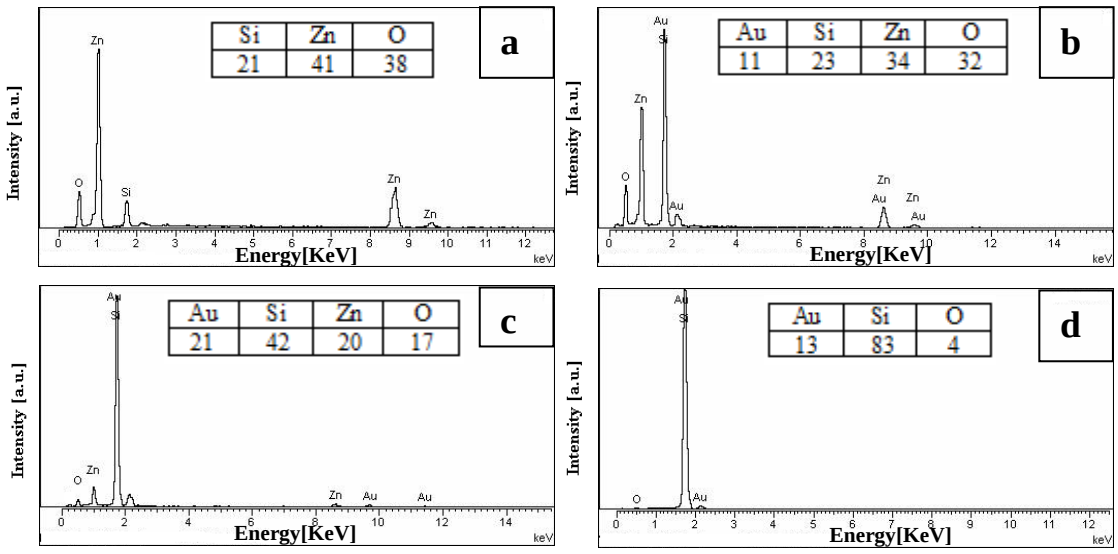

Fig.4.27. EDX spectra of ZnO nanostructures formed on gold-coated silicon substrates at (a) 1200°C, (b) 1100°C, (c) 1000°C and (d) 950°C furnace temperatures. The substrates were kept at 11 cm far from the source. Ar flow rate was 40 sccm. The deposition time was 30 min and the mass ratio of ZnO:C was 1:1.

Different morphologies of ZnO nanostructures were obtained on gold-coated silicon substrate at different furnace temperature. Aligned nanowires with 50 nm to 500 nm diameters and 3-5 μm lengths were formed on the substrate at 1200°C furnace temperature as illustrated in Fig. 4.26 (a). EDX result shows peaks of O and Zn as well as Si (from silicon substrate) as shown in Fig. 4.27 (a). This result shows a low atomic proportion of silicon element which indicates a high growth density of ZnO nanostructures. In addition, no Au signals are recorded on EDX result and this is may be due to the high density growth of ZnO nanostructures. As the furnace temperature was decreased to 1100°C, non-aligned nanowires are observed on top of the gold-coated silicon substrate as shown in Fig. 4.26 (b). The length of these nanowires is ranged from 2-4 μm with the average diameter is about 100 nm. According to EDX result (Fig. 4.27(b)), Au peak starts to appear on EDX spectrum, while Si peak is increased compared to that of the EDX spectrum of the

nanostructures grown at 1200°C furnace temperature (Fig. 4.27(a)). At 1000°C furnace temperature, very short ZnO nanowires are observed as shown in Fig. 4.26 (c). These nanowires seem as if they have just emerged from the substrate. EDX results show a very low atomic proporation of Zn and O which, confirms that a very low growth density ZnO nanostructures are formed at 1000°C furnace temperature as shown in Fig. 4.27 (c). On the other hand, no ZnO nanostructures are observed on the top of the substrate which was at 950°C furnace temperature as illustrated in Fig. 4.26 (d). EDX result shows that no Zn signals have been recorded as well as a very low proportion of O was present as shown in Fig. 4.27 (d). For samples grown at 1200°C and 1100°C furnace temperatures, EDX analyses indicate that the grown nanostructures contain Zn and O elements at an approximate atomic ratio of 1:1 demonstrating that the products are ZnO. In contrast, Fig. 4.27(c) demonstrates that ZnO nanostructures grown at 1000°C furnace temperature has an Zn:O atom ratio 1.18:1, which shows that the nanostructures are Zn rich. This may due to the low local temperature of the substrate making less oxygen being absorbed on the surface.

The XRD patterns of the deposited ZnO nanostructures on the gold-coated silicon substrates at different furnace temperatures are shown in Fig. 4.28. At 1200°C furnace temperature, all the corresponding diffraction peaks assign to the standard hexagonal wurtzite ZnO. No diffraction peaks from Zn or other impurities are found on the samples. The diffraction peak at 2θ=34.4° can be assigned to (002) of the hexagonal structure of bulk ZnO. This indicates the preferential (002) growth of ZnO on the gold-silicon substrate. Gold (111), (200) and (220) peaks are detected in the sample that was grown at 1100°C furnace temperature. According to XRD result, weak ZnO peaks are detected in the samples grown at 1000°C. In contrast, no ZnO diffraction peaks are assigned to the

nanostructures grown at 950°C source temperatures and all the peaks correspond to gold particles. As a result, the ZnO nanostructures deposited at higher source temperatures are denser than those deposited at lower substrate temperatures. This is due to the increase of the vapor pressure which is positively affected the growth of ZnO nanostructures. In addition, no growth at 950°C furnace temperature may be due to the insufficient local temperature of the substrate. In other words, the local substrate temperature was below the gold and zinc eutectic temperature, which is 684°C [113].

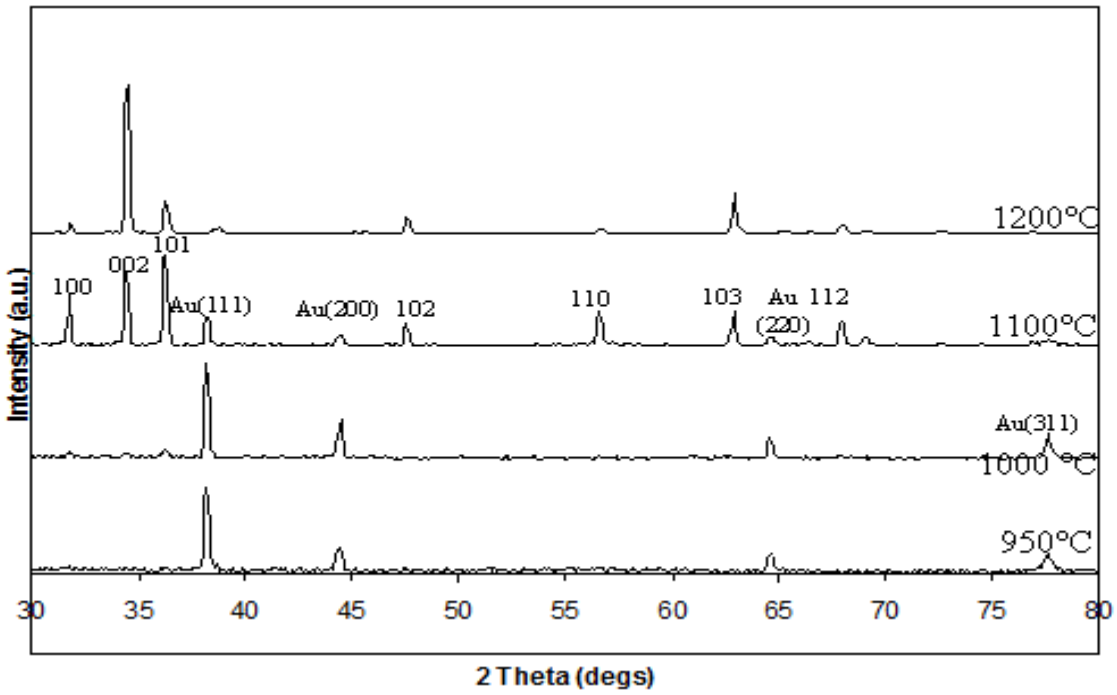

Fig. 4.28. XRD patterns of the deposited ZnO products formed on gold-coated silicon substrates at different furnace temperatures. The substrates were kept at 11 cm far from the source. Ar flow rate was 40 sccm. The deposition time was 30 min and the mass ratio of ZnO:C was 1:1.

4.3.4 Effect of Ar flow rate

The growth of ZnO nanostructures was performed under various Ar flow rates, including 10, 30, 50 and 70 sccm for substrates located at 11 cm away from the source. The source was ZnO:C (1:1) heated at 1100°C for 15 min. Fig. 4.29 shows Typical FESEM images that indicate the morphologies of ZnO nanostructures grown on gold-coated silicon substrates at different Ar flow rates. In addition, Fig. 4.30 demonstrates the EDX results of `ZnO nanostructures grown at different Ar flow rates.

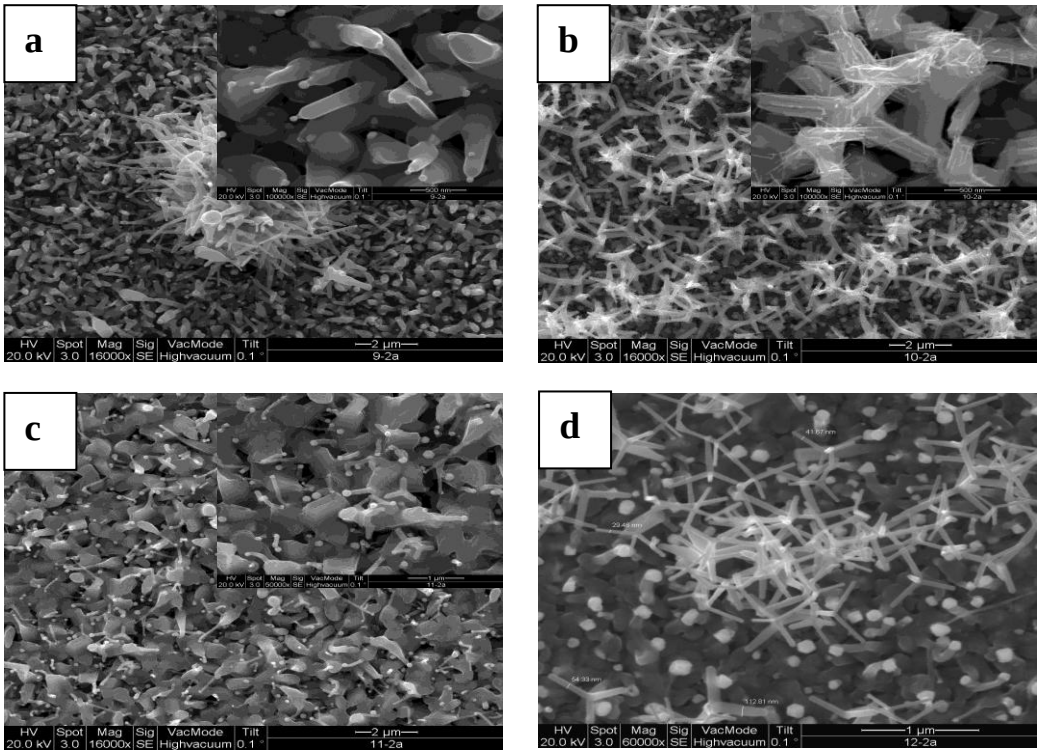

Fig. 4.29. FESEM images of ZnO nanostructures formed at on gold-coated silicon substrates at (a) 10 sccm (b) 30 sccm, (c) 50 sccm and (d) 70 sccm Ar flow rates. The substrates were located at 11 cm away from the source, which is ZnO:C (1:1) heated at 1100°C furnace temperature for 15 min.

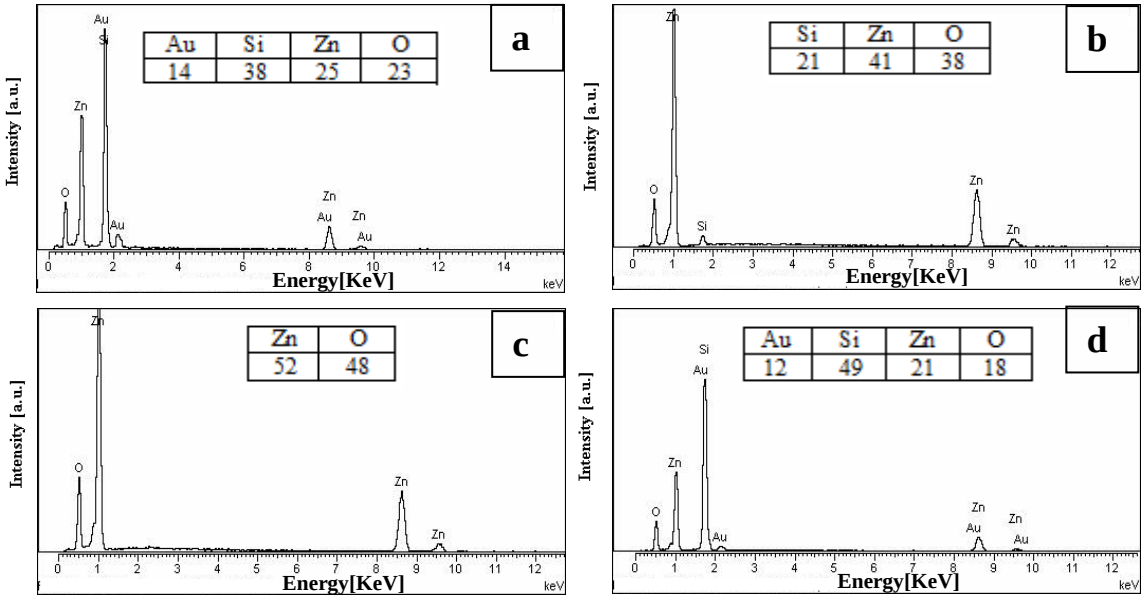

Fig. 4.30. EDX spectra of ZnO nanostructures formed on gold-coated silicon substrates at (a) 10 sccm, (b) 30 sccm, (c) 50 sccm and (d) 70 sccm Ar flow rates. The substrates were located at 11 cm away from the source, which is ZnO:C (1:1) heated at 1100°C furnace temperature for 15 min.

Obviously, all the grown samples exhibit almost the same morphology. In Fig. 4.29 (a), ZnO nanocones with end tips were formed with high density growth at 10 sccm Ar flow rate. The end tip of ZnO nanocones is consisted of solidified alloy droplet which contributed to VLS growth mechanism [99]. The typical diameter and length of nanocones are about 50–200 nm and 0.5-1 μm, respectively. EDX result shows that these nanocones are indeed ZnO. They contain Zn and O as shown in Fig. 4.30 (a). As the Ar flow rate increases from 10 to 30 sccm, the density of ZnO nanostructures increases. Si signal is suppressed in EDX spectrum for the sample grown at 30 sccm as shown in Fig. 4.30 (b). At high magnification of FESEM image, ZnO nanofibers are growing on the main body of nanostructures as shown in Fig. 4.29 (b). Fig. 4.29 (c) illustrates the sample grown at 50 sccm Ar flow rate. Semi-aligned nanowires ended with alloy tips are obtained on the top of the substrate. Noticeably, EXD result shows

that no Si peak is detected on the spectra (Fig. 4.30 (c)). As a result, these nanowires are formed with a very high growth density. This indicates that as the flow rate increases from 10 to 50 sccm, the growth densities of nanostructures were increased. However, EDX results for 10, 30 and 50 sccm Ar flow rates show that the compositions of ZnO nanostructres are roughly maintained around the stoichiometry of ZnO. As the gas flow rate increases, more vapor components are carried to the substrate hence, more ZnO nanostructures are obtained. In contrast, there are few ZnO nanostructures formed at 70 sccm Ar flow rate as demonstrated by Fig. 4.29 (d). EDX result shows that a high signal of Si is recorded for the substrate grown at 70 sccm Ar flow rate as shown in Fig. 4.30 (d). This indicates that the vapor components generated from the crabothermal reaction are carried away rapidly from the substrates at high flow rates (more than 50 sccm). In addition, EDX result for nanostructures grown at 70 sccm shows that the molar atomic ratio of Zn:O is 1.17: 1, which indicates that there is excessive zinc. This may due to the high flow rate of Ar which leads to less O existing at the substrate.

XRD patterns of the ZnO nanostructures grown at different Ar gas flow rates are illustrated in Fig. 4.31. Weak gold peaks are detected on the samples grown at 10, 30 and 50 sccm flow rates. The diffraction peak at 2θ=34.4° can be assigned to (002) hexagonal structure of bulk ZnO. This indicates the preferential (002) growth of ZnO on the gold-silicon substrate at 10 and 50 sccm flow rate. On the other hand, XRD spectrum of 30 sccm flow rate sample exhibits high intensities of ZnO diffraction peaks. This gives good evidence to the increase a growth density of the ZnO nanostructures. It is clear that the sample grown at 70 sccm shows a low growth density of ZnO nanostructures because of the high intensities of gold peaks and weak intensities of ZnO peaks are detected in the XRD result. In addition, ZnO diffraction peak at 2θ=56.59° is too broad which shows that the

grown nanostructures have inferior crystal structure. As a result, XRD results agree well with the FESEM and EDX results.

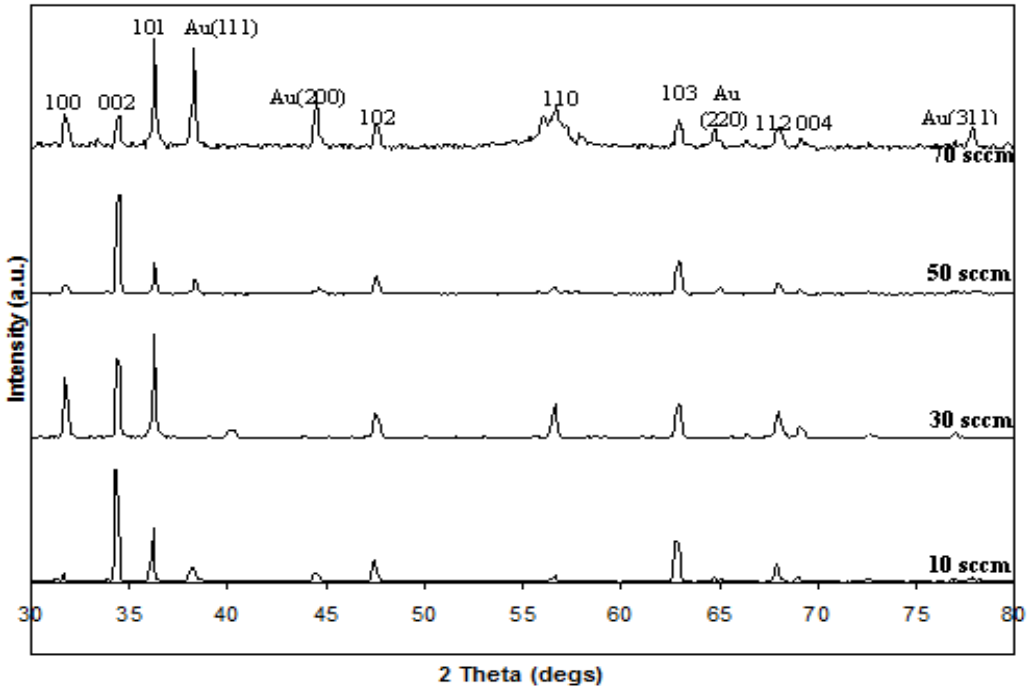

Fig. 4.31. XRD patterns of the different ZnO nanostructures formed on gold-coated silicon substrates at different Ar gas flow rates. The substrates were located at 11 cm away from the source, which is ZnO:C (1:1) heated at 1100°C furnace temperature for 15 min.

4.3.5 Effect of deposition time

The deposition time was varied to study its effect on ZnO formations. The gold-coated silicon substrates are placed 11 cm away from the source material. The deposition time was varied as 15, 30, 45 and 60 min, respectively. The ZnO:C mass ratio, Ar flow rate and furnace temperature are set at 1:1, 40 Ar flow rate sccm and 1100°C. Representative FESEM images and EDX results of the synthesized ZnO nanostructures at different deposition time are shown in Fig. 4.32 and Fig. 4.33, respectively.

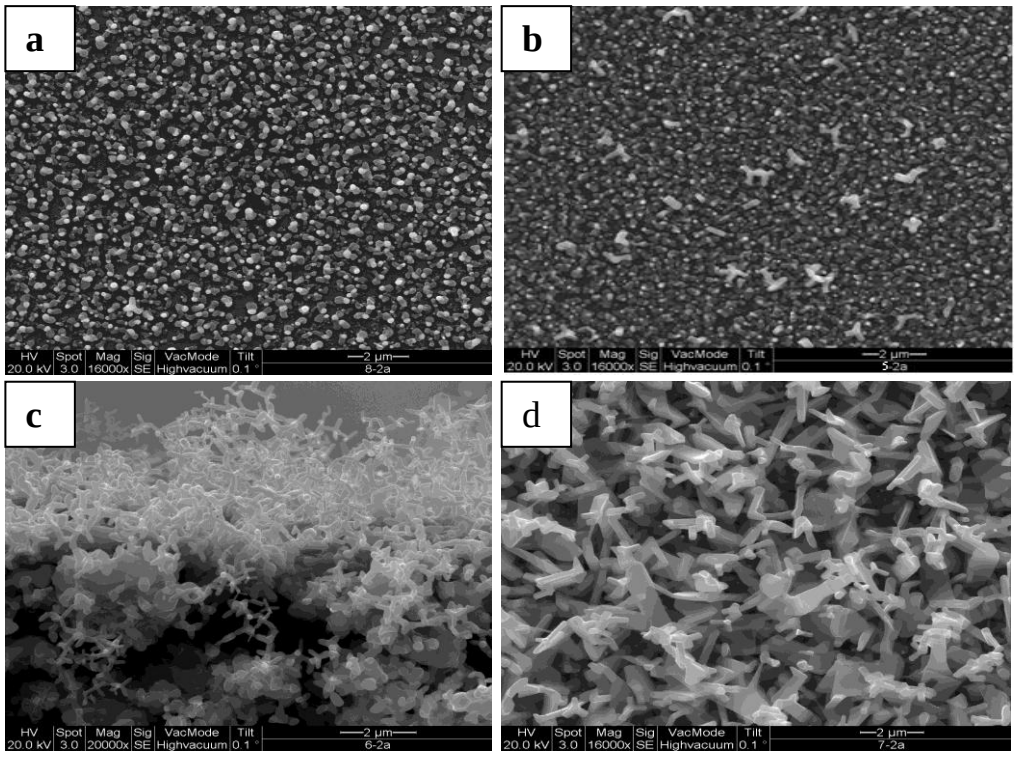

Fig. 4.32. FESEM images of ZnO nanostructures formed on gold-coated Si substrates with different (a) 15 min, (b) 30 min, (c) 45 min and (d) 60 min deposition times. The substrates were located at 11 cm away from the source, which is ZnO:C (1:1) heated at 1100°C under 40 sccm Ar flow rate.

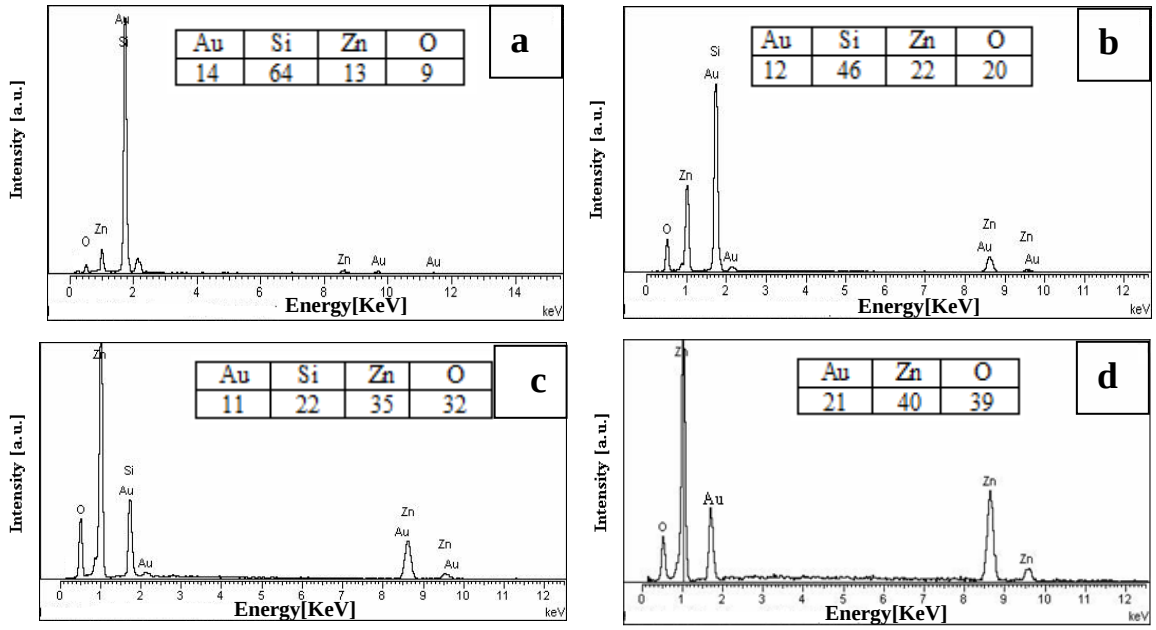

Fig. 4.33. EDX spectra of ZnO nanostructures formed on gold-coated Si substrates with different (a) 15 min, (b) 30 min, (c) 45 min and (d) 60 min deposition times. The substrates were located at 11 cm away from the source, which is ZnO:C (1:1) heated at 1100°C under 40 sccm Ar flow rate.

As shown in Fig. 4.32 (a), very short ZnO nanowires are obtained for the sample with 15 min deposition time. These nanowires are almost identical in the length and they grow in one direction. The EDX spectrum of the sample grown with 15 min deposition time is shown in Fig. 4.33 (a). The peaks are assigned to Zn, O, Au and Si, while no trace of other impurities can be seen in the EDX spectrum. The contents of Zn and O are low compared to Si and Au, which indicate that the grown nanowires have just formed and they are short. As deposition time increases to 30 min, longer ZnO nanowireswere are formed. These ZnO nanowires are similar in shape to the nanowires obtained with 15 min deposition time but, they have longer stems. In addition, these nanowires are appeared with ended cap or tip as shown in Fig. 4.32 (b). EDX spectrum (Fig. 4.33 (a)) confirms that the

atomic proportion of Zn and O elements is increased while, the atomic proportion of Si and Au is decreased compared to that of the ZnO nanostructures grown with 15 min deposition time. This result shows that as deposition time increases from 15 to 30 min, the growth density of ZnO nanowires is increased dramatically. A high yield of ZnO nanostructures are obtained in the sample grown with 45 min deposition time as illustrated in Fig. 4.32 (c). EDX investigation also reveals of ZnO nanostructures increased for the sample prepares with 45 min deposition time as shown Fig. 4.33 (c). Transformation of ZnO nanostructure shapes from nanowires to nanoplates and nanosheets occurrs for the sample with 60 min deposition time as illustrated in Fig. 4.32 (d). The average diameter of nanosheet is 800 nm. Fig. 4.33 (d) shows the typical EDX spectrum of the ZnO nanosheets grown with 60 min deposition time. Remarkably, there is no Si signal detected on the EDX spectrum. This reveals a very high growth density for nanosheets formed on Si/Au substrate with 60 min deposition time. For all the grown samples, the ratio of oxygen to zinc (O/Zn) is larger than 1 and this ratio becomes closer to 1 for the nanostructures grown with longer deposition time resulting in better crystallinity.

Fig. 4.34 shows the typical XRD patterns for all the samples grown at different deposition times. According to XRD result, all the samples grown have almost the same XRD patterns which are consisted of ZnO and gold catalyst peaks. As deposition time is increased more than 30 min, the ZnO nanostructures started to grow randomly. This is can be clearly seen from the multiple ZnO peaks appear in XRD patterns for the samples grown with 45 and 60 min deposition times, respectively. As a result, the density of the ZnO nanostructures is increased with the deposition time due to the increase of vapor components that is carried by the Ar carrier gas to the gold-coated silicon substrates.

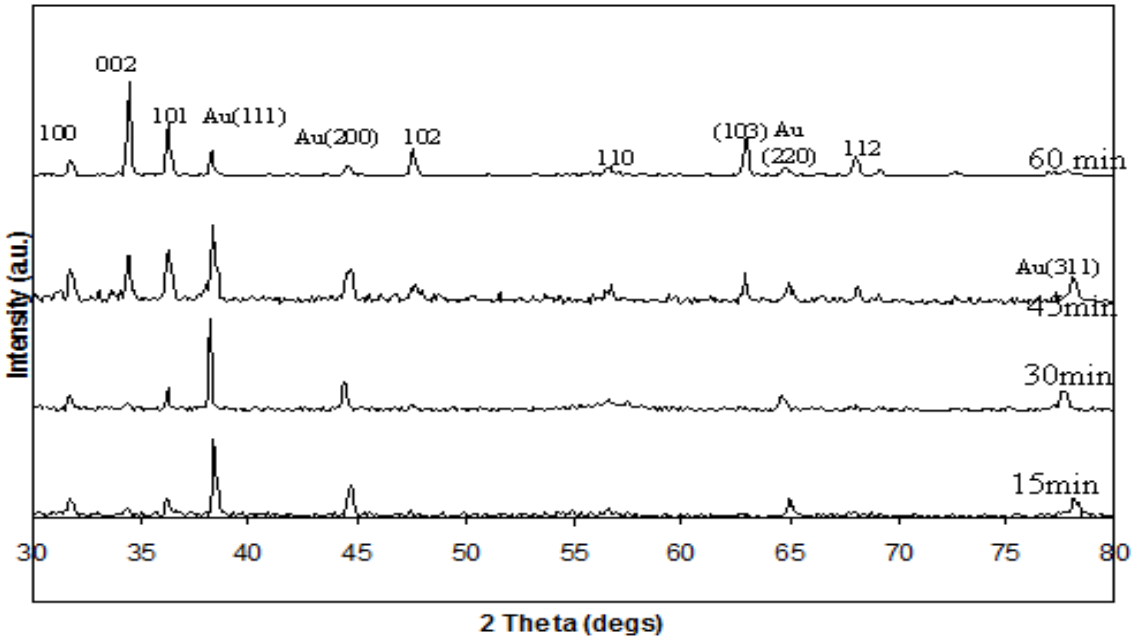

Fig. 4.34. XRD patterns of ZnO nanostructures grown with different deposition times on the gold-coated silicon substrates. The substrates were located at 11 cm away from the source, which is ZnO:C (1:1) heated at 1100°C under 40 sccm Ar flow rate.

4.3.6 Effect of ZnO:C mass ratio

To study the effects of the ZnO:C mass ratio, the mass ratio was varied from (1:1) to (2:1), (1:2), (3:1) and (1:3). The Ar flow rate was 30 sccm and the furnace temperature was fixed at 1100°C. The substrate was located at 11 cm from the source. The deposition time was kept constant 15 min during the growth process. The general morphologies of the fabricated ZnO nanostructures with different ZnO:C mass ratios are shown in Fig. 4.35. Furthermore, EDX results of the grown ZnO nanostructures with different Zn:C mass ratios are shown in Fig. 4.36.

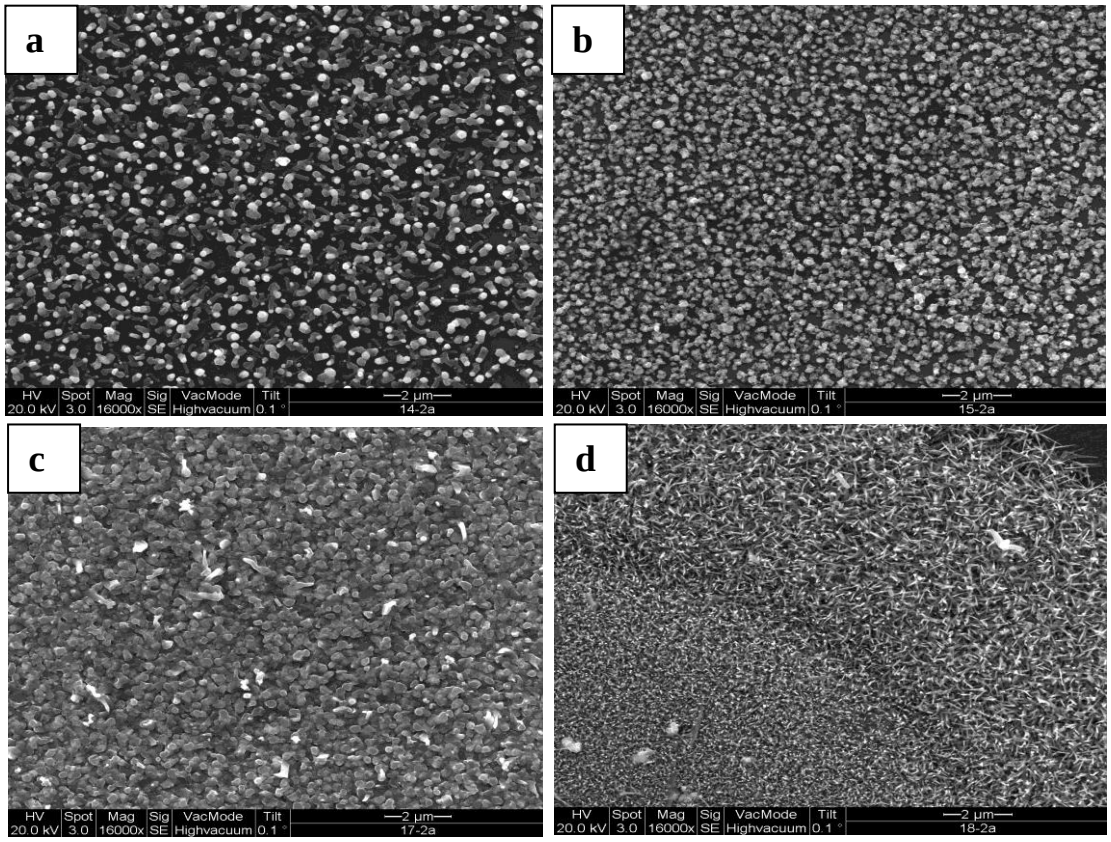

Fig. 4.35. FESEM images of ZnO nanostructures obtained from the ZnO:C source ratios of (a) (2:1), (b) (3:1), (c) (1:2) and (d) (1:3). The gold-coated silicon substrates were located at 11 cm away from the source under 30 sccm Ar flow rate. The source was heated at 1100°C for 15 min.

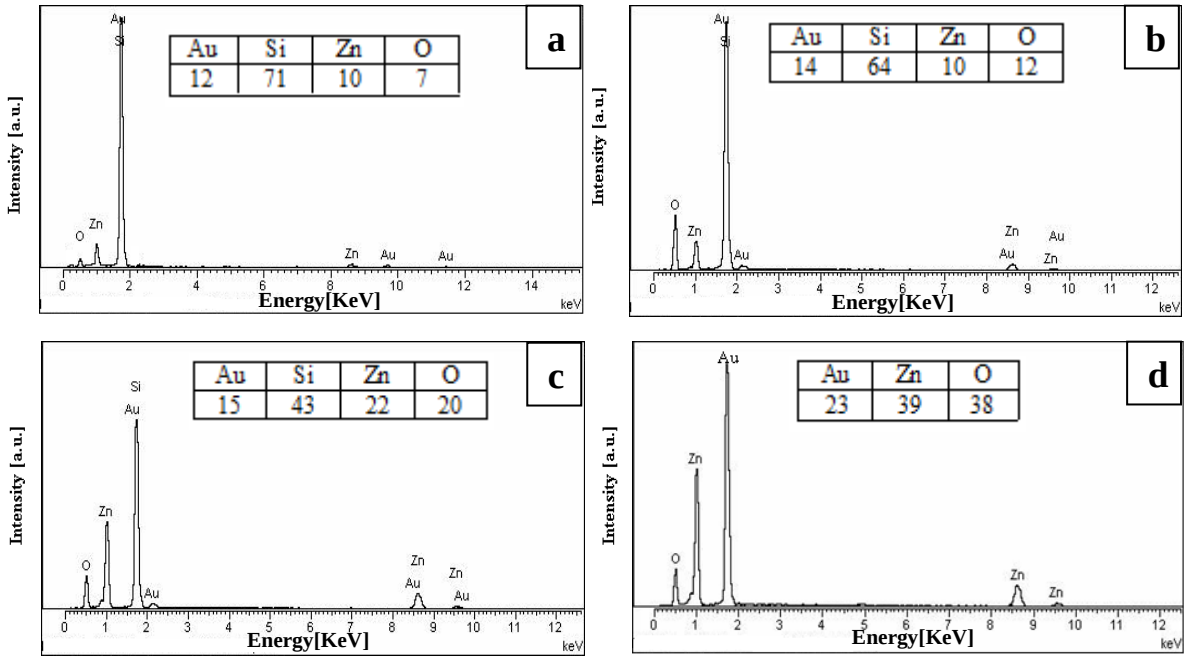

Fig. 4.36. EDX spectra of ZnO nanostructures formed by using (a) (2:1), (b) (3:1), (c) (1:2) and (d) (1:3) ZnO:C mass ratios. The gold-coated silicon substrates were located at 11 cm away from the source under 30 sccm Ar flow rate. The source was heated at 1100°C for 15 min.

Lower ZnO nanostructures density is obtained when a small quantity of carbon powders are mixed with ZnO powders as reactants, when excess carbon powders are added into the reactants, the density of nanostructures is increased. According to FESEM results, there is a slight change on ZnO morphology when ZnO:C mass ratio was altered from 2:1 (Fig. 4.35 (a)) to 3:1 (Fig. 4.35 (b)). EDX results agree well with FESEM results via the slightly change on the atomic components of Zn and O as ZnO:C mass ratio increases from 2:1 (Fig. 4.36 (a)) to 3:1 (Fig 4.36 (b)). In contrast, there is a significant change in the ZnO nanostructure morphologies as the ZnO:C mass ratio is increased from 1:2 (Fig. 4.35 (c)) to 3:1 (Fig. 4.35 (d)). According to EDX results, no Si signals are detected when the mass ratio of the carbon is three times more than the mass ratio of ZnO (Fig. 4.35 (d)) comparing to (1:2) ZnO:C mass ratio (Fig. 4.35 (c)). The EDX results show that when the

carbon mass is higher than the ZnO mass, the atomic ratio of Zn and O elements is an approximate of 1:1. As a result, carbon mass ratios enhance the growth rate as well as the growth density of ZnO nanostructures.

Fig. 4.37 shows XRD patterns of the ZnO nanostructures grown on gold-coated Si substrates at different ZnO:C mass ratios. There are strong gold peaks and weak diffraction peaks of ZnO when the mass ratios of ZnO:C are (2:1), (1:2) and (3.1) confirming a low growth yield of ZnO nanostructures. In contrast, the best crystal structures of ZnO is obtained with (1:3) ZnO:C mass ratio. The big size of the (002) ZnO diffraction peak indicates that most of ZnO nanostructures are preferred to grow in a aligned direction which is perpendicular to the substrate surface.

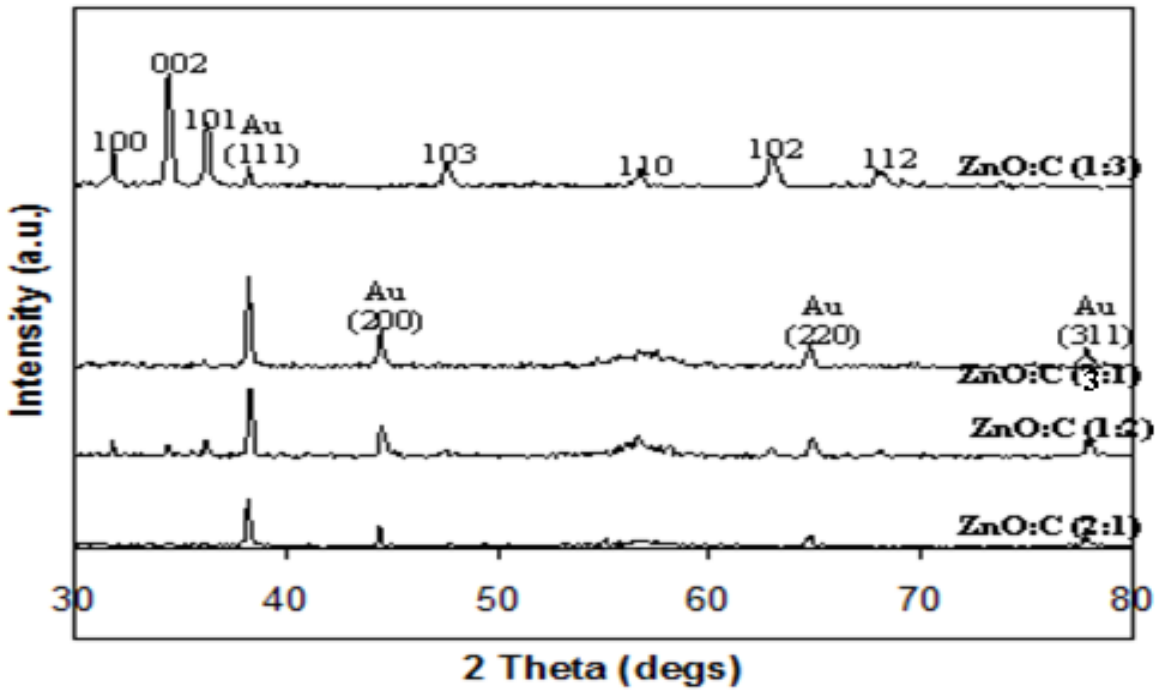

Fig. 4.37. XRD patterns of ZnO nanostructures formed at different ZnO:C mass ratios. The gold-coated silicon substrates were located at 11 cm away from the source under 30 sccm Ar flow rate. The source was heated at 1100°C for 15 min.

4.3.7 Mechanism of ZnO nanostructure growth

The growth mechanism of ZnO nanostructures with gold as a catalyst is not fully understood, however there are numerous models that have been suggested for catalytic ZnO nanostructures growth. Vapor–liquid–solid (VLS) mechanism is a well-known model that explains the growth of ZnO nanostructures via external metal catalyst as it was explained in section 2.10.1. According to VLS mechanism, when the temperature of the furnace has reached the melting point of the thin gold film, the gold film starts to melt and form large quantity of melting liquid droplets with size close to that of the original solid metal particles as shown in the model sketched in Fig. 4.38 (a) and (b). Subsequently, as the vapor components in the inlet flow, which are generated from the carbothermal reaction, are absorbed by the melting gold droplets resulting in Zn/Au droplets. These droplets serve as the nuclei for the ZnO nanostructure growth as shown in Fig. 4.38 (c). The absorption of the vapors is continued until the supersaturation of the droplet is occurred. Then, the ZnO nuclei are segregated out from the droplets at substrate/droplet interference and growth of ZnO nanostructures is starting as shown in Fig. 4.38 (d). The growth of ZnO nanostructures continues as long as the appropriate quantities of the source metal reactants are available and the gold catalyst is still active. In other words, the temperature of Zn/Au alloy is above the eutectic temperature of Zn-Au (684°C). Finally, as the growth of ZnO nanostructures is terminated, Zn/Au droplets are solidified at the end of nanostructures formed as a cap or a tip as demonstrated in Fig. 4.38 (e).

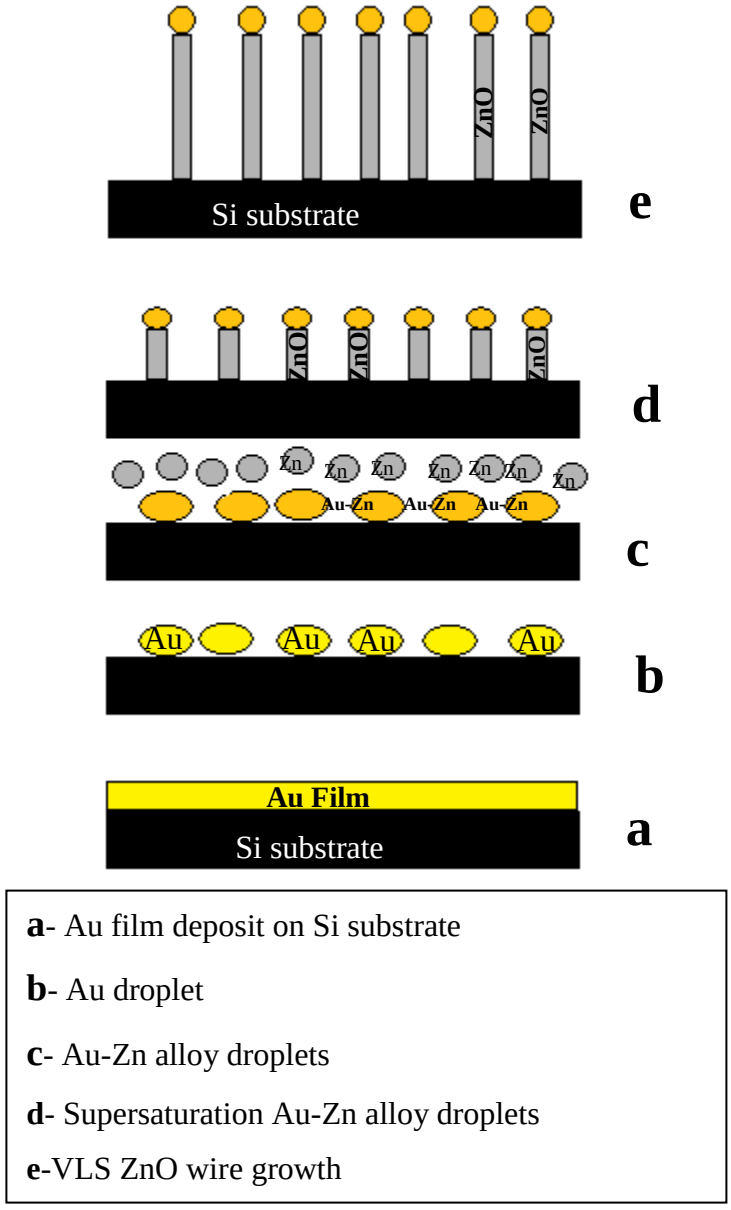

Fig. 4.38. A schematic diagram illustrated the steps of the nucleation and the growth of ZnO nanostructures using gold as catalyst according VLS process.

According to this study, the above steps of VLS process have been traced during the formation of ZnO nanostructures. The best method to elaborate the functions of the gold catalyst is the observation during the growth process. The gold droplets (appear white in the image) have just started to dissolve the vapor components at short growth time (5min) as shown in Fig. 4.39 (a). The tendency of gold droplets to attract the vapor components is attributed to the high accommodation coefficient (sticking coefficient). The circle shape is indicats one of the ZnO nanowires just emerged from the gold droplet. As growth time increases to 15 min, more ZnO nanowires have emerged from the gold droplets and all the grown nanowires ended with tips as shown in Fig. 4.39 (b). The observed nanowires have only grown from Au droplet, while no growth is observed at the black area of the silicon substrate. Fig. 4.39 (b) shows an example of the growth mechanism of ZnO nanowire. EDX spectra of two different spots of the FESEM for one ZnO wire are shown in Fig. 4.39 (c). At the end wire, EDX reveals Zn, O, Si and Au peaks. Si peak is attributed to the background signal of the substrate while Au signals reveal the presence of gold particles at the wire tip. On the other hand, the second EDX spot is focused on the black area shows only one peak which is corresponding to the silicon substrate. According to FESEM and EDX results, the gold droplet plays a key role on the growth mechanism of ZnO nanostructures. In other words, gold droplet triggers and guids the growth of ZnO nanostructures. It is worthy to report that the diameter of the grown ZnO nanostructures is not constant during the growth process. The diameter is fluctuated during growth process as illustrated in Fig. 4.40. As long as the catalyst droplets and vapor components are present during growth, the sidewalls of nanostructures remain stable and smooth but, once the gold droplet is consumed through the migration process [127] or the carbothermal reaction is stopped, the growth rate is terminated (Fig 4.40 (a)). The growth rate is overcome by a

direct transverse growth on sidewalls and often dramatically altering nanostructures geometry.

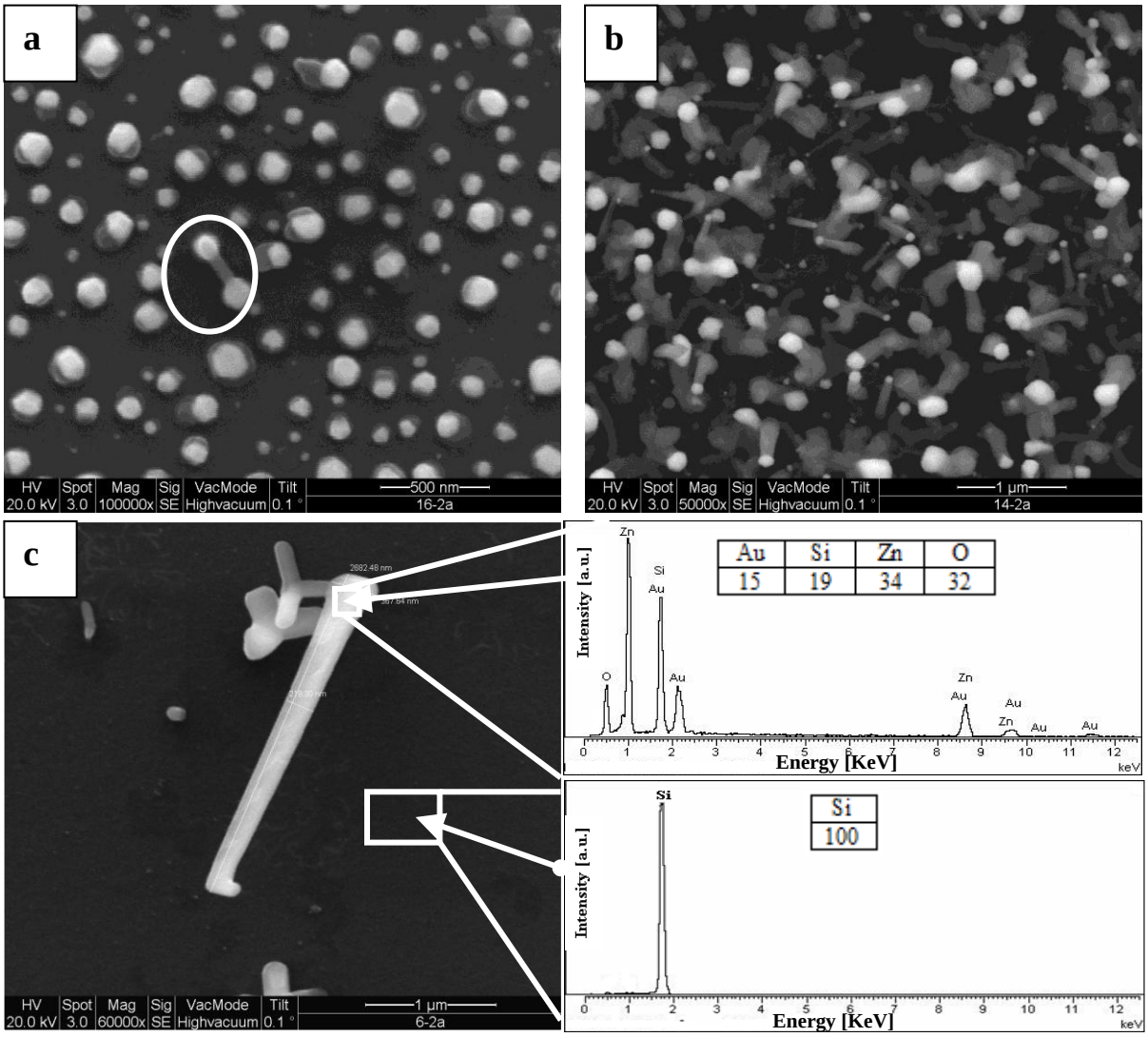

Fig. 4.39. FESEM and EDX results that prove the growth of ZnO nanostructures is triggered and guided via the gold catalyst. The gold-coated silicon substrates were located at 11 cm away from the source under 20 sccm Ar flow rate. The source ZnO:C was (1:1) and heated at 1200°C for (a) 5 min and (b) 15 min.

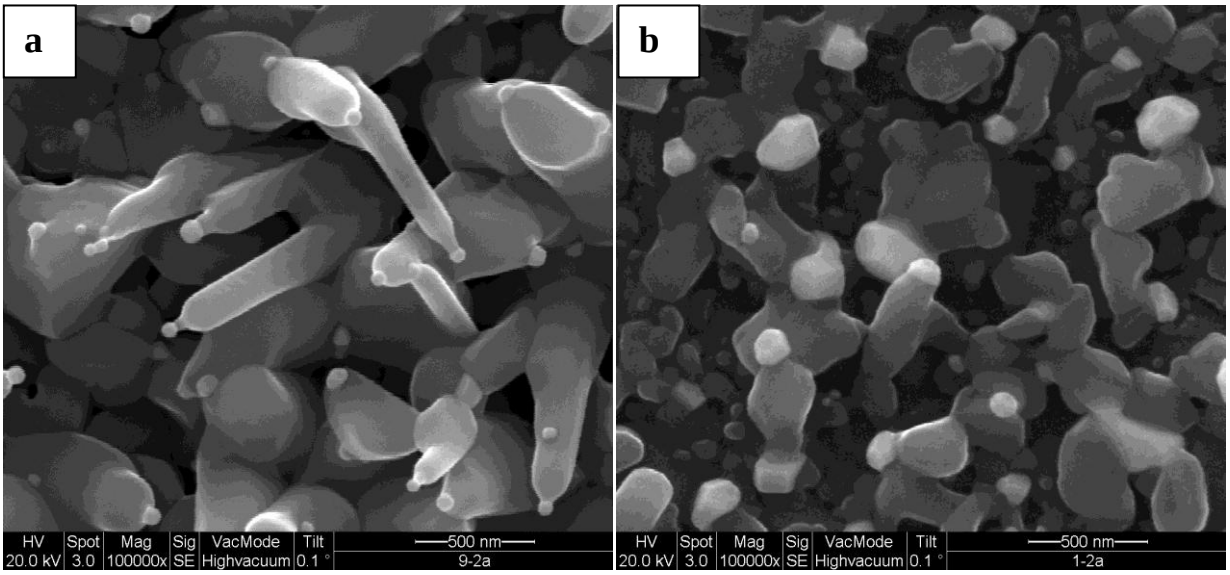

Fig. 4.40. FESEM images of ZnO nanowires with varying diameters during the growth process. The gold-coated silicon substrates were located at 11 cm away from the source under 10 sccm Ar flow rate. The source of ZnO:C was (1:1) and was heated at 1100°C for 15 min.

4.4 Comparative study between ZnO nanostructures grown without and with Au catalyst

The morphologies of the ZnO nanostructures with catalyst-free and with Au as catalyst are different. Fig. 4.41 (a) and (b) show FESEM images of ZnO nanowires grown on bare and gold-coated silicon substrates at same growth conditions (The growth temperature was 1200°C, the substrate location was 11 cm, Ar flow rate was 40sccm, growth time was 30 min and ZnO:C mass ratio was 1:1). The hexagonal wurtzite structured ZnO nanowires are obtained on both types of the substrates. These ZnO nanowires grow with a preferred orientation in *c*-axis along the substrates. According to FESEM images, the growth density of ZnO nanostructures grown on gold-coated silicon substrate is much higher than that grown on bare silicon substrate. It is obvious that the catalyst plays an important role on the growth density of ZnO nanostructures.

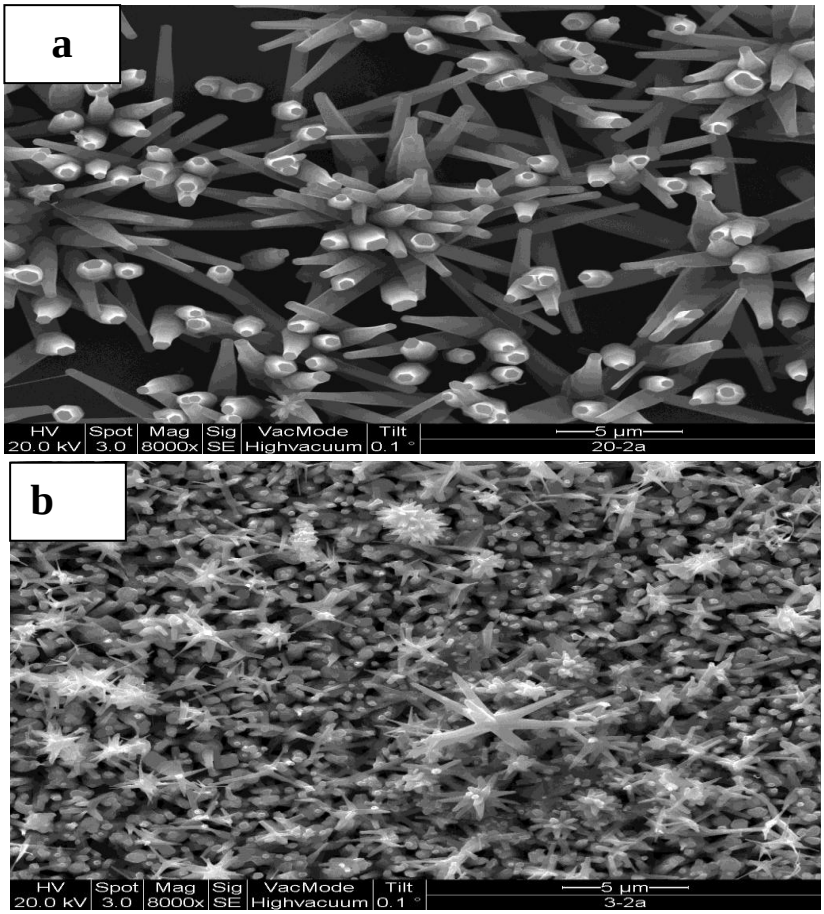

Fig. 4.41. FESEM images of ZnO nanowires grown on (a) bare and (b) gold-coated silicon substrates at same conditions The growth temperature was 1200°C, the substrate location was 11 cm, Ar flow rate was 40sccm, growth time was 30 min and ZnO:C mass ratio was 1:1).

Fig. 4.42 shows the XRD spectra of ZnO the pure powder of ZnO and the grown ZnO nanowires grown on (a) catalyst-free and (b) gold-coated silicon substrates. In the spectrum of the pure ZnO powder (Fig. 4.42 (a)), nine peaks appear at 2θ = 31.7º, 34.4º, 36.3º, 47.5º, 56.6º, 62.3º, 66.5º, 67.9º, and 69.1º, which are corresponding to (100), (002), (101), (102), (110), (103), (200), (112), and (201) wurtzite hexagonal ZnO, respectively. In contrast, only six peaks of ZnO are present in XRD for the samples grown on bare and

gold-coated silicon substrates (Fig. 4.42 (a) and (b)). These XRD peaks are assigned to (100), (002), (101), (102), and (110) wurtzite ZnO peaks. No other observable peaks from Zn or impurities can be observed besides ZnO peaks. It seems that both ZnO nanowires samples have a high crystallinity structure. However, compared with the strong (101) orientation preference in the pure ZnO powder, the ZnO nanowires grown on bare and gold-coated silicon substrates lost the (101) orientation preference and became (002) oriented, as shown in Fig. 4.42. In addition, Fig. 4.42 also shows that the XRD intensity ratios of the ZnO powder and ZnO nanowires grown on bare and gold-coated silicon substrates. It is interesting to note that ratio of the intensity of (110) peak to maximum intensity is constant in all XRD patterns. This may be due to the stability of ZnO (110) crystal face. In addition, it is found that the ratio of the intensity of (100), (101), (102) and (103) peaks to that of (002) peak of ZnO nanowires grown on gold-coated substrate is considerably increased compared with that of nanowires grown on bare silicon substrate as shown in Fig. 4.42. This indicates that the growth density of ZnO nanowires grown using gold as a catalyst is much higher than those of nanowires grown on bare silicon substrate at same growth conditions. In contrast, ZnO nanowires grown without catalyst exhibit a peak intensity of the *c*-plane (002) is higher than that of the *c*-plane of ZnO nanowires grown on gold-coated silicon substrate. Therefore, it is suggested that the ZnO nanowires grown without catalyst have a preferential orientation along the (002) orientation better than that grown with gold catalyst. As a result, catalyst-free mechanism shows better orientation of ZnO nanowires than that grown with Au catalyst.

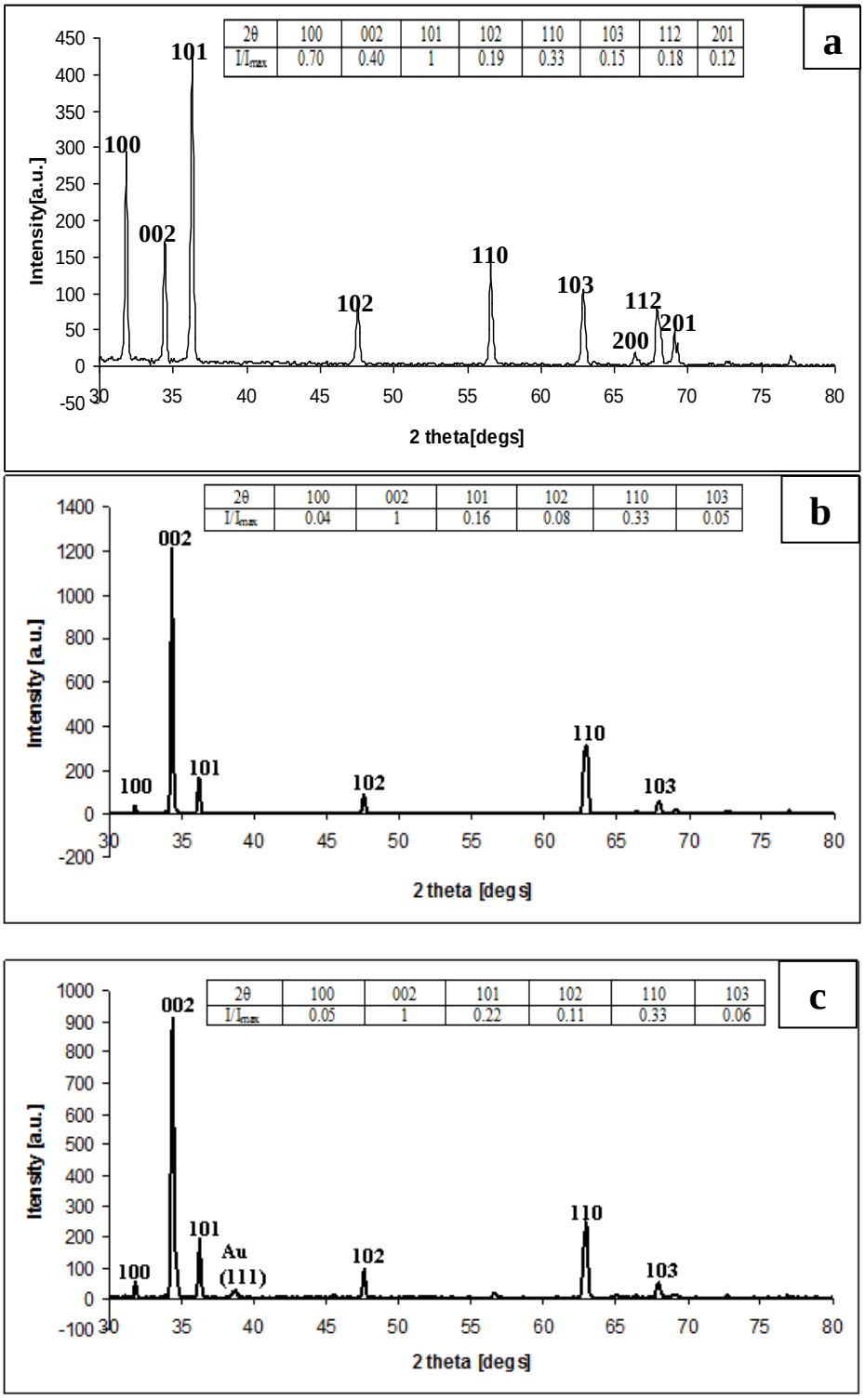

Fig. 4.42. XRD spectra of (a) pure ZnO powder and ZnO nanowires grown on (b) catalyst-free and (c) with Au catalyst silicon substrates at same conditions The growth temperature was 1200°C, the substrate location was 11 cm, Ar flow rate was 40sccm, growth time was 30 min and ZnO:C mass ratio was 1:1.

4.5 Optical properties of ZnO nanostructures

Photoluminescence (PL) has been widely used to investigate the optical properties of ZnO nanostructures. In this study, PL measurements are carried out at room temperature, with an excitation wavelength of 325 nm, to examine the emission spectra of the nanostructures fabricated on bare silicon substrates at various furnace temperatures of 1200°C, 1100°C, 1000°C and 950°C as illustrated in Fig. 4.43.

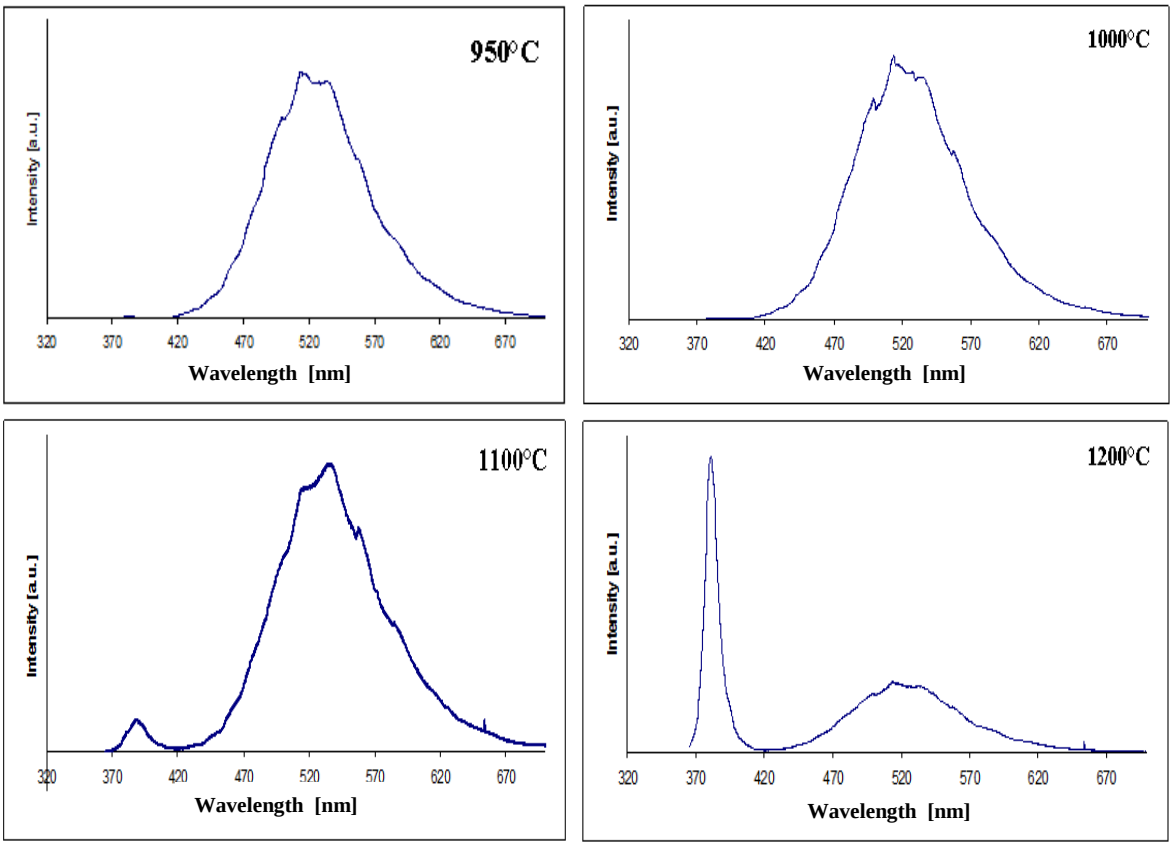

Fig. 4.43. PL spectra of the deposited ZnO nanostructures at different furnace temperatures on bare silicon substrates. The Si substrates were kept at 11 cm from the source. Ar gas flow rate was 40 sccm. The deposition time was 30 min. The mass ratio of ZnO:C was 1:1.

A relatively wide emission band is observed, which ranges from 420 to 650 nm centered at around 520 nm corresponding to the deep level emission for ZnO nanostructures formed at 950 and 1000°C furnace temperatures. According to the emission type, the broad band spectra (420-600 nm) can be divided into two major regions: a green emission region ranges from 420 to 550 nm and a red or orange emission around 600 nm [128]. The deep level emission is generally attributed to the impurities and structural defects, such as oxygen vacancies and interstitials of zinc. Thus, the emission resulted from the radiative recombination of a photo-generated hole with an electron occupying the oxygen vacancy. As the furnace temperature is increased to 1100°C, a weak UV emission at 382 nm appeared together with wide green and red emission. The UV emission is attributed to the near-band-edge emission (NBE) generated by the recombination of the free excitons through an exciton–exciton collision process. The PL emission for the ZnO nanostructures grown at 1200°C source temperatures shows a high intensity of UV luminescence at 381 nm while, the broad emission is suppressed. In addition, a shift of UV luminescence is observed from 3.82 to 3.81 nm compared to ZnO nanostructures grown at 1100°C source temperatures. The shift in UV peak by an amount $\Delta\lambda = 1$ nm towards the higher energy for nanostructures grown at 1200°C, means that the optical energy gap is increased may be due to the decrease in ZnO nanostructure size. This result suggests that the band gap can be controlled by controlling the experimental situation. It is observed that the NBE UV emission is enhanced when the source temperature is increased. In addition, the absence of UV emission indicates that ZnO nanostructures grown at 950 and 1000°C have more defects. Based on PL results, ZnO nanostructures obtained on silicon substrate at 950 and 1000 °C furnace temperatures have lower quality and have more defects such as a lack of oxygen or excess of zinc. On the other hand, the green emission peak decreased

with increasing the source temperature. The progressive increase of the green light emission intensity relative to the UV emission as the source temperature decrease suggests that there is a greater fraction of oxygen vacancies in the nanostructures that grown at 950°C, 1000°C and 1100°C.

In order to investigate the effect of the annealing process on the optical properties of ZnO nanostructures after the growth process, Fig. 4.44 shows the PL spectra of ZnO nanostructures grown on bare silicon substrates before and after the annealing process.

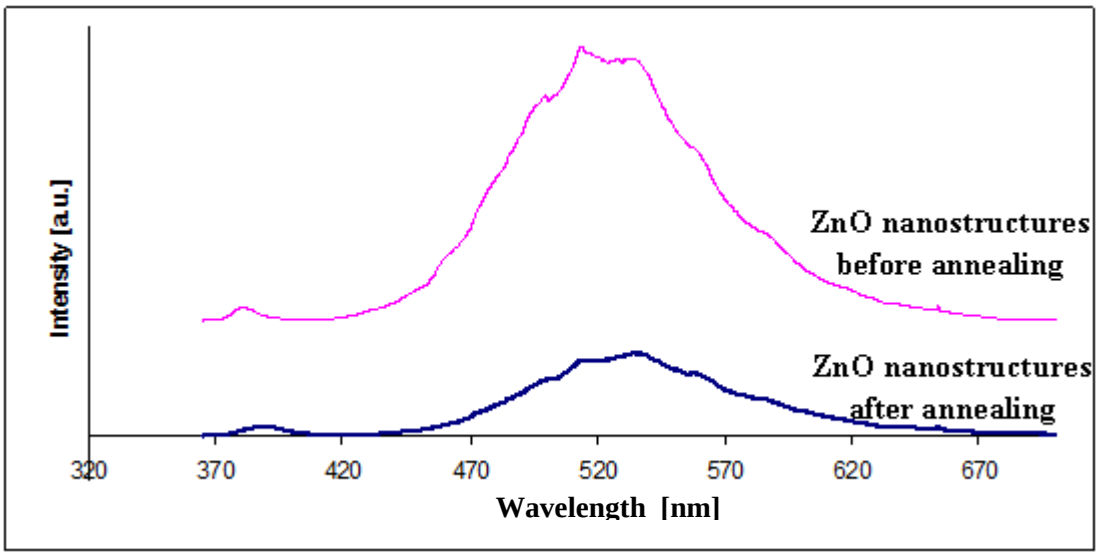

Fig. 4.44. PL spectra of ZnO nanostructures at room temperature: before and after heat treatment at 1000 °C in the air for 1 h.

It is clear that the annealing process strongly affect the luminescence behavior of ZnO nanostructures. The green emission intensity of the nanostructures decreased dramatically as ZnO nanostructures are annealed in the air for 60 min as shown in Fig. 4.44.This can be explained as follows. The more singly ionized oxygen vacancies there are, the stronger the intensity of the green luminescence is and the weaker green light emission from annealed nanostructures is related to the reduced oxygen vacancy concentration. This

suggests that the optical property of the ZnO nanostructures is tunable by controlling the oxygen vacancy concentration.

In addition, Fig. 4.45 shows a comparison study on PL spectra between the grown ZnO nanostructures on gold-coated silicon and bare silicon substrates which they have the same growth conditions; (The growth temperature was 1200°C, the substrate location was 11 cm, Ar flow rate was 40sccm, deposition time was 30 min and ZnO:C mass ratio was 1:1).

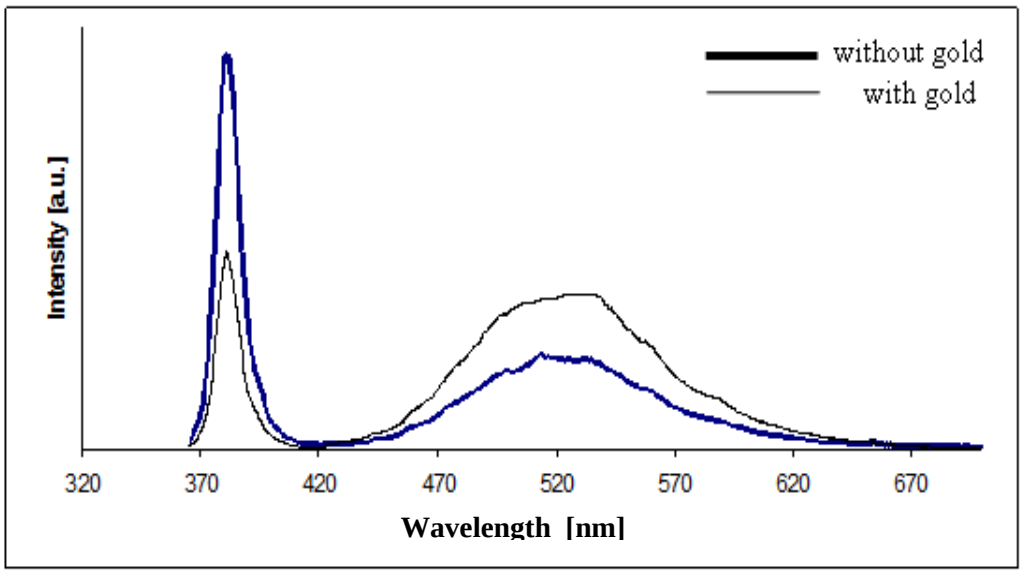

Fig. 4.45. PL spectra of grown ZnO nanostrctures on gold-coated silicon and bare silicon substrates.

According to the PL spectra (Fig. 4.45), the UV emission peak in ZnO nanostructures grown on silicon substrate is much higher than that grown on Si/Au substrate, indicating a better optical quality. In addition, the deep level emission peak in the ZnO nanostructures grown on gold-coated silicon substrate is much stronger that grown on the bare silicon substrate. This suggests that more defects and higher concentrations of oxygen vacancies are existed in the ZnO nanostructures which are synthesised on gold-coated silicon substrate. In contrast, ZnO nanostructures grown on the bare silicon substrate

show better optical properties. This may be due to the gold catalyst which may cause more structural defects in ZnO nanostructures during the growth process. As a result, the difference in the optical properties of the ZnO nanostructures with and without catalysts is attributed to the different growth mechanism.

4.6 Different Forms of Zinc Oxide nanostructures

ZnO has the richest family of nanostructures among all materials. According to this study, assortments of some of ZnO nanostructures that have successfully been grown on bare and gold-coated silicon substrates will be presented.

4.6.1 Flower-like structure

Fig. 4.46 (a) and (b) show flower-like ZnO nanostructures deposited on bare and gold coated Si (100) substrates, respectively.

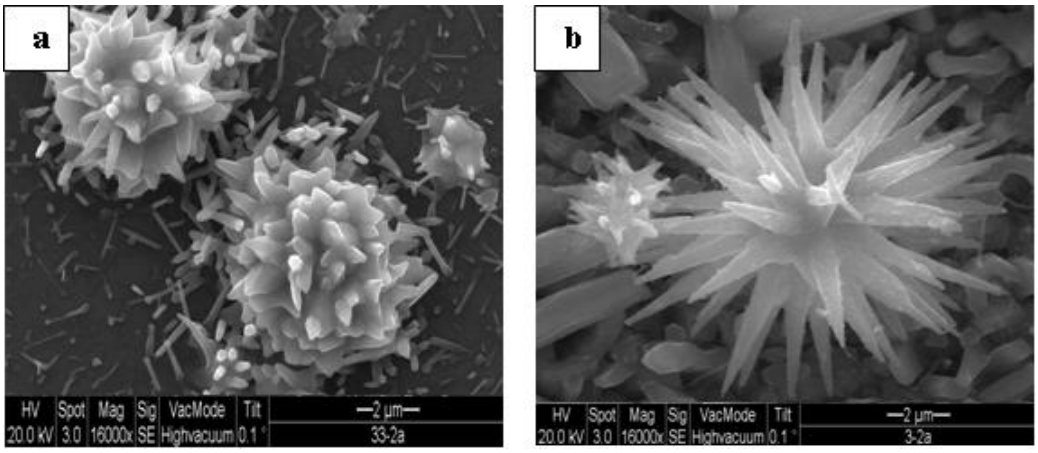

Fig. 4.46. FESEM images of flower-like ZnO nanostructures grown on (a) bare and (b) gold-coated silicon substrates (1100°C furnace temperature, 11cm substrate location, 30 sccm Ar flow rate, 15 min deposition time and ZnO:C (1:3) mass ratio).

Fig. 4.46 (a) shows flower-like structure obtained on bare silicon substrate at (1100°C furnace temperature, 11 cm substrate location, 30 sccm Ar flow rate, 15 min deposition time and ZnO:C (1:3) mass ratio) growth conditions. The typical length of one leaf is about 200–400 nm while, the diameter at the bases and tips are in the ranges of 400–900 nm and 100–200 nm, respectively. Moreover, the full width of one ZnO flower-like is 2.0–5.0 μm. Since no metal catalyst has been used, the growth mechanism of ZnO flower-like is attributed to the deposition of layer by layer growth [192]. According to this mechanism, each layer contains several leaves and the sizes of the leaves at the upper part to the lower one are different. In contrast, Fig. 4.46 (b) shows a typical FESEM image of ZnO flower-like structure which was obtained on the gold coated silicon substrate at (1200°C furnace temperature, 11 cm substrate location, 40 sccm Ar flow rate, 30 min deposition time and ZnO:C (1:1) mass ratio) growth conditions. ZnO flower-like nanostructure has uniform leaves and these leaves are like ZnO nanorods with a smooth surface and uniform diameter originating from one centre. In addition, the upper portion of these leaves shows sharp tips. The average lengths and diameters of one leaf of a flower-shaped structure lie in the ranges 2–4 μm and 200–400 nm, respectively. The full width of one collection is about 6 μm. The growth mechanism of the ZnO flower-like nanostructures obtained upon Si gold-coated substrate can be attributed to VLS mechanism. Fig. 4.47 (a) and Fig. 4.47 (b) show EDX spectra of flower-like obtained on bare and gold coated Si (100) substrates. Fig. 4.47 (a) reveals that no metal catalyst or other impurities had been detected. Si peak indicates the background silicon substrate. EDX result in Fig. 4.47 (b) reveals that the presence of gold particles on flower-like structures which was obtained on gold-coated substrate.

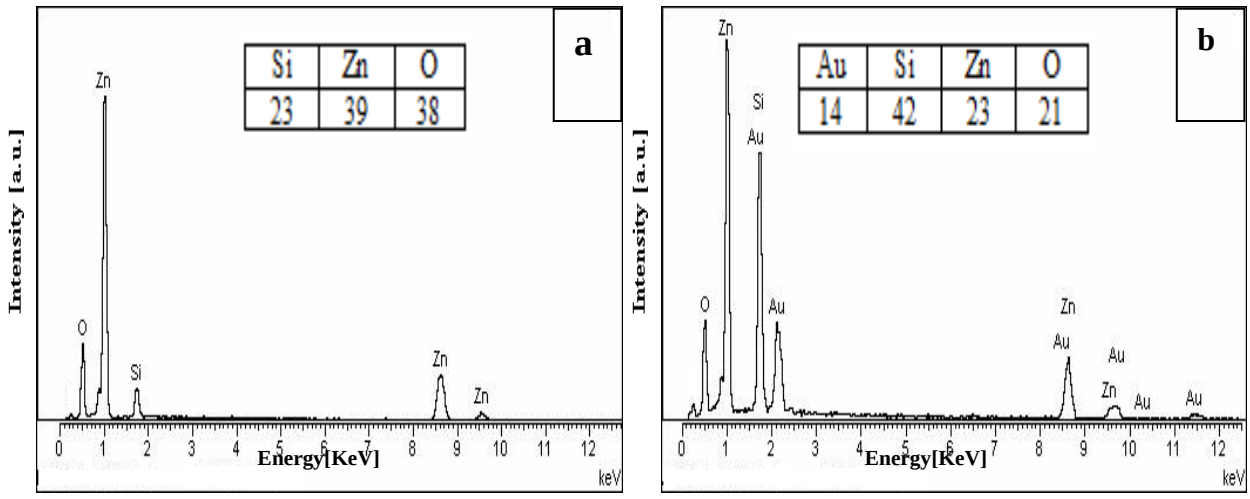

Fig. 4.47. EDX spectra of flower-like obtained on (a) bare and (b) gold coated Si substrates.

4.6.2 Nano-bottle structure

To the best of our knowledge, there is no report about the fabrication of ZnO nano-bottle structure. Fig. 4.48 shows the ZnO nano-bottle structure that was obtained upon gold-coated silicon substrate.

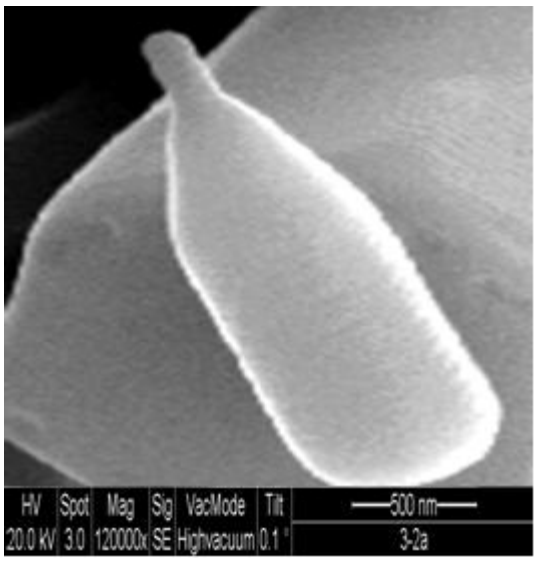

Fig. 4.48. FESEM image of ZnO nano-bottle structure was obtained at (1100°C furnace temperature, 11cm substrate location, 10 sccm Ar flow rate, 14 min deposition time and ZnO:C (1:1) mass ratio) growth conditions.

The typical diameters at the roll base and roll neck are 400 nm and 100nm, respectively. The typical length from top to bottom is 2 μm. This type of structure was obtained at (1100°C furnace temperature, 11cm substrate location, 10 sccm Ar flow rate, 14 min deposition time and ZnO:C (1:1) mass ratio) growth conditions. Fig. 4.49 (a) and (b) show the EDX spectra of the middle and the tip cab of the fabricated ZnO nano-bottle. According to EDX results, there is no gold peak detected on the middle of the bottle, whereas gold peaks were only observed at the tip cap. In addition, this result confirms that the growth mechanism of ZnO nano-bottle proceeds via VLS process.

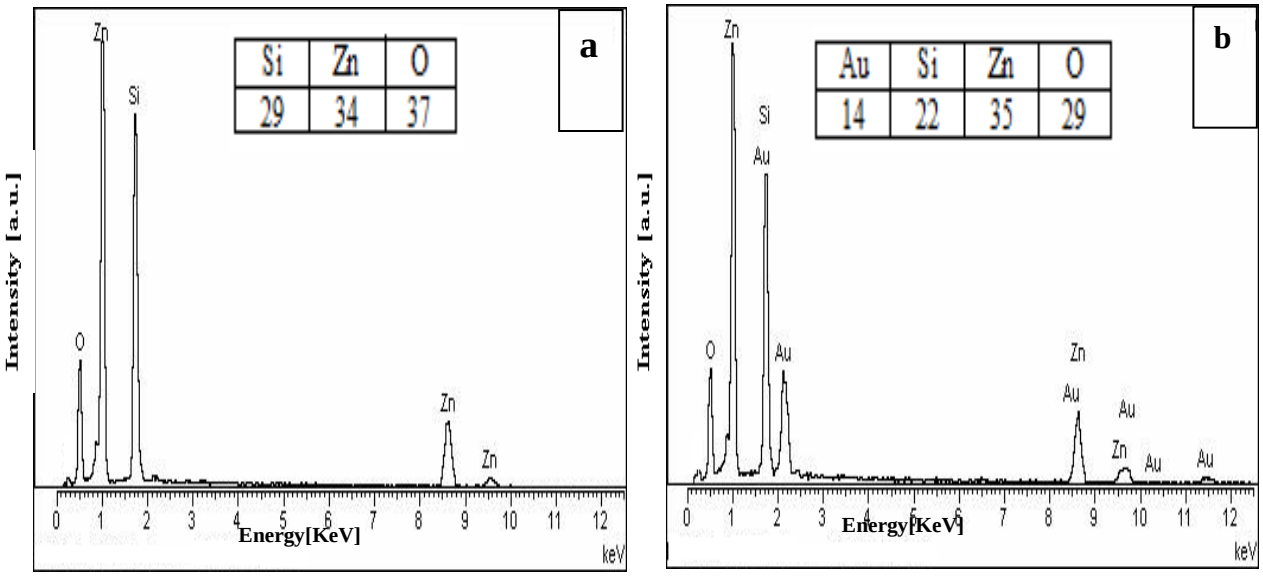

Fig. 4.49. EDX spectra of (a) the middle and (b) the tip cab of fabricated ZnO nano-bottle correspondingly.

4.6.3 Nanocomb-like structure

The ZnO nanocomb-like nanostructures were also obtained as shown in Fig. 4.50. The ZnO nanocomb-like nanostructures content of two parts; backbone and teeth. It is worthy to point out that the nanocomb-like was only observed at gold-coated substrate, which was located at 15 cm far from source material ZnO:C (1:1) heated at 1200°C for 30 min under 40 sccm Ar gas flow rate. The usual width of the backbones of the nanocombs is about 400 nm to 1 μm, and the thickness is around 50–100 nm, while the length is up to several tens of microns. The branches (teeth) are attached along one side of the backbones and are arranged in a proper manner. The teeth have diameters ranging from about 50 to 100 nm and length ranging from hundreds nanometers to several microns. It is interesting to note that no gold signals were detected in EDX result as Fig. 4.51 illustrated.

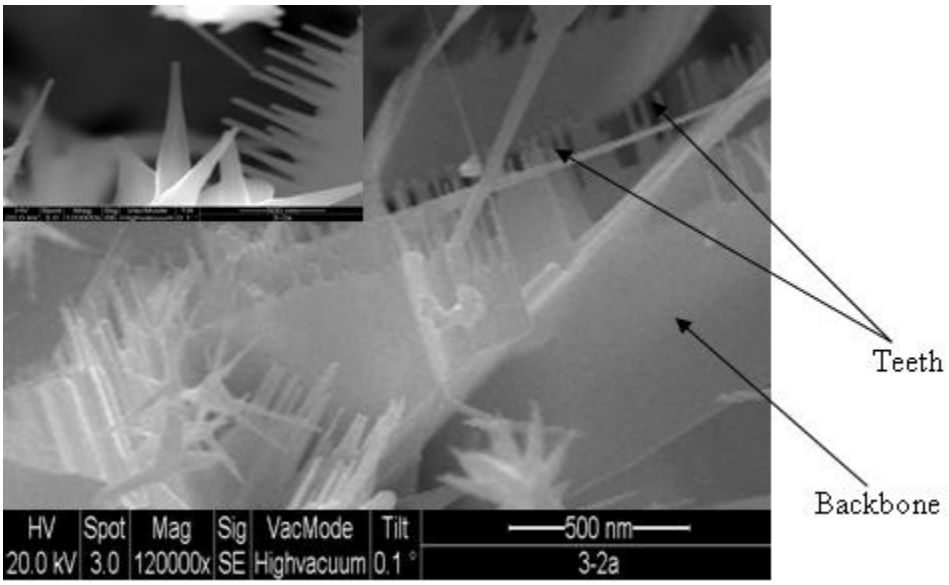

Fig. 4.50. Low and high magnification FESEM images of the ZnO nanocomb-like structures at gold-coated substrate located at 15 cm far from source material source ZnO:C (1:1) heated at 1200°C for 30 min under 40 sccm Ar gas flow rate.

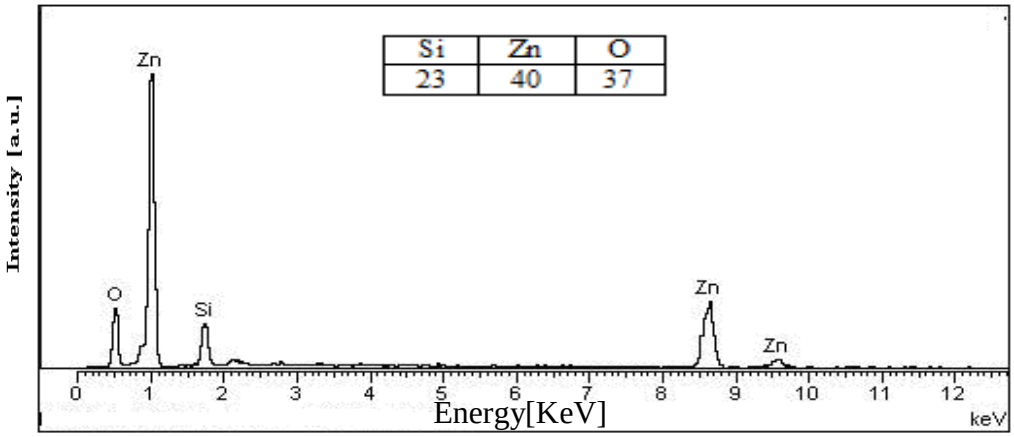

Fig. 4.51. EDX spectrum for ZnO nanocomb-like structure.

4.6.4 Cages and Shells structures

Nano-cages and shells are two examples of the most interesting structures formed by zinc oxide. The FESEM image in Fig. 4.52 shows the as-synthesized ZnO cages and shells obtained on the substrate surface. The cage and shell structures exhibit the regular polyhedral shapes. The growth conditions of these structures were discussed in section 4.3.2. The typical shapes observed can be classified into two groups; hexagon-based cages and spherical shells. The polyhedron is enclosed by (001) (top and bottom surface), (100) (side surfaces), stepped (101) (inclined surfaces), and high index planes with rough surfaces and this result agrees well with Wang *et al.*[130]. In contrast, no corners or side opened cages and shells had been obtained in this work. In addition, ZnO cages and shells have different sizes and they have thick walls. The typical diameters of nanocages and nanoshells lie in the ranges 300 nm-1.5 μm and 200 nm to 2 μm, respectively. To investigate the related shapes of the cages and shell, the as-synthesized ZnO cages and shells were investigated using EDX technique as shown in Fig. 4.53. EDX result indicates that the atomic proportion of zinc is a very high comparing to atomic proportion of oxygen. This result confirms that the nanocage and nanoshell structures are mainly metallic zinc.

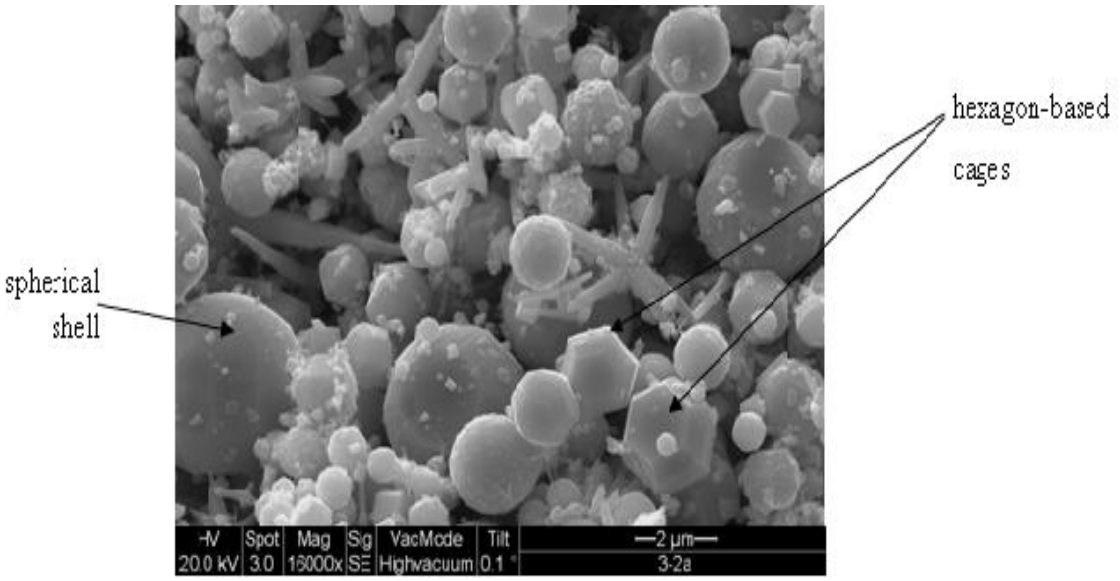

Fig. 4.52. FESEM image of the as-synthesized ZnO cages and shells distributed on the substrate surface.

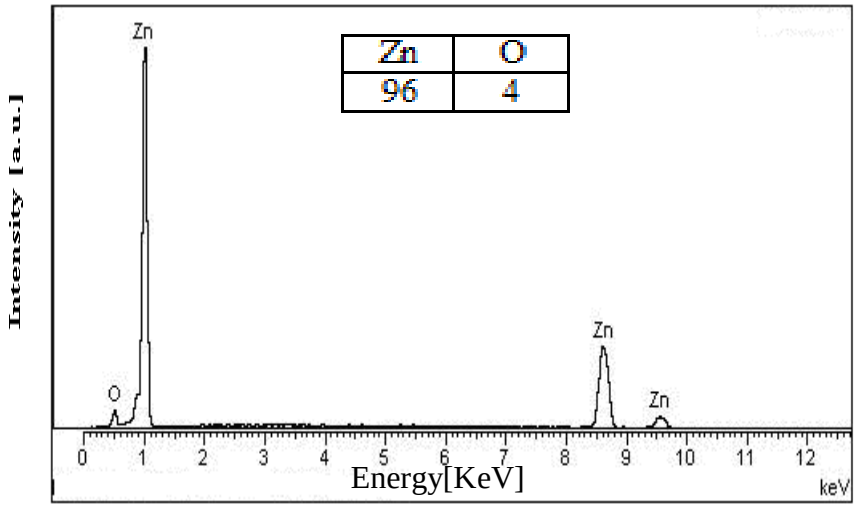

Fig. 4.53. EDX spectrum of the as-synthesized ZnO cages and shells.

4.6.5 Nanowires/nanorods structures

Nanowires and nanorods are the representatives of 1-D nanostructures due to their high aspect ratio. According to the orientation alignment, nanowires can be categorized to four types; well aligned, aligned, randomly oriented and intermixed wires. In this study, three types of ZnO nanowires were obtained as shown in typical FESEM images (Fig. 4.54). Fig. 4.55 shows the XRD patterns of the aligned and randomly oriented ZnO nanowires.

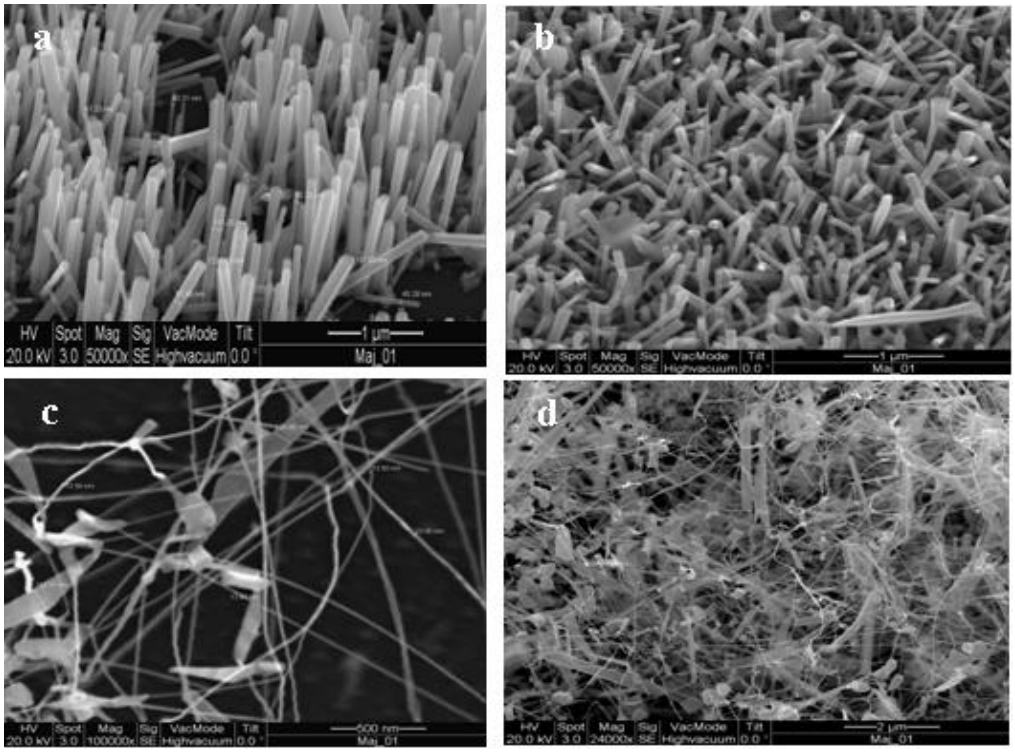

Fig. 4.54. FESEM images of (a) aligned, (b) randomly oriented and (c) and (d) intermixed nanowires.

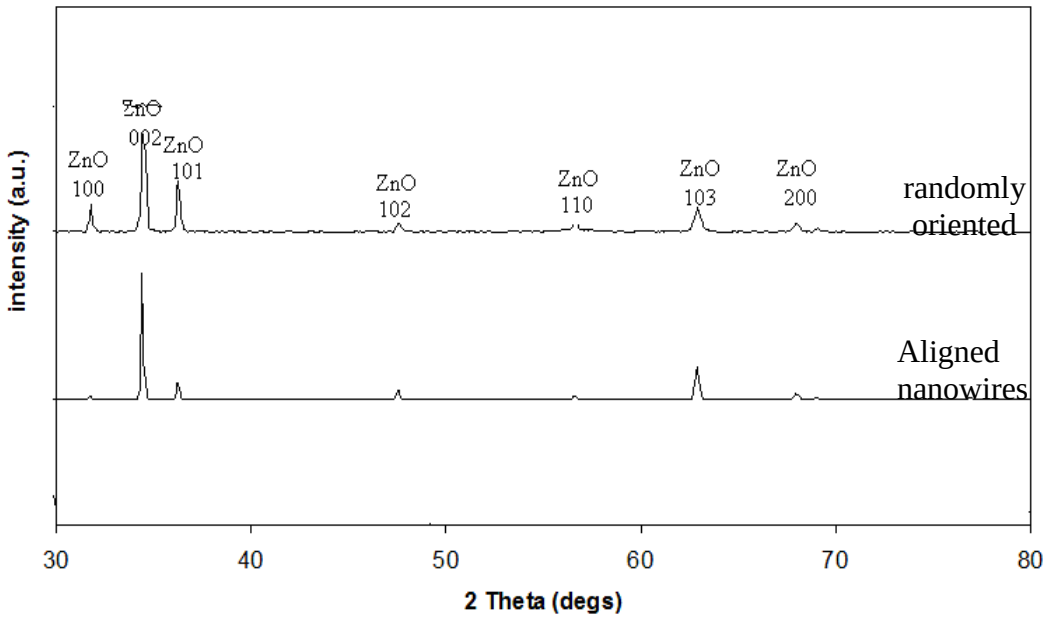

Fig. 4.55. XRD patterns of the aligned and randomly oriented nanowires.

In randomly oriented ZnO nanowires, XRD result indicates that the nanowires exhibit different growth directions. In contrast, XRD pattern of aligned ZnO nanowire shows a main peak at 2θ =34.3°, which indicates that almost the ZnO nanowires tend to grow in one direction, which is perpendicular to the substrate. The average diameter of nanowires ranged from 10 nm to 200 nm. Aligned ZnO nanowires were obtained in both bare and gold coated silicon substrates at 1200°C furnace temperature, 11 cm substrate location, 40 sccm Ar flow rate, 30min deposition time and ZnO:C (1:1) mass ratio) growth conditions. The non-aligned and intermix ZnO nanowires were obtained at 1100°C furnace temperature, 11cm substrate location, 40 sccm Ar flow rate, 30min deposition time and ZnO:C (1:1) mass ratio) growth conditions. The growth mechanism of nanowires depends on the metal catalyst. In catalytic process, the growth mechanism is attributed to the VLS mechanism whereas process without catalyst the growth mechanism is attributed to self-catalytic VLS.

4.6.6 Nanoneedles-like structure

Nanoneedles-like structures are nanowires/ nanorods ended with sharp tips. Recently, these needles-liked attract more attention for their novel properties. For example, electrons are more easily emitted from ZnO nanoneedles with sharp tips than from nanowires with uniform diameters [131]. For this property, nanoneedles can be used as probing tips with a high spatial resolution in both vertical and horizontal dimensions or field-emission tips due to the increased field [132]. Fig. 4.56 shows a typical FESEM image of ZnO nanoneedle-like was formed on gold-coated silicon substrate at 1100°C furnace temperature, 11 cm substrate location, 40 sccm Ar flow rate, 30 min deposition time and ZnO:C (1:1) mass ratio) growth conditions. It is interesting to note that the diameter of these nanostructures decreases with increasing the length of the nanostructures from the bottom to the top. The bottom diameter of the nano-needles normally ranges from 100 to 250 nm and the lengths are 1–4 μm long, while the tip has an average diameter around 60 nm. In addition, the tip of the nano-needles is well developed without the formation of metal catalyst. The growth mechanism of ZnO nanoneedle-like is accredited to VLS and the diameter reduction seems to be due to the decrease of the amount of reacting species (Zn, CO,CO_2) supplied to substrate during the reaction.

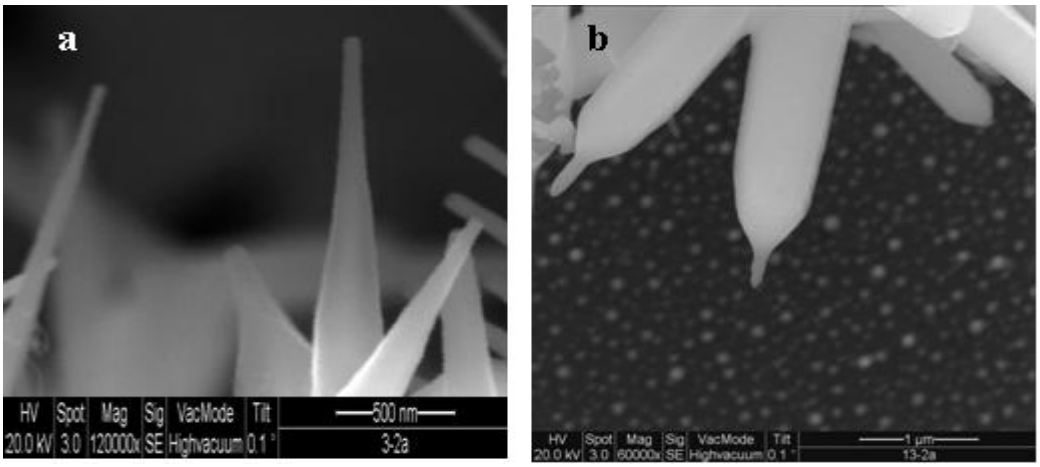

Fig. 4.56. FESEM picture of ZnO nanoneedle-like.

4.6.7 Possible growth mechanism of grown ZnO nanostructures

Different ZnO nanostructures formed on bare and gold-coated silicon substrates have different growth mechanisms. Based on FESEM, EDX and XRD results, the growth mechanism of previous ZnO nanostructures will be explained through the VLS and self-catalytic VLS point of view.

4.6.7.1 Nano-bottle structure

Since the ZnO nano-bottle structure was obtained on gold-coated silicon substrate and based on FESEM result (Fig.4.48) and EDX result (Fig.4.49), the growth mechanism is attributed to VLS process. Fig. 4.57 (a), (b) and (c) illustrate the growth process of ZnO nano-bottle proceeds via VLS route. First, the gold element forms a droplet on the silicon substrate at suitable temperature (Fig. 4.57 (a)). Second, the Zn and ZnOx vapors are transported by Ar gas to low-temperature region and then, attract by Au droplet to form the nanorods (Fig. 4.57 (b)). At the end of the experiment, the vapors concentration decreases dramatically and this leads to reduce the vapors that arrived to the Au droplet resulting in a

sharp decrease in the diameter of the nanorods and hence, the neck of the bottle was formed.

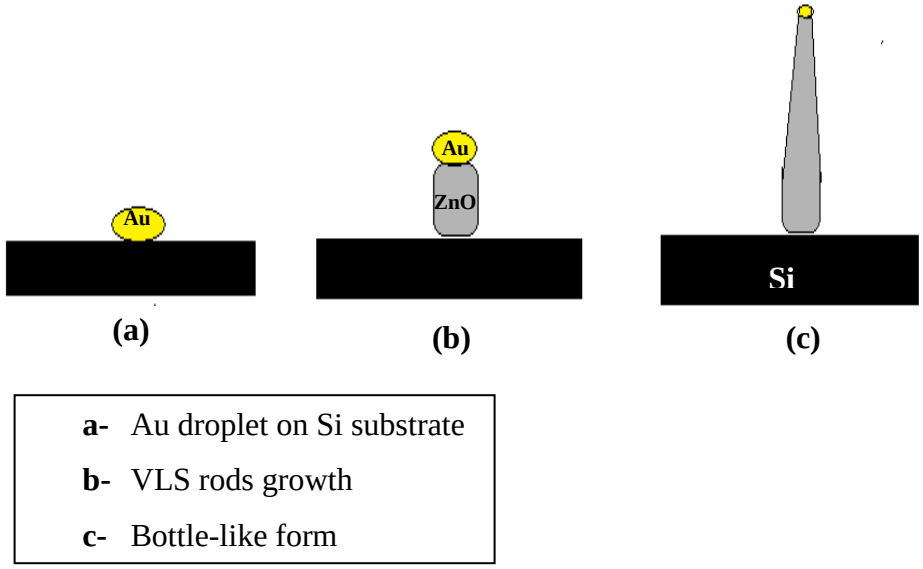

Fig. 4.57. (a), (b) and (c) are illustrated the growth process of ZnO nano-bottle proceeds via VLS mechanism.

4.6.7.2 Nanocomb-like structure

The nanocomb-like growth process can be attributed to two growth process; VLS and self- catalytic VLS. First of all, the growth of nanowires was occurred and this process was controlled by the catalyst droplet. This is followed by dendritic sidebranch nanowires growth along the basal nanowires and the side branches growth was attributed to self-catalytic growth. For more illustration, Fig. 4.58 explains more details about two different growth processes [4,133]. According to Fig. 4.58, Au–Zn alloy tip moves upward leave ZnO nanowire downward in the Au-catalyzed VLS process.

In contrast, there are no Au catalysts present along the branches (teeth) so, the growth mechanism of the teeth cannot be attributed to the aid of catalysts. In this regards, dendritic crystals in homogeneous and epitaxial crystal growth is generally attributed to the diffusion-limited process in a supersaturated environment [134]. The dendrites can be developed by the morphological instability via self-catalytic VLS growth mechanism. In addition, thin sheet can be formed due to the fill up of interspacing between the branches. According to this study, the pervious explanation agrees well with FESEM result. ZnO nanowires grow as side branches from the main root of nanocomb backbone and as more vapors introduce, the filled-up process is continued between branches and resulting in thin-sheets. Fig. 4.59 shows an example of ZnO nanosheet structure, which has 1.5 μm diameter

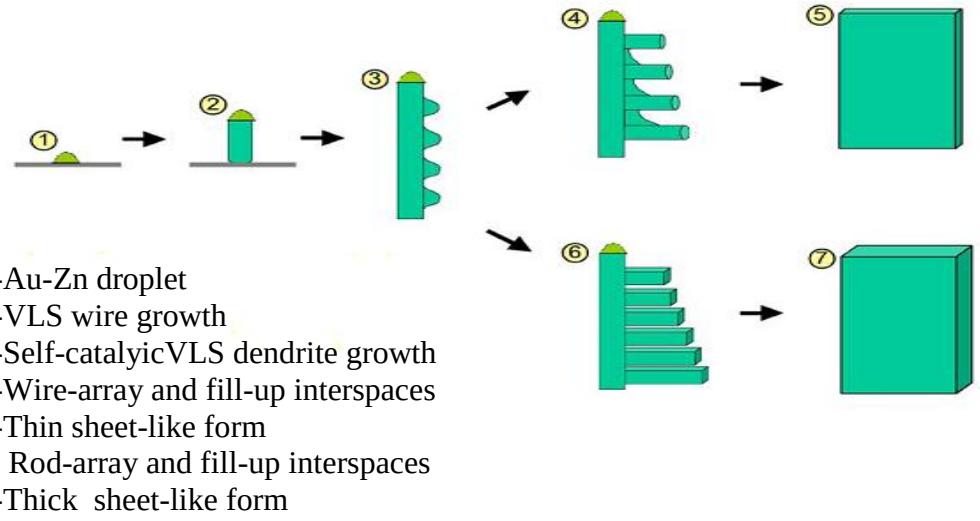

1-Au-Zn droplet
2-VLS wire growth
3-Self-catalyicVLS dendrite growth
4-Wire-array and fill-up interspaces
5-Thin sheet-like form
6. Rod-array and fill-up interspaces
7-Thick sheet-like form

Fig. 4.58. A schematic diagram showing the possible growth mechanisms of ZnO nanocomb and nanosheet structures.

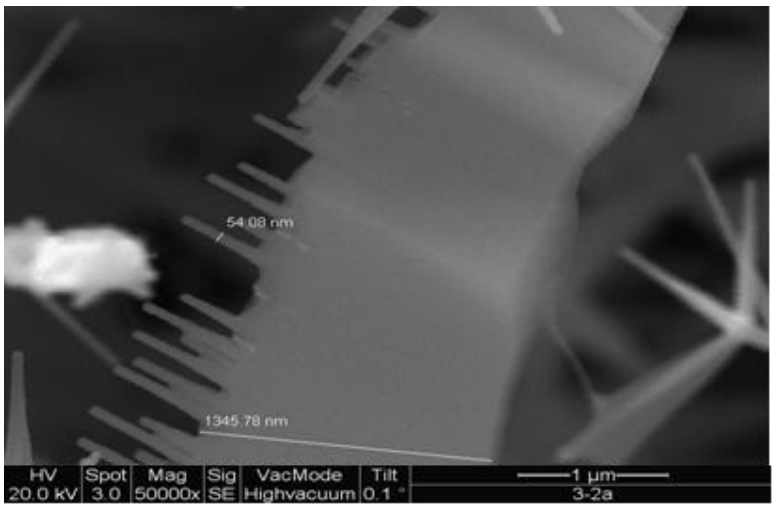

Fig. 4.59. FESEM image of ZnO nanosheet structure formed as filled-up process between branches.

4.6.7.3 Shell and cage-like structures

The growth mechanism of the ZnO shell and cage structures is proposed to be a process comprised of solidification of liquid droplets, surface oxidation, and sublimation [135]. According to this mechanism, a Zn vapor form, first, from the carbothermal reaction Then, Zn vapor is carried downstream by the Ar carrier gas. The ZnO shell and cage structures are formed at lower substrate temperature. When the Zn atoms reached the substrate at low temperature, they condense and form liquid clusters which tend to deposit fairly onto the substrate. The liquid droplets are quickly solidified at the lower temperature zone, forming faceted single crystalline Zn polyhedra, which are enclosed by (001), (100) and (101) facets. The residual oxygen in the growth chamber oxidizes the surface of the Zn polyhedron. Because of the oxidation rates on different crystal surfaces are different, the surface with the lowest energy tends to be most stable and may resist being oxidized, while the high energy surfaces will be quickly oxidized, resulting in the formation of an oxide layer with a non uniform thickness on the Zn polyhedral surface. Zn has a much lower (melting point 419°C) than that of ZnO (1975°C) for; an increase in local temperature

between 300 and 500°C during the growth leads to the sublimation of Zn but not ZnO, resulting in the formation of the ZnO shell/cage structure. In some cases, the shell collapsed after the vaporization of the Zn core possibly because the oxide layer is thin and the local temperature is high enough to cause sintering, forming various collapsed structures. In this study, no collapsed cages or shells were obtained.

4.7 Doping of ZnO nanostructures with Phosphorous

As illustrated in section 2.6.2.2, ZnO nanostructures are naturally n-type semiconductors. Therefore, there have been attempts to produce *p*-type ZnO nanostructures with high quality but, to date; no significant success has been reported. Production a good quality of *p*-type ZnO nanostructures has been problematic, mainly due to the defects caused by dopant induced stresses in the crystal. Here, ZnO nanostructures doped with phosphorus have been successfully achieved on a bare silicon substrate. In this study, phosphorus pentoxide (P_2O_5) had been used as a dopant source. The dopant source was mixed with ZnO and graphite powders in equal proportion (growth conditions: 1200°C, 11 cm, 40sccm, 30 min) as descried in the experimental section. At evaluate temperature, the graphite redact P_2O_5 into phosphorus and CO as indicated in Equation (4.4) [136].

$$P_2O_{5\,(s)} + 5C_{\,(s)} \rightarrow 2P_{\,(g)} + 5CO_{(g)} \quad \text{---------- 4.4}$$

Then, the phosphorus deposited with Zn on the substrate down stream and the contributed together to form P-doped ZnO nanostructures via self-catalytic VLS. Fig. 4.60 shows FESEM images of the P-doped ZnO nanostructures. Fig. 4.60 (a) shows a low

magnification FSEM image of a large area of the P-doped ZnO nanostructures grown on the silicon substrate, while Fig 4.60 (b) shows a high magnification image.

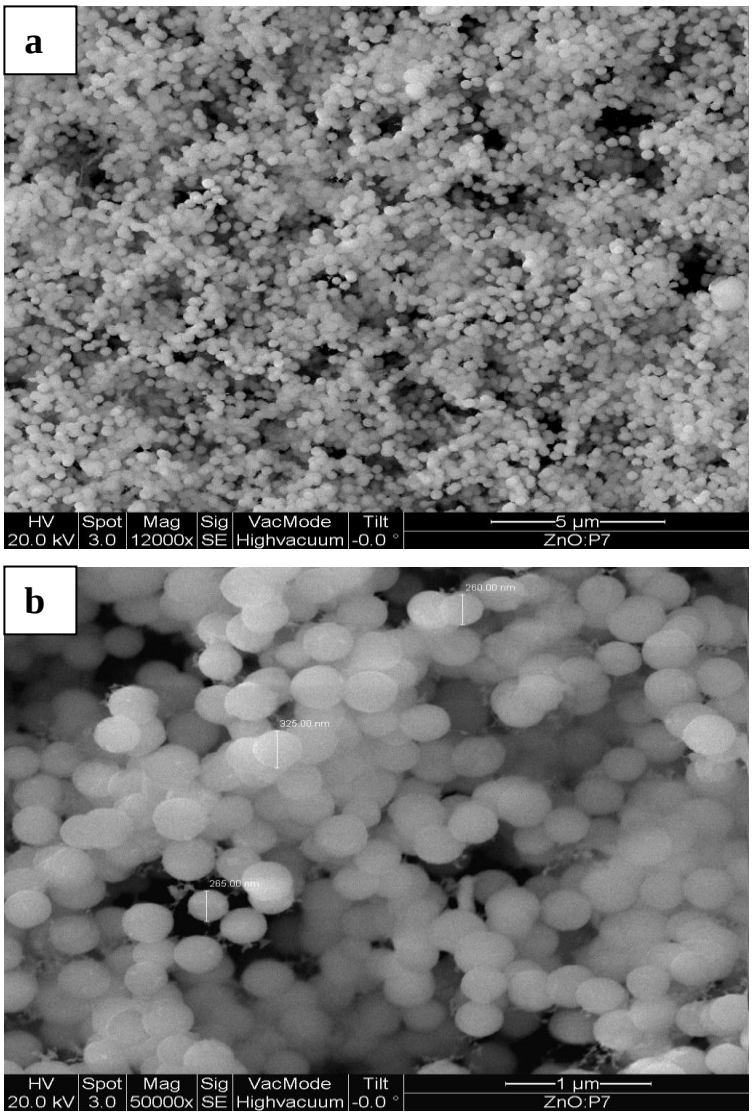

Fig. 4.60. FESEM of P-doped ZnO nanostructures at (a) low and (b) high magnifications.

FESEM images show nanoballs-like ZnO:P nanostructures. The diameter of balls is ranging from 90 to 300 nm. EDX analysis shows that these nanoballs are indeed composed of Zn, P and O as shown in Fig. 4.61. According to EDX result, the nanoballs are grown in a high yield because no Si peak is detected. Interestingly, there is a change in ZnO nanostructures morphology during the doping process comparing to the morphology obtains during the same experiment conditions without doping. The same experiment conditions were applied without doping process, smi-aligned ZnO nanowires were obtained on Si(100) substrate as shown in Fig. 4.62. As a result, a hexagonal-like shape of ZnO nanostructures was altered to a spherical shape when doping of ZnO with P ions as shown in Fig. 4.60 and Fig. 4.62, respectively. The modification of ZnO nanostructures shape during doping process at the same experiment conditions was also reported by Fan *et al.* [137] and Wang *et al.* [138].

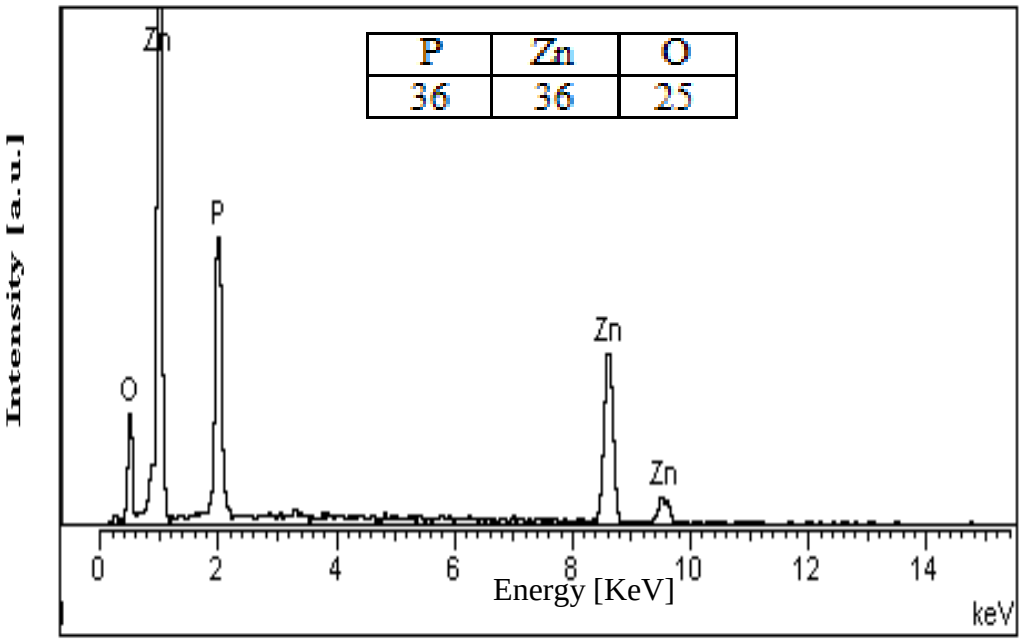

Fig. 4.61. EDX spectrum of synthesized P- doped ZnO nanoballs.

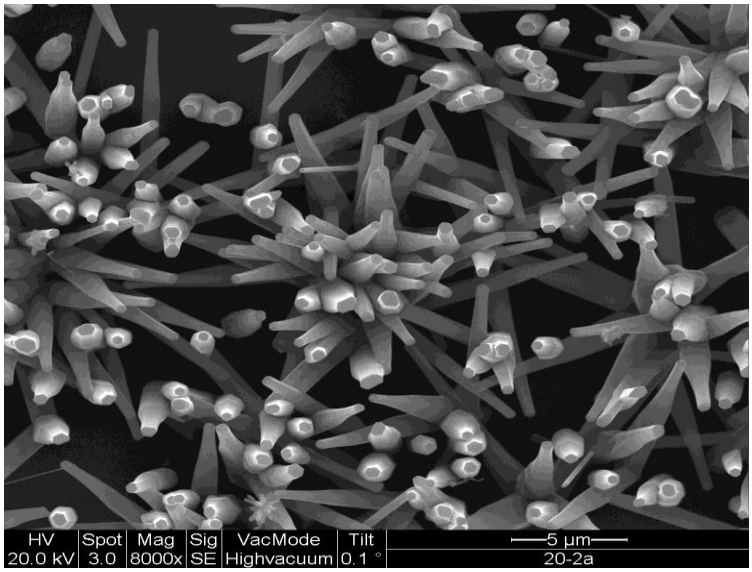

Fig. 4.62. FESEM image of the synthesized undoped ZnO nanowires.

Fig. 4.63 shows typical FESEM images of an area which had no nanostructures were observed. Cracked flower-like microstructures were viewed on silicon surface as shown in Fig. 4.63 (b). The average diameter of these microstructures is about 30 µm. EDX result shows that a very low atomic percentage of Zn and P was presented on silicon substrate compared to a high percentage of silicon and oxygen as illustrated in Fig. 4.64. As a result, flower like microstructures was attributed to some defects were presented on the surface of silicon substrate. The crake's formation can be attributed to the poor wetting effect between the silicon substrate and the deposited components [139].

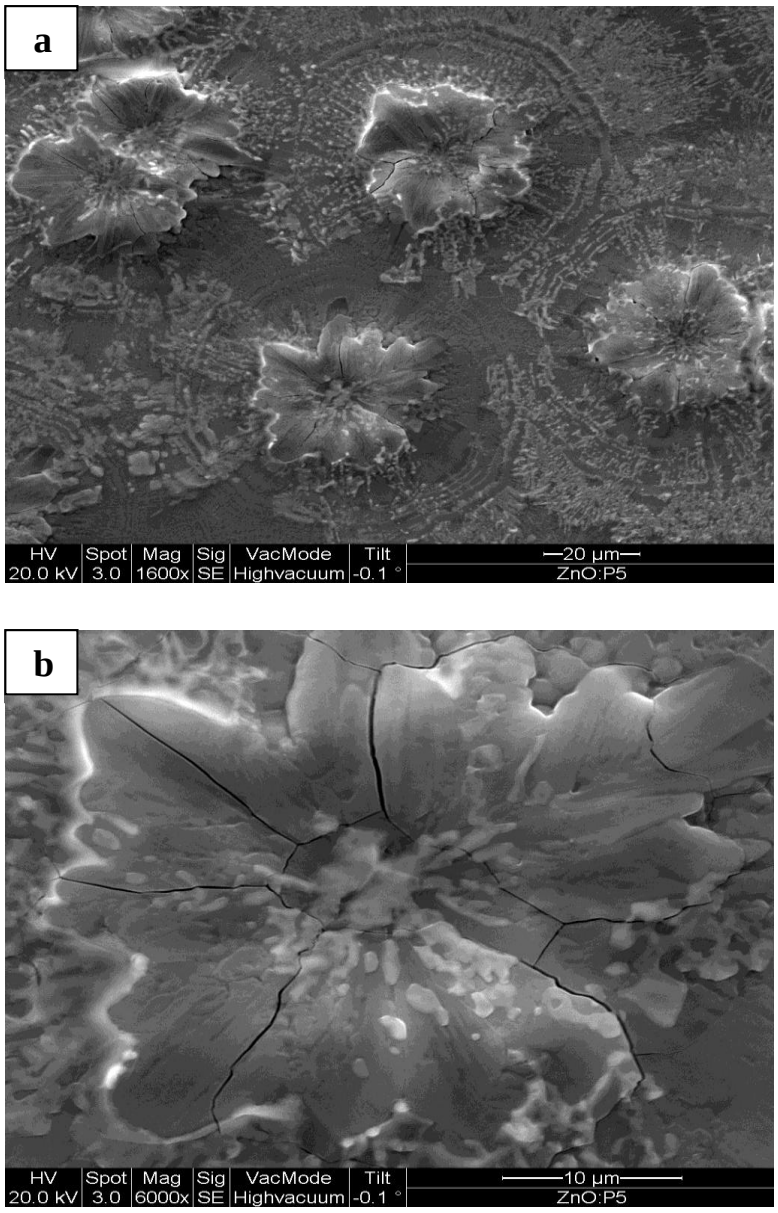

Fig. 4.63. FESEM images (a) low magnification without grown nanostructures surface and (b) cracked flower like microstructures.

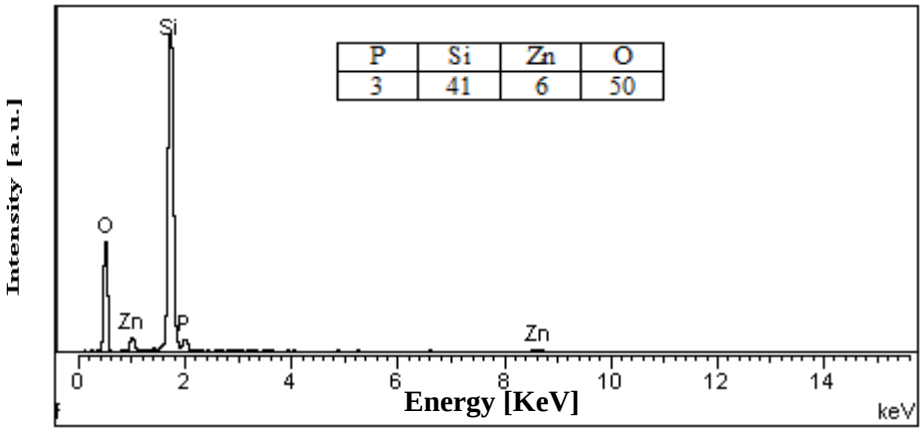

Fig 4.64. EDX spectrum of flower like microstructures.

The XRD spectra for both doped and undoped ZnO nanostructures are shown in Fig. 4.65. All the diffraction peaks in XRD data show peaks corresponding to wurtzite ZnO. No other diffraction peaks from Zn, Zn-P or other impurities were detected. However, compared with the strong (002) orientation preference in undoped ZnO nanostructures, ZnO:P deposited on silicon substrate lost the (002) orientation preference and became randomly oriented, as shown in Fig. 4.65. This result is in good agreement with published results in doping ZnO films [140]. It is worthy to note that there is slightly shifted towards higher angles for the P doped ZnO nanostructures in the XRD pattern. For example, the peak (002) is centered at $2\theta = 34.45°$ for P doped ZnO nanostructures while, that for undoped sample is $2\theta = 34.40°$ with the peak shift $\Delta 2\theta = 0.05°$, which means that the lattice parameter of ZnO had been decreasing due the doping process. The same result reported by many authors due to incorporation of doping elements with ZnO [141,142]. In addition, XRD pattern of remain powder after doping process showed only graphite peaks which is indicated that no remain P or Zn on it as it is shown in Fig. 4.66. According the XRD spectra, two diffraction peaks were detected at $2\theta=13.8°$ and $2\theta=26.5°$ which they attributed to graphite oxide (100) and carbon (002), respectively.

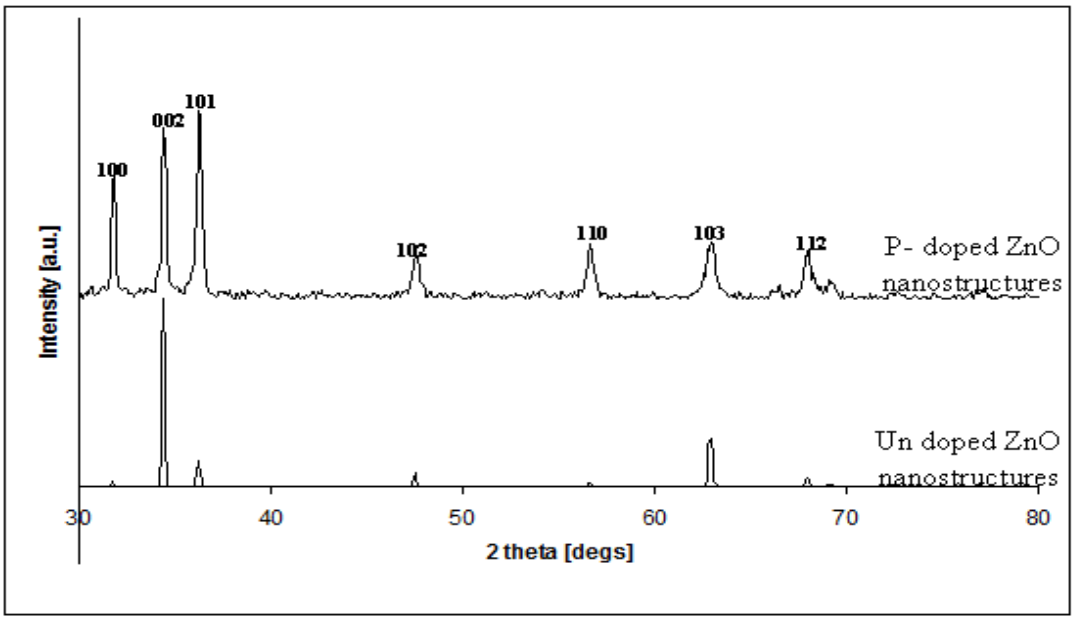

Fig. 4.65. XRD spectra of both doped and undoped ZnO nanostructures.

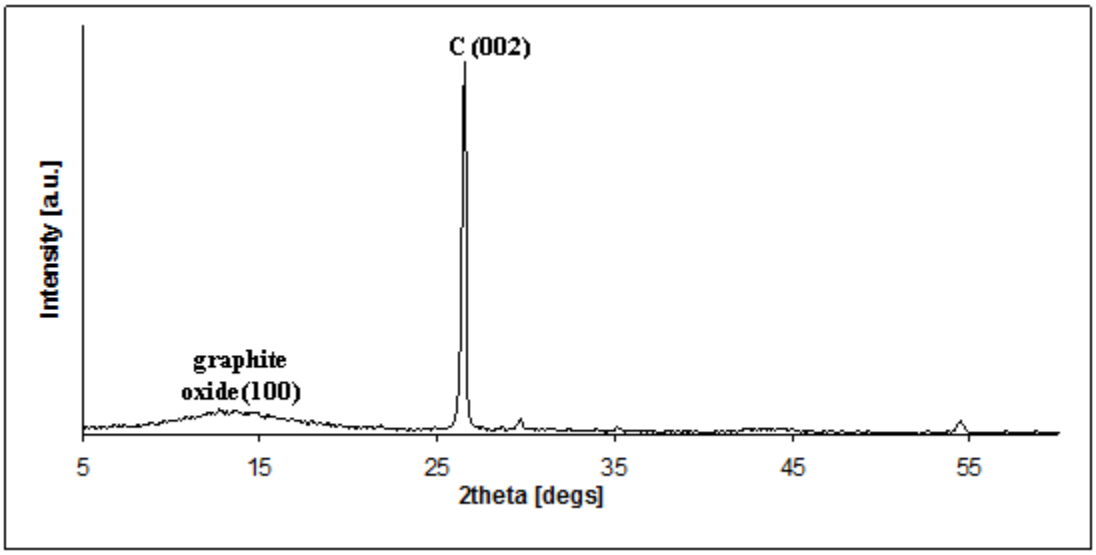

Fig. 4.66. XRD spectrum of remain powder after doping ZnO nanostructures.

The PL spectra of undoped and doped ZnO nanostructures are shown in Fig. 4.67. PL spectra for both undoped and P-doped ZnO nanostructures reveal two emission peaks, the near band edge and the green broad emission peak. The details of these peaks were discussed in section 4.5. It can be observed from Fig. 4.67 that the two emission peaks can be affected by the ZnO nanostructures doping process with phosphorus element. On the one hand, the UV peak can be suppressed or eliminated through the doping process as shown in PL spectrum of P-doped ZnO nanostructures. On the other hand, the green broad emission peak in P-doped ZnO nanostructures is broader than that of the undoped ZnO nanostructures. The broader and high intensity of green emission is mainly attributed to the defects in ZnO and it is caused may be due to the presence of phosphorus atoms in the ZnO nanostructures. The prepared phosphor doped ZnO nanostructures emitted green luminescent light with high efficiency was reported widely [143-145].

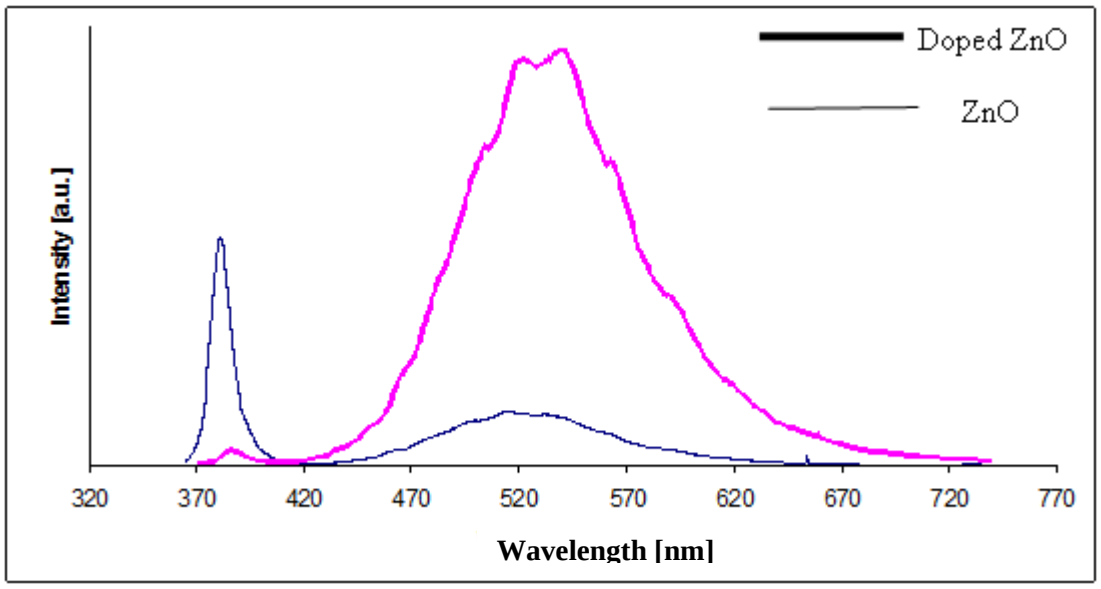

Fig. 4.67. PL spectra of undoped and P-doped ZnO nanostructures